COMPUTER SIMULATION OF DIRECT WEATHERING OF FELDSPAR TO GIBBSITE THROUGH DIFFUSION

by

PARTHA PRATIM DE

DEPARTMENT OF CIVIL ENGINEERING

INDIAN INSTITUTE OF TECHNOLOGY, KANPUR

AUGUST 1988

To

MY PARENTS

24/7/98

CERTIFICATE

This is to certify that the present work, entitled "COMPUTER SIMULATION OF DIRECT WEATHERING OF FELDSPAR TO GIBBSITE THROUGH DIFFUSION" has been carried out by Mr. PARTHA PRATIM DE under our joint supervision and the same has not been submitted elsewhere for a degree.

NIRUPAM CHAKRABORTI
Assistant Professor
Department of Metallurgical Engineering
I.I T. Kanpur-208016

BIKASH C. RAYMAHASHAY
Professor
Department of Civil Engineering
I.I.T. Kanpur-208016

ACKNOWLEDGEMENTS

I wish to express my sincere gratitude to my joint thesis supervisors Dr B.C Raymahashay and Dr. N. Chakraborti for suggesting me this interesting problem, their valuable guidance throughout and critical review of the manuscript.

I avail this opportunity to thank Shri A.K. Sen, Director, G.S.I , who was kind enough to send me a copy of his important paper on East Coast bauxite, written in collaboration with Shri S. Guha, G.S.I.

I also thank Shri Jayakumar of Civil Engineering for supplying me a rainfall data.

Lastly, I fondly remember all my friends at I.I.T. Kanpur, too numerous to mention individually, for their support, enthusiasm and the friendly environment they created around me during my stay.

- PARTHA P. DE

ABSTRACT

The common weathering sequence of feldspars at surface pressure-temperature condition involves these steps, feldspar to mica, mica to clay and clay to gibbsite. On the otherhand, some recent reports suggest that a direct conversion of feldspar to gibbsite is possible bypassing the intermediate phases. This thesis reviews the physico-chemical conditions for direct gibbsitization of feldspars. Factors like structural changes, Al^{+3} Co- ordination, Eh-pH controls and thermodynamic viability have been discussed at length It was shown that direct conversion of feldspar to gibbsite requires special conditions like pH > 10, quick removal of silica etc.

Chemical mass balance of four soluble cations viz: Na, K, Ca and Mg between parent rock, weathered product and ground water was used to calculate the time of weathering in several known bauxite deposits. It was found that the rate of weathering varies widely, from 2.3 metres per million years to as high as 1300 metres per million years, for same element in different rocks and also for different elements in the same rock.

A diffusion controlled computer model for weathering of feldspar to gibbsite was developed. Variables included ground water velocity, concentrations of H^+ and dissolved silica species e.g., H_4SiO_4 and rock size. Effects of these parameters on the time required to attain steady

state were evaluated For diffusion through a fixed distance of the order of 50 cms to 70 m, the time required to attain steady state was found to be 3.17 years to 77689 years In comparison, the time of weathering of a rock having similar thicknesses calculated by mass balance was found to be of the order of few thousand years to few million years. This showed that diffusion plays a significant role only in the initial stage of weathering. After attainment of steady state it is likely to be controlled by the chemical reaction:

$$KAlSi_3O_8 + H^+ + 7H_2O = Al(OH)_3 + K^+ + 3H_4SiO_4$$

amorphous

CONTENTS

LIST OF TABLES

CHAPTER 1

INTRODUCTION AND OBJECTIVES

Weathering is a complex physico-chemical process of mechanical degradation and chemical alteration of primary rock forming minerals. Study of weathering processes is significant both from an academic as well as from an economic point of view. Many minerals of economic importance owe their origin to weathering processes. Notable among these is bauxite.

Weathering reactions are, in general, extremely slow, incomplete and often irreversible (Krauskopf, 1979). One of the reasons for this slowness, is the pressure-temperature conditions at earth's surface (1 atm: pressure and 25^{o}C temperature) under which most of the weathering reactions take place.

It is well known that bauxite deposits are dominated by three minerals, namely, gibbsite, diaspore and boehmite. Bauxite is a product of tropical weathering of feldspathic rocks. Existing views regarding genesis of bauxite can be broadly divided into two groups.

According to one group, weathering of feldspars gives rise to gibbsite, but through an intermediate phase of clays (Valeton, 1972; Grubb, 1979; Kronberg et al., 1979). Another group advocates a direct derivation of gibbsite from feldspars (Mackenzie, 1958 quoted in Keller (1979),

Grubb, 1970; Keller, 1979). There are however, evidence of gibbsitization by both the processes in the same deposit. For example, Sen and Guha (1987) have reported direct gibbsitization of feldspathic rocks in older weathering profiles and desilication of kaolinite to gibbsite in recent profiles.

Opinion is also divided on another aspect. According to some workers, weathering of feldspars involves removal of silica from the structure, leaving behind an Al-rich layer. Subsequent weathering rate depends upon the rate of diffusion of dissolved species through this layer. After a threshold value of silica concentration is reached in the external solution, back reaction is promoted, whereby kaolinite is formed (Wollast, 1967; Dobrovolsky, 1986). The other idea emphasizes total dissolution of feldspar in the associated solution and thereafter recombination of dissolved Al^{+3} and OH^{-} ions to give rise to gibbsite (Keller, 1954; Krauskopf, 1979). A third mechanism favours selective dissolution of feldspar from structurally weak sites such as crystal edges, zone of dislocation etc. However, the Al-rich residue left locally on the feldspar surface is apparently too thin to be detectable by existing instrumental techniques (Berner, 1978; Berner and Holdren, 1978(a) and (b)).

In view of the above lack of agreement on the mechanism of direct gibbsitization among previous workers, this thesis project was carried out with the following

objectives :

1. To review the existing literature regarding direct gibbsitization and gibbsitization through intermediate clay phases

2. To derive the precise physico-chemical constraints under which indirect and direct gibbsitization of feldspars can take place, from thermodynamic stability diagrams.

3. To estimate the time of weathering of a given thickness of parent rock and its replacement by weathered product of equal thickness, by means of chemical mass balance of four soluble cations (viz. Na, K, Ca and Mg) and hence determining the rate of weathering.

4. To utilize the boundary conditions derived above in a diffusion controlled weathering model of feldspar. This highlights the role played by rock size, percolation velocity of ground water etc on the time required to attain steady states for diffusion over fixed distance.

5. To compare steady state time obtained by diffusion mechanism with calculated time of weathering and to draw relevant conclusions therefrom.

CHAPTER 2

WEATHERING OF FELDSPARS

2 1 WEATHERING PROCESS

Most rock forming minerals are out of equilibrium at pressure and temperature conditions in which they are exposed at the earth's surface. Therefore, there is a natural tendency of these minerals to convert to secondary minerals which are more stable in surface pressure and temperature conditions, i.e., 1 atmosphere and 25° C respectively. This process of adjustment is collectively known as weathering. Leaving aside special contribution of biological processes, we can treat weathering as a chemical reaction between minerals and natural agents - principally water.

The reaction of natural waters with rock forming minerals are further accentuated by the presence of dissolved CO_2 gas. A solution of CO_2 is mildly acidic. For example, it can be calculated that water saturated with atmospheric CO_2 at a partial pressure of $10^{-3.5}$ atms· has a pH value about 5.7 at 25° C (Garrels and Christ, 1965). This feebly acidic solution reacts with rock forming minerals by a process of ion-exchange between H^+ from solution and cations from the minerals. Thus Kaolinization of potash Feldspar can be depicted as :

$$2KAlSi_3O_8 + 2CO_2 + 11H_2O = Al_2Si_2O_5(OH)_4 + 2K^+ + 4H_4SiO_4 + 2HC$$

$$2H^+ + 2HCO_3^- = 2CO_2 + 2H_2O$$

$$2KAlSi_3O_8 + 2H^+ + 9H_2O = = Al_2Si_2O_5(OH)_4 + 2K^+ + 4H_4SiO_4$$

On the basis of field observation and laboratory experiments, common mafic and felsic minerals can be arranged in a series, according to their susceptibility to weathering (Krauskopf, 1979).

		Mafic	Felsic
Increasing weatherability	↑	Olivine	Ca-Na feldspar
		Pyroxene	Na-Ca feldspar
		Amphibole	K-feldspar
		Biotite	Muscovite
			Quartz

It is clear from the weatherability series that in a felsic parent rock, feldspars are the more weatherable minerals. Among them, plagioclase feldspars are more weatherable than alkali feldspars. A common weathering sequence is :

Feldspars ⟶ Mica ⟶ Clay ⟶ Gibbsite

Out of these four minerals, gibbsite is a hydroxide and the other three are silicates.

In this thesis we are concerned with formation of

gibbsite by direct weathering of feldspars. It will be, therefore, necessary to discuss the weathering process in terms of crystal structure of the primary feldspars and the intermediate weathering sequence through mica and clay upto gibbsite.

2.2 CRYSTAL STRUCTURE OF FELDSPAR

Feldspars belong to the "Framework type" of silicates, in which SiO_4 tetrahedra are linked to one another by shared oxygens in all four corners, giving rise to a three dimensional network. For convenience of understanding the structure, the atomic arrangement may be conceived as linking of chains in two directions perpendicular to their length, although well defined chains of tetrahedra (as in pyroxenes and amphiboles) are not present (Deer, Howie and Zussman, 1979). The chains themselves are formed by the linking of inclined rings of four tetrahedra (Fig.2.1(a) and 2.1(b)). The repeat distance along the chain axis, i.e., a-crystallographic axis, is about four times the height of a tetrahedron.

From a crystallo-chemical point of view, feldspars can be considered as modifications of quartz. When all four corners of SiO_4 tetrahedron are shared, the formula of the unit cell is Si (4, 1/2 O), i.e, SiO_2 In feldspars, one-fourth of the Si^{+4} positions are substituted by Al^{+3}. So, the formula becomes $Al_{1/4}\ Si_{3/4}\ O_2$ or $AlSi_3O_8$.

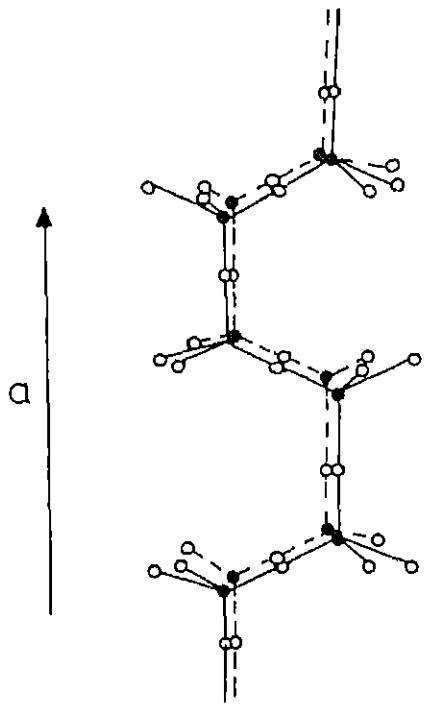

Fig. 2.1(a) Ideal illustration of feldspar chains (after Deer, Howie and Zussman, 1979)

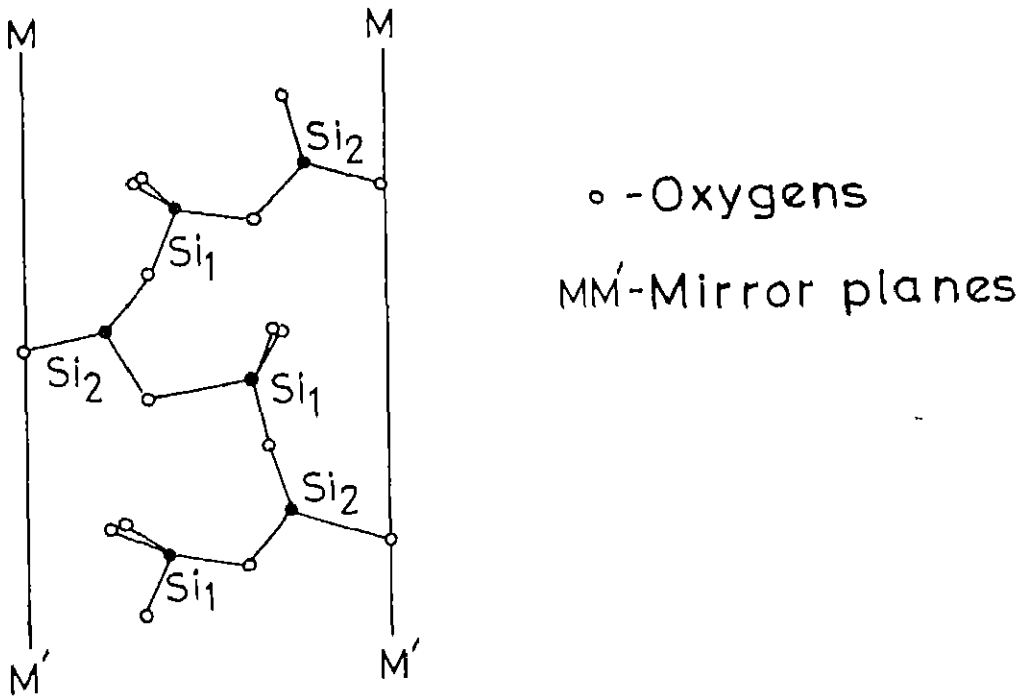

Fig 2.1(b) Part of sanidine ($KAlSi_3O_8$, Monoclinic) structure viewed along normal to (001) (After Deer, Howie and Zussman, 1969)

However, substitution of Al^{+3} for Si^{+4} causes a deficiency of positive charge which is balanced by incorporating cations in the structure. Thus, in potash feldspars, the structural formula is $KAlSi_3O_8$. Similarly, albite is $NaAlSi_3O_8$ Anorthite is $CaAl_2Si_2O_8$ where Ca +2 balances the deficiency caused by substitution of two Al^{+4} ions for two Si^{+4} ions Natural feldspars show solid solution series between these three end member compositions

2.3 CRYSTAL STRUCTURE OF GIBBSITE

The fundamental unit of the structure of gibbsite is a layer of Al^{+3} ions sandwiched between two sheets of close packed hydroxyl ions (Deer, Howie and Zussman, 1979). Each Al^{+3} ion is octahedrally coordinated, i.e , bonded with six neighbouring hydroxyl (OH) ions, three of which are situated above it and three below (part of this arrangement is shown in Fig.2.2(a)). The gibbsite layer may be regarded as built up of octahedron linked laterally by sharing faces. In gibbsite, only two out of three octahedrally coordinated sites are occupied by Al^{+3} .Therefore, the structural formula is : Al^{+3} (6, 1/2 OH) i.e., $Al(OH)_3$ or $Al_2(OH)_6$. A schematic diagram of gibbsite layer is shown in Fig. 2.2(b).

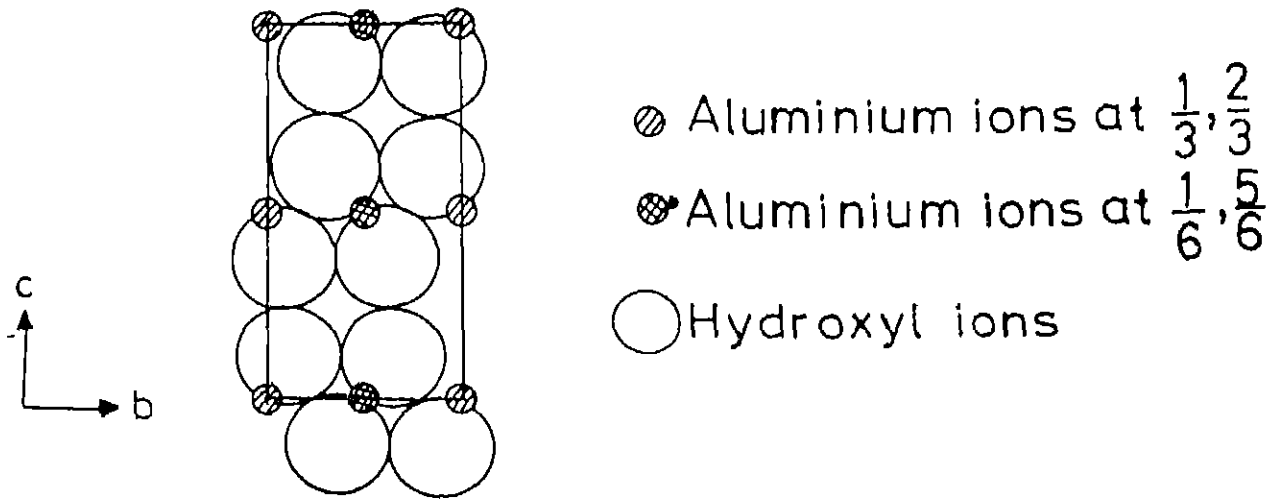

Fig. 2.2(a) Ideal structure of gibbsite projected along X-axis

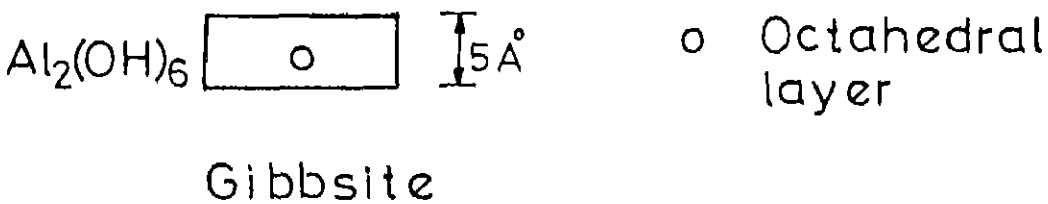

Fig. 2.2(b) Schematic representation of the structural unit of Gibbsite

2.4 CRYSTAL STRUCTURE OF KAOLINITE

Clay minerals and micas are sheet silicates, where the basic structural unit is a silicate sheet formed by linking of three corners of the Si-O tetrahedron leaving the fourth corner free. The structural formula of the building block is therefore Si, (3, 1/2, 0), (1,0), i.e., $(SiO_{5/2})$ or Si_2O_5. This unit has a net negative charge of -2, which is balanced in sheet silicates by a unique linking with modified gibbsite layer having Al^{+3} in octahedral (i.e., six-fold) coordination. For example, in Kaolinite $(Si_2O_5^{-2})$ tetrahedral sheet is linked to one $(Al_2(OH)_4)^{+2}$ octahedral layer in which two out of six OH corners of the gibbsite structure are replaced by oxygen atoms of the tetrahedral sheet (Fig.2.3(a)). Thus, the structural formula of Kaolinite becomes $Al_2Si_2O_5(OH)_4$ or $Al_2O_3 .2SiO_2.2H_2O$. Fig. 2.3(b) shows the schematic representation of Kaolinite structure.

2.5 CRYSTAL STRUCTURE OF MICA

As stated above, micas are also sheet-silicates with $(Si_2O_5)^{-2}$ tetrahedral layers. However, in contrast to Kaolinite, the building block is a three-layered T-O-T structure with one octahedral Al-O layer linked on both sides with tetrahedral Si-O layers. As a result the basic formula of the Mica Group is - $(Si_2O_5)^{-2}$ - $(Al_2(OH)_2)^{+4}$ -

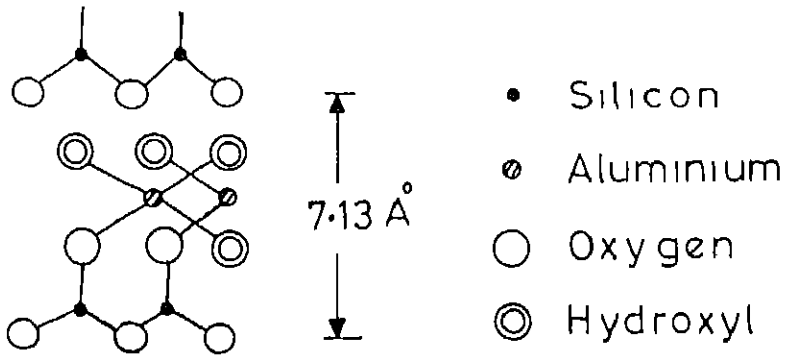

Fig 2.3(a) Structure of kaolinite when viewed along X-axis (after Deer, Howie and Zussman, 1979)

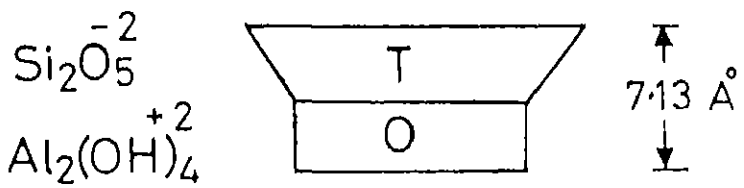

Fig. 2.3(b) Schematic representation of the kaolinite structure

$(Si_2O_5)^{-2}$ or $Al_2Si_4O_{10}(OH)_2$, which actually represents the mineral pyrophyllite. Micas have essentially the pyrophyllite structure with substitution of Si^{+4} by one Al^{+3} ion. To restore charge neutrality, K^+ ion is incorporated in the structure which occupies the interlayer position (Fig.2.4). The overall structural formula of muscovite thus can be written as

$$KAl_2^{VI}(Al^{IV}Si_3)O_{10}(OH)_2$$

IV - Al^{+3} in four fold co-ordination

VI - Al^{+3} in six fold co-ordination

2.6 STRUCTURAL CHANGES DURING WEATHERING

From the above descriptions of minerals, it is clear that the conversion of feldspar to gibbsite through intermediate steps of mica and Kaolinite is in fact a sequential formation of successively simpler Si-O-Si linking in silicates and ultimately formation of an octahedrally coordinated Al-OH structure. For example :

Four corner shared feldspar ⟶ three corner shared mica ⟶ three corner shared kaolinite ⟶ No silica tetrahedra in gibbsite.

There is a corresponding change in Al^{+3} co-ordination also. In feldspars, all the Al^{+3} ions were in tetrahedral coordination. In mica (muscovite), two out of three Al^{+3} ions in the structural unit are octahedrally coordinated. When the sheet structure of mica breaks down to give rise

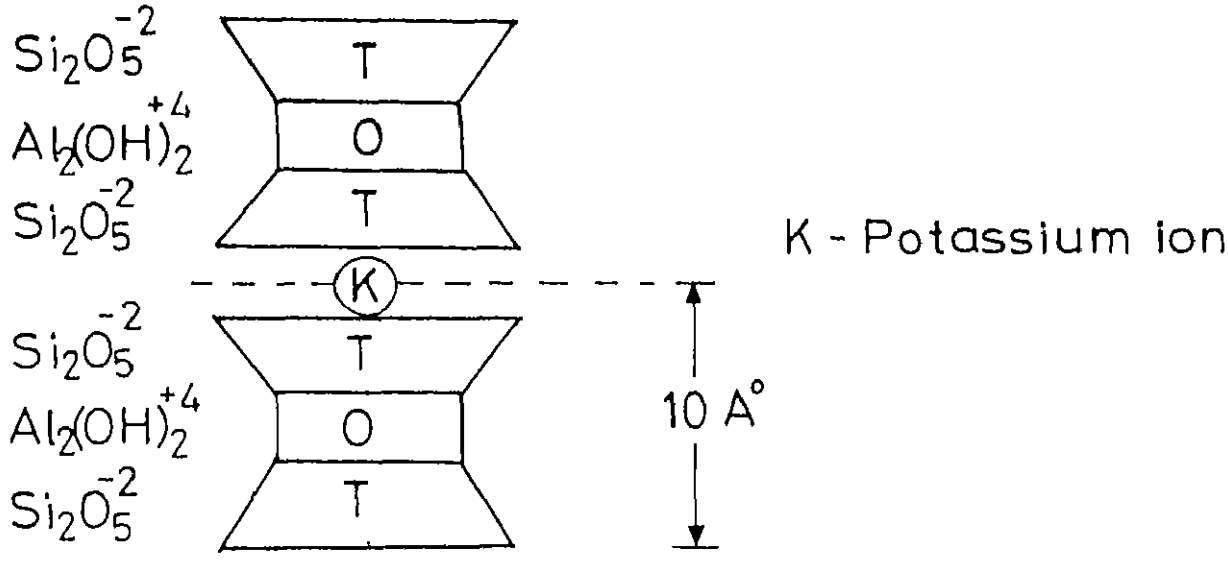

Fig. 2.4 Schematic representation of muscovite structure

to kaolinite, there is a further structural simplification. Two tetrahedral and one octahedrally coordinated layers are now reduced only to one tetrahedral and one octahedral layer. All the Al^{+3} ions present are now octahedrally coordinated. When kaolinite is weathered to yield gibbsite, the two-tier arrangement of octahedral and tetrahedral layers breaks to give way to a single octahedrally coordinated $Al_2(OH)_6$ layer.

The initiation of feldspar weathering takes place by the first surficial exchange of loosely bound K^+ in the structure with H^+ of the water. This renders the lattice weak and subsequent arrangement and adjustments take place in the structure. De Vore (1959) as quoted in Loughnan (1969), has discussed the mechanism of formation of layered-lattice minerals, such as the micas, from feldspar. He pointed out that decomposition of the feldspar structure releases chains which have a certain degree of stability and retain the original Si-Al ordering of the tetrahedra. If these released chains are from the (100) and (010) surfaces of the feldspar, they can polymerize directly into tetrahedral sheets of composition $(Al, Si_3)O_{10}$ Combination with octahedral cations (e.g., Al^{+3}, Mg^{+2}, Fe^{+2} and Fe^{+3}) and K^+ would lead to the formation of clay minerals. However, if the released chains breakdown into individual tetrahedra, aluminium contained therein would be expected to assume its preferred octahedral coordination. In such cases, layered-lattice

silicates requiring at least part of the Al^{+3} in the tetrahedral sheets could not develop

It is pertinent, at this point, to mention that as we proceed from primary feldspar to secondary gibbsite via intermediates like muscovite and kaolinite, there is a successive decrease in Si:Al ratio. In alkali feldspars the ratio is 3.1, in muscovite and kaolinite it is 1 1, while in gibbsite it is zero. Thus, with progression of weathering, there is a progressive loss of not only cations but also silica from the structure. However, if in a particular case, Si Al ratio remains same in both parent and product mineral (e.g., in Anorthite ($CaAl_2Si_2O_8$) to kaolinite ($Al_2Si_2O_5(OH)_4$) or muscovite ($KAl_3Si_3O_{10}(OH)_2$ to kaolinite) there is no silica loss from the parent mineral structure. In certain cases, where there is an increase in Si Al ratio from the parent mineral to the product mineral, silica has to be added in the system to ensure such transformations.

For example :

Anorthite $\longrightarrow$ Ca-montmorillonite

$CaAl_2Si_2O_8$ $\qquad$ $Ca_{.17}Al_{2.33}Si_{3.67}O_{10}(OH)_2$

(Raymahashay, 1984). These relationships are guided by the stoichiometry of weathering reactions in which Al^{+3} is assumed to be immobile and is, therefore, locked up in the parent mineral.

The above mentioned normal sequence of weathering of feldspars to kaolinite and kaolinite to gibbsite has been

recorded in numerous kaolinite and bauxite deposits (Valeton, 1972, Grubb, 1979, Kronberg, et al., 1979; Sen and Guha, 1987). However, weathering of feldspars directly to gibbsite is also recorded and is discussed further in the following paragraphs.

2.7 EVIDENCES IN FAVOUR OF DIRECT GIBBSITE FORMATION

In recent years, quite a number of field evidences brought to light the fact that direct gibbsitization of feldspar does take place in nature. Kaolinite, if present, is only the product of re-silication of gibbsite. One of the earliest examples is that of Arkansas Bauxite Deposits, U.S.A., where frequent preservation of parent rock textures within the bauxite (gibbsite) was noted and conclusions were drawn in favour of direct alteration of feldspar to gibbsite (Mackenzie, 1958 as quoted in Keller (1979). Similar conclusion was also drawn by Grubb (1970) for the bauxites of Mitchell plateau, victoria, Australia, where basaltic (parent rock) textural features were preserved. Keller (1979) studied the Arkansas bauxite samples under scanning electron microscope and provided visual proofs of direct gibbsitic alteration of feldspars Very recently, Sen and Guha (1987) reported feldspar grains altered along the margins, directly to gibbsite, from the East Coast Bauxite Deposits, Orissa, India.

In all the above cases, evidences of direct alteration

of feldspars to gibbsite, bypassing the intermediate kaolinite stage, are overwhelming. From a structural point of view, this is somewhat unusual and enigmatic In the scheme of successive structural simplification through removal of silica and cations, this can be described as a "step-jump", where under certain combination of physico-chemical conditions, complex and tightly packed feldspar structure directly yields simple gibbsite structure.

For this reason, direct gibbsitization of feldspar can be considered as a special case. This thesis work is aimed at the details of special conditions which are needed to weather feldspars directly to gibbsite.

2.8 KAOLINIZATION VERSUS GIBBSITIZATION - WITH REFERENCE TO Al^{+3} CO-ORDINATION.

In contrast to Si^{+4} in alkali silicate solution, which on neutralization changes from six to four fold co-ordination (Iler, 1955), Al^{+3} in alkali aluminate solution changes rapidly from four to six fold co-ordination on falling to pH 0. However, in presence of silicic acid (H_4SiO_4), Al^{+3} in four fold coordination may be stable down to pH3 (Grubb, 1970). Hence, the conclusion follows that at a pH value below 3, when six-fold Al co-ordination is favoured, gibbsite formation is accentuated with rapid removal of silica. When aluminium becomes mobile, it leaves the parent mineral structure to enter the solution

and eventually precipitates as $Al(OH)_3$. Here, role of OH^- ions should be conspicuous in raising the ion activity product of Al^{+3} and OH^- ions above the solubility product of $Al(OH)_3$ (gibbsite), so that gibbsite could precipitate. According to Garrels and Christ (1965), gibbsite formation, unlike kaolinite formation is largely the result of unbuffered rise in pH (due to continuous uptake of H^+ from the solution and removal of silica) during weathering. On the otherhand, if gibbsite were to be formed from kaolinite, it can simply form at any ordinary intermediate pH by desilication and consequent structural rearrangement of kaolinite.

It will be pertinent, at this point, to have a closer look on dependence of aluminium mobility on pH. Fig. 2.5 depicts the stability fields of various species of aluminium. The isoelectric point for the aluminium and aluminate ions is around pH6 On the left hand side of it Al^{+3} is the predominant ion in solution, while on the right hand side of it, $Al(OH)_4^-$ is the predominant ion in solution. Furthermore, at around pH6, $Al(OH)_3$ (gibbsite) has the minimum solubility value. So, the effect of very high or very low pH is to mobilize aluminium effectively from the parent mineral as soluble ions. Once aluminium is in solution, the solution pH should be centred around pH6 in order to have maximum gibbsite precipitated. This sudden change in pH, however, cannot be accounted for with certainty.

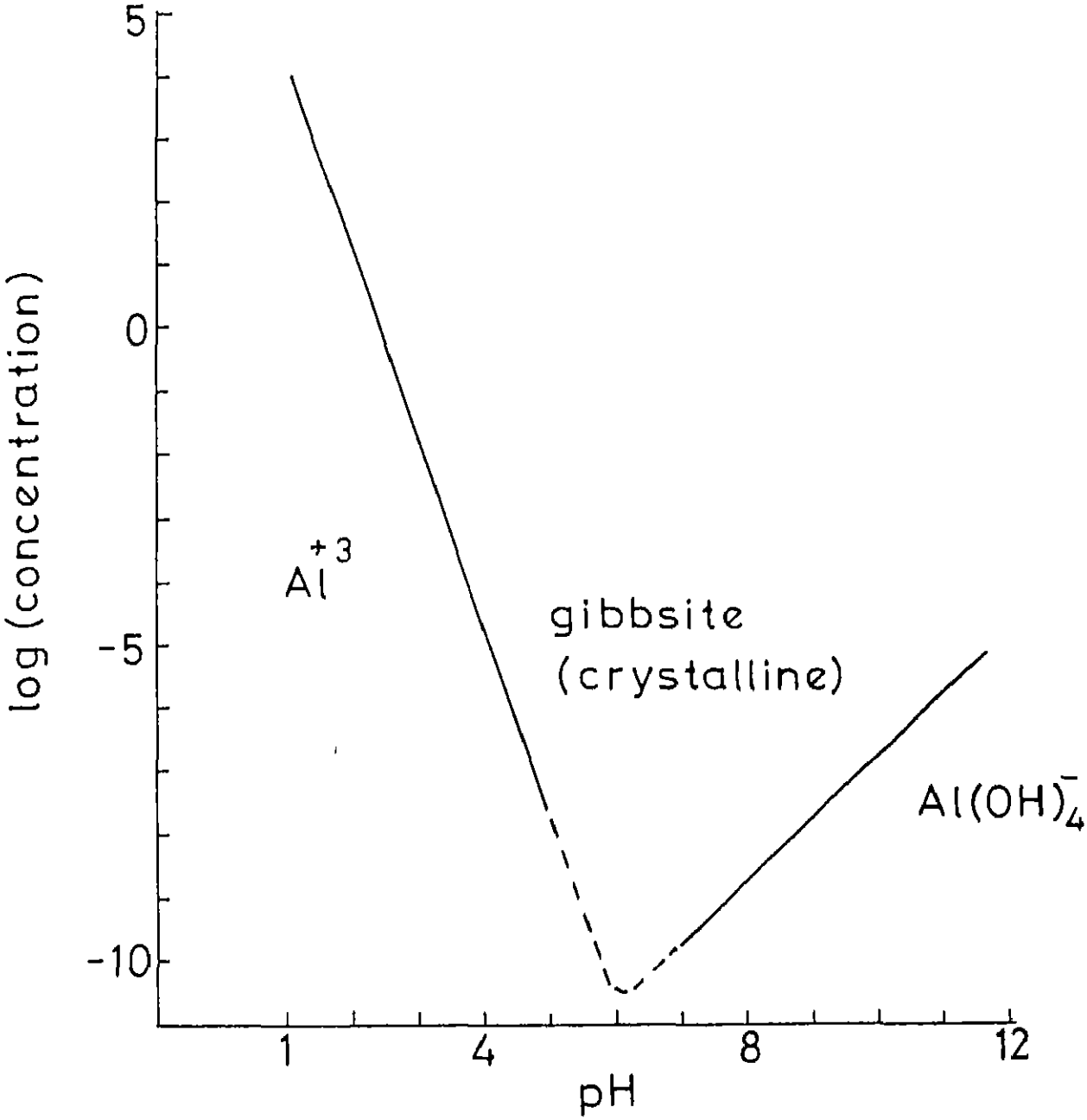

Fig. 2 5 Stability fields of various species of aluminium

All these evidences point towards the fact that with respect to pH range also, direct gibbsitization of feldspars is a special case, which is only possible at a very low or very high pH.

2.9 KAOLINIZATION VERSUS GIBBSITIZATION - WITH REFERENCE TO STABILITY DIAGRAMS

Fig. 2.6 (drawn from the data of Appendix 1) shows the stability relationships among various phases of K-feldspar, kaolinite, muscovite mica and gibbsite. The diagram is, actually, a superposition of stability relationships among members of two systems. One is the system K-feldspar-muscovite mica-kaolinite-gibbsite, all being in crystalline state. The other is the system K-feldspar (crystalline) - muscovite mica (crystalline) - kaolinite (poorly crystalline)-gibbsite (amorphous).

The various phase boundaries are as follows .

1. Equilibrium boundary between crystalline kaolinite and crystalline gibbsite
2 Equilibrium boundary between K-feldspar and crystalline kaolinite
3. Equilibrium boundary between muscovite mica and crystalline kaolinite

1'- Equilibrium boundary between poorly crystalline kaolinite and amorphous gibbsite

2'- Equilibrium boundary between K-feldspar and

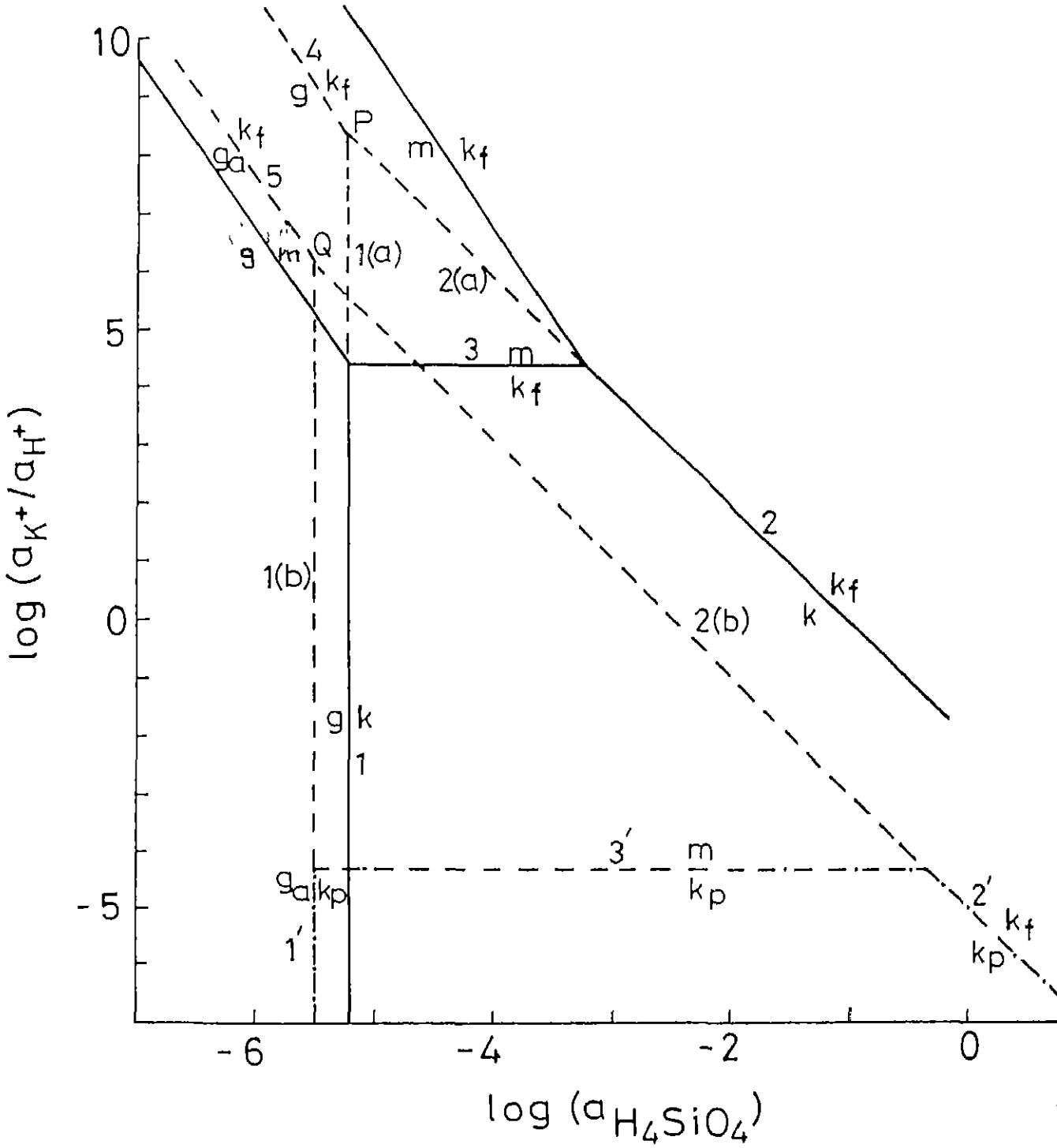

Fig. 2 6 Stability diagram for Gibbsite, kaolinite, Muscovite and K-feldspar at 25°C

K_f - K-feldspar (crystalline)

m - mica (crystalline)
g - crystalline gibbsite
g_a - amorphous gibbsite

k - crystalline kaolinite
k_p - poorly crystalline kaolinite

poorly crystalline kaolinite

3'- Equilibrium boundary between mica and poorly crystalline kaolinite

1(a) - Metastable extension of equilibrium boundary 1

1(b) - Metastable extension of equilibrium boundary 1'

2(a) - Metastable extension of equilibrium boundary 2

2(b) - Metastable extension of equilibrium boundary 2'

Lines 1(a) and 2(a) meet at point P and lines 1(b) and 2(b) meet at point Q.

4 - Metastable equilibrium boundary between K-feldspar and crystalline gibbsite

5 - Metastable equilibrium boundary between K-feldspar and amorphous gibbsite.

It can be seen in the diagram that in both the cases of crystalline and poorly crystalline or amorphous phases, K-feldspar and kaolinite have common boundary and so have kaolinite and gibbsite. This indicates that formation of kaolinite from K-feldspar and gibbsite from kaolinite is thermodynamically predictable This can occur under a wide range of pH variation along with silica removal. On the other hand, nowhere K-feldspar and gibbsite have a stable equilibrium boundary. This rules out the possibility of direct conversion of K-feldspar into gibbsite via stable equilibrium relationship. This, therefore, calls for metastable extensions of relevant phase boundaries, by which, we arrive at two points P and Q as described earlier Lines 4 and 5 start from P and Q respectively.

So, P is the lowest point on the line 4 which furnishes the composition of water, where K-feldspar and gibbsite (both in crystalline phases) are in metastable equilibrium. On the otherhand, Q is the lowest point on the line 5 which furnishes the composition of water, where K-feldspar (crystalline) and amorphous gibbsite are in metastable equilibrium.

At P, $\log \frac{a_{K^+}}{a_{H^+}} = 8.4$ or, $a_{H^+} \frac{a_{K^+}}{a_{H^+}} = 10^{8.4}$ or $a_{H^+} = a_{K^+} \times 10^{-8.4}$

At Q, $\log \frac{a_{K^+}}{a_{H^+}} = 6.2$ or, $\frac{a_{K^+}}{a_{H^+}} = 10^{6.2}$, or, $a_{H^+} = a_{K^+} \times 10^{-6.2}$

Taking the average concentration of K^+ in natural stream water as 2.3 ppm ($= 10^{-4.23}$ m/l) (Mason and Moore, 1982), we get two different values of pH, viz: 12.63 and 10.43 corresponding to P and Q respectively. Both indicate solutions of high alkalinity. This lends support to the contention that direct alteration of K-feldspar to gibbsite takes place at high pH conditions.

In Na- and Ca- systems, however, direct conversion of albite and anorthite to gibbsite is thermodynamically stable. In Na-system (Fig. 2.7, drawn from the data of Appendix 1), the point R lies at the point of intersection of kaolinite-gibbsite and albite-kaolinite equilibrium boundaries This is the lowest point on the equilibrium boundary between crystalline albite and crystalline gibbsite It furnishes composition of water, where crystalline albite and crystalline gibbsite are in stable

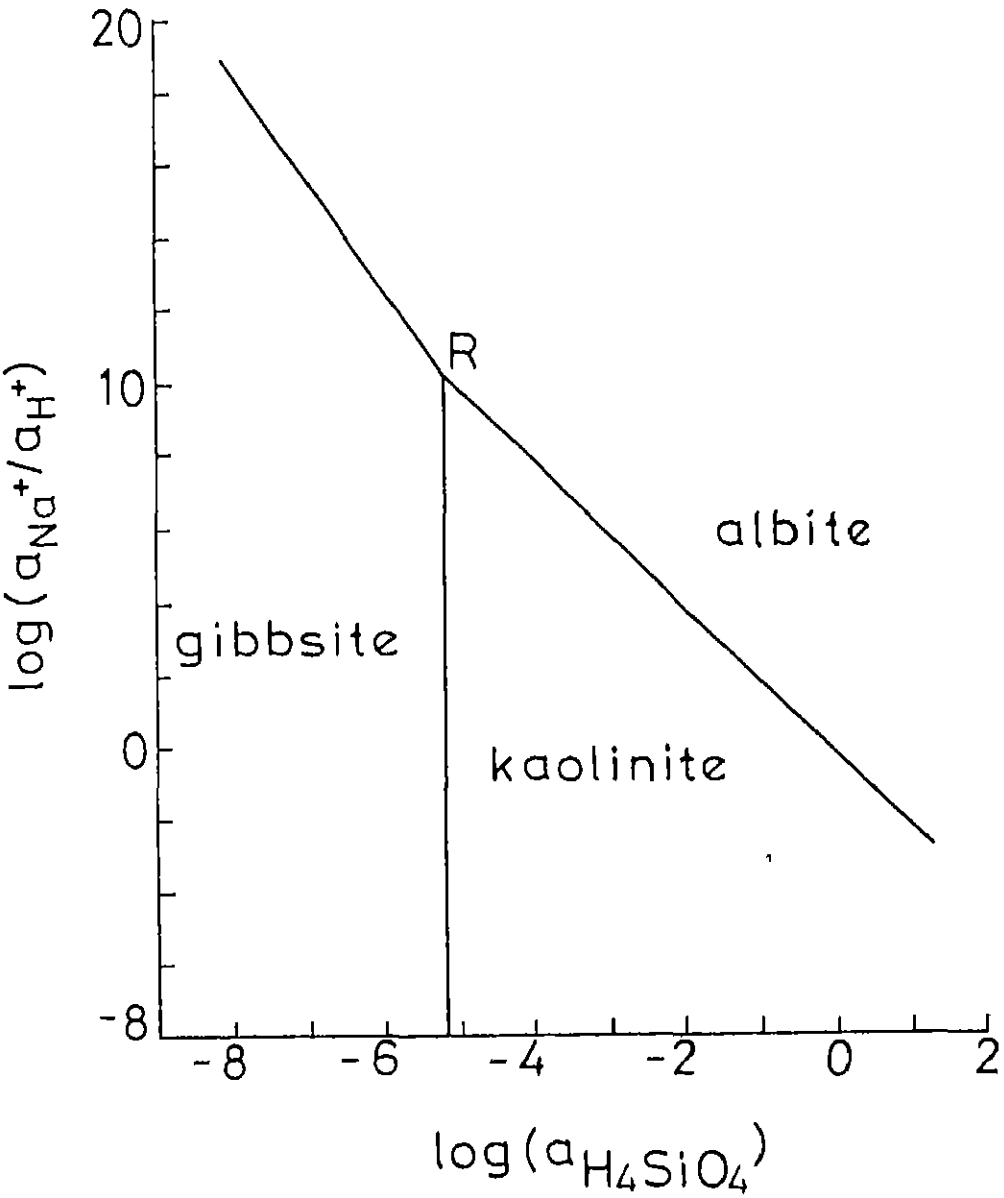

Fig. 2.7 Stability diagram for gibbsite, kaolinite and albite at 25 ^{o} C

equilibrium. Taking the average Na concentration in natural stream water as 6.3 ppm (= $10^{-3.56}$ m/l) (Mason and Moore, 1982), we get the pH of the water as follows

From R, $\log \frac{a_{Na^+}}{a_{H^+}} = 10.20$ $\quad \therefore \frac{a_{Na^+}}{a_{H^+}} = 10^{10.20}$

or, $a_{H^+} = 10^{-3.56} \times 10^{-10.20} = 10^{-13.76}$

$\therefore$ pH = 13.76

In Ca-system (Fig. 2.8, drawn from the data of Appendix 1), the point S lies at the point of intersection of kaolinite-gibbsite and anorthite-kaolinite (all in crystalline state) equilibrium boundaries. This is the lowest point on the equilibrium boundary between crystalline anorthite and crystalline gibbsite. It furnishes composition of water, where crystalline anorthite and crystalline gibbsite are in stable equilibrium. Taking the average Ca concentration in natural stream water as 15 ppm (= $10^{-3.42}$ m/l) (Mason and Moore, 1982), we get the pH of the water as follows .

From S, $\log \frac{a_{Ca^{+2}}}{(a_{H^+})^2} = 17.27$ or, $\frac{a_{Ca^{+2}}}{(a_{H^+})^2} = 10^{17.27}$

or, $(a_{H^+})^2 = 10^{-3.42} \times 10^{-17.27} = 10^{-20.69}$

or, $a_{H^+} = 10^{-10.345}$ $\quad \therefore$ pH = 10.345

In both the above cases, pH values deduced lie in highly alkaline range.

These calculations indicate that direct gibbsitization

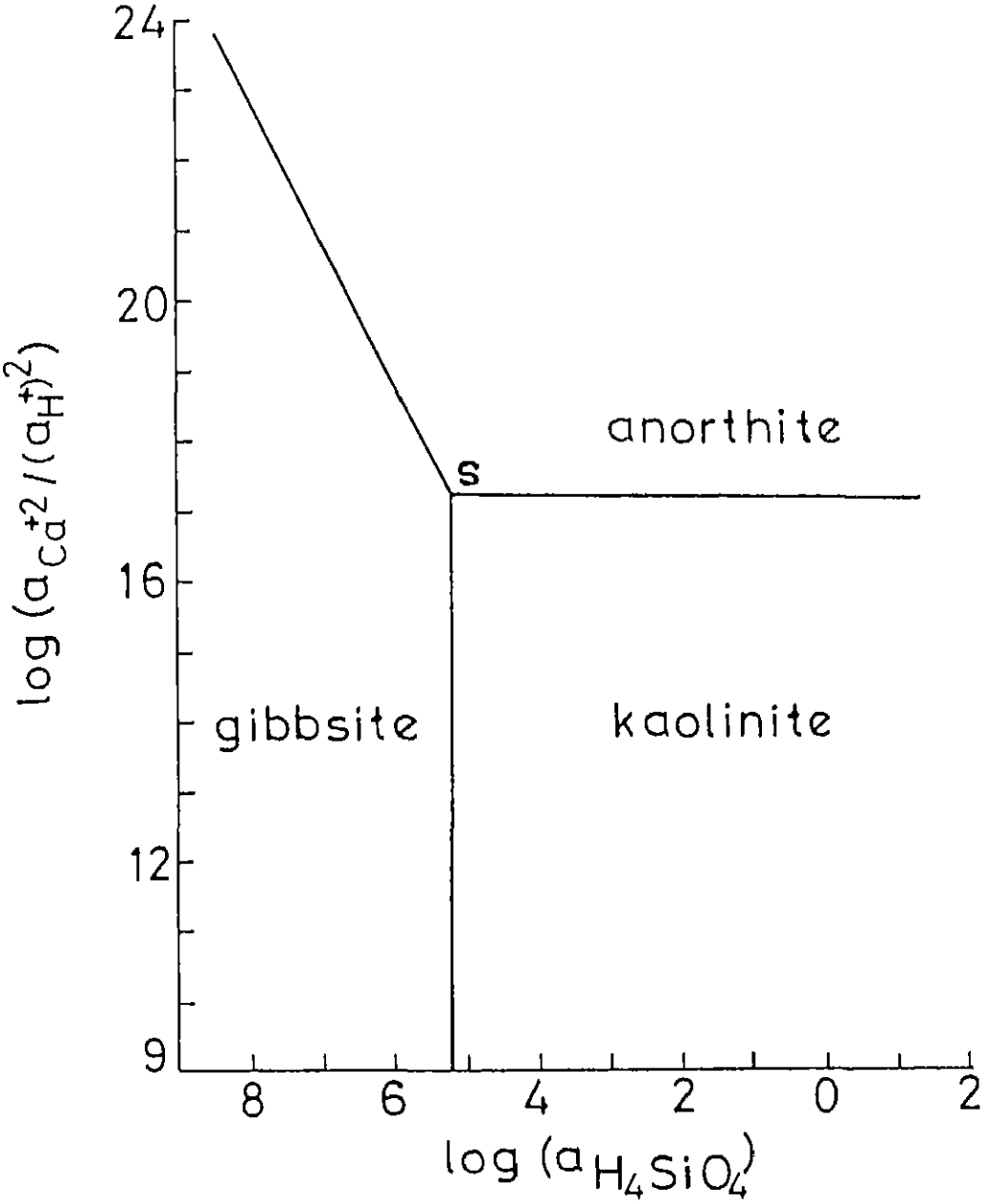

Fig. 2.8 Stability diagram for gibbsite, kaolinite and anorthite at 25°C

of K, Na and Ca-feldspars requires highly alkaline solution pH value While Na and Ca feldspars can be in stable equilibrium with gibbsite, K-feldspar can convert to gibbsite only under metastable equilibrium conditions.

2.10 ROLE OF REDOX POTENTIAL (Eh) IN DIRECT GIBBSITIZATION

Redox potential or "Eh" value of water has a well defined role in the formation of latesites, which are normally associated with bauxites. This is because, higher Eh value helps in oxidizing Fe^{+2} ions to Fe^{+3} state, whereby it is precipitated in the form of $Fe(OH)_3$, and mobility of $Fe(OH)_3$ is much less compared to its ferrous counterpart. On the otherhand, any change in Eh of the solution does not affect Al^{+3} ion and the process of gibbsite formation. These aspects can be illustrated with the help of following diagrams (Fig.2.9(a) and (b)). Fig.2.9(a) shows the iron-stability fields, where it can be observed that the field for ferric iron (Fe^{+3}) lies in the extremely high Eh range. On the contrary, the stability field of gibbsite covers a wide range of Eh from positive to negative (Fig.2.9(b)).

Furthermore, evidences in favour of gibbsite formation both under high and low Eh values can be found. For example, Keller et al (1954), as quoted in Grubb (1970), has found gibbsite formed under oxidizing conditions. On the otherhand, in the Gippland Bauxite Deposit, Australia,

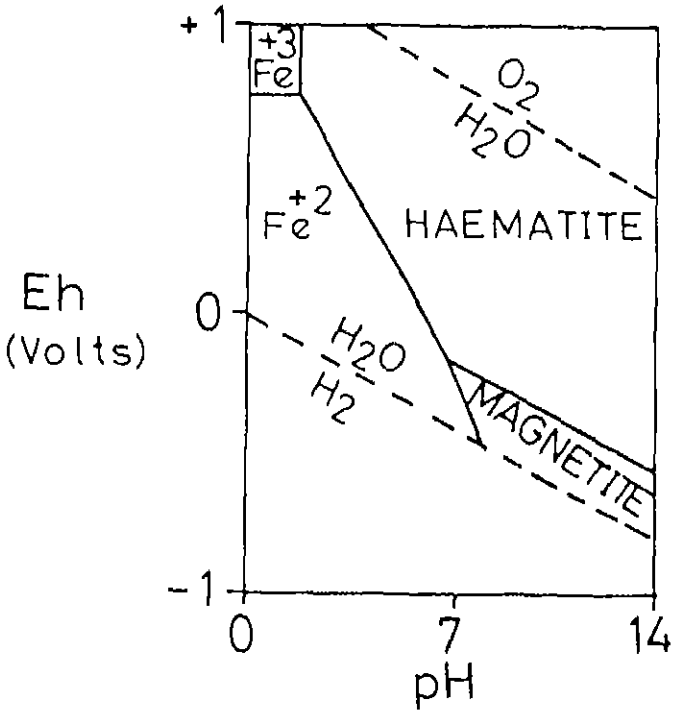

Fig 2.9(a) Eh-pH diagram for the system Iron-water at 25°C, after Garrels and Christ (1965) (from Petersen, 1971)

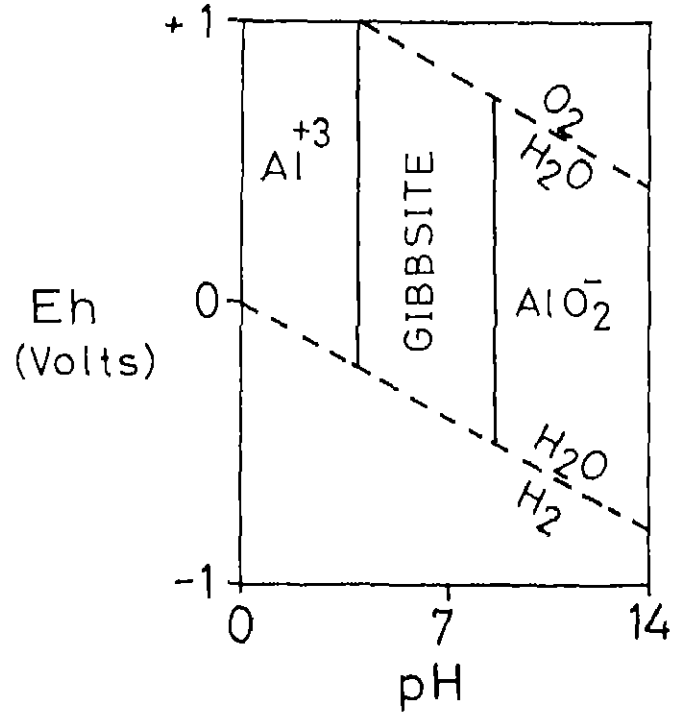

Fig. 2.9(b) Eh-pH diagram for the system Aluminium-water at 25°C, after Pourbaix, 1966 (from Petersen, 1971)

bauxite is in association with small amount of residual sulphide minerals, which indicates a reducing environment (Grubb, 1970).

Besides the aforesaid chief factors, other factors like dense vegetation cover with intense rainfall (available in tropics), rugged topography and higher atmospheric temperature are also required to promote direct gibbsitization. Rugged topography helps in quick drainage of silica. Certain tropical forests can extract significant amount of silica from soil, thus help in silica removal (Lovering, 1959, quoted in Sen and Guha, 1987). According to Okamoto et al (1957) as quoted in Sen and Guha, 1987, solubility of silica gel and the rate of its dissolution increase three-fold from temperature 0^{o} to $58^{o}C$ Thus, higher ambient temperature also facilitates quick silica removal. Sen and Guha (1987) also emphasized the roles played by vegetation, rainfall and rugged topography in the direct gibbsitization of feldspathic rocks in the East Coast Bauxite Deposit of India.

To sum up, following points seem most important in considering direct gibbsitization of feldspars as a special case as opposed to the existence of an intermediate kaolinite stage :

1. A sudden jump in the sequence of gradual simplification of compact feldspar structure
2. Tendency of aluminium to change into six-fold co-ordination (from four-fold co-ordination in feldspars) at

very low (< 4) and at very high (> 10) pH solutions.

3. Between pH values 4 and 10, aluminium practically remains immobile. Only at pH values outside this range, aluminium gains mobility in the form of water soluble ions and gibbsite can form from such a solution by precipitation at pH near the isoelectric point of aluminous species.

4 Redox potential of water does not appear to play any conspicuous role in gibbsitization.

5. Very high rainfall, good drainage and ample vegetation cover (as available in tropical regions) are needed in order to flush out silica and promote direct formation of gibbsite from parent feldspar. A fluctuating water-table can serve as a possible mode of silica removal.

6. The following flow sheets furnish transformation relationships among different varieties of feldspare, mica, kaolinite and gibbsite, i.e., different pathways of gibbsite as well as kaolinite formation are shown. In all these transformations, at indicated pH, aluminimum is always considered to be immobile.

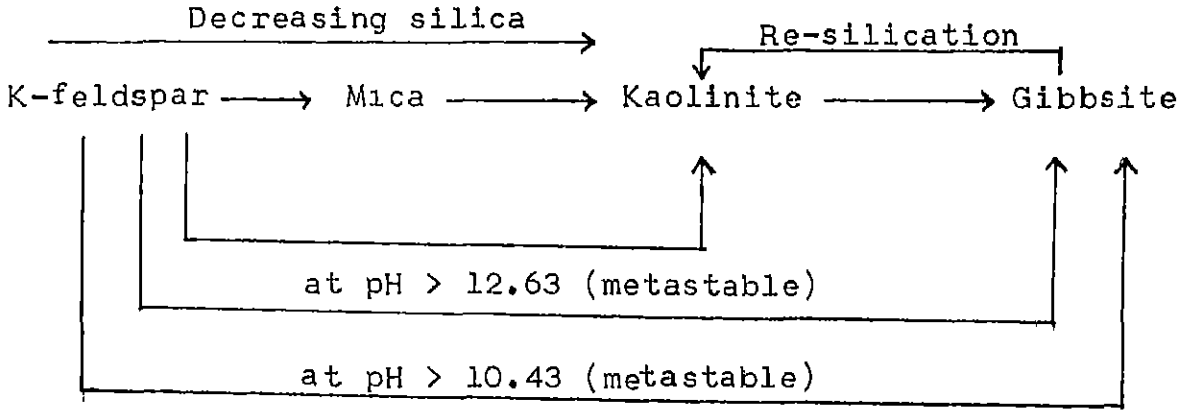
Decreasing silica
Re-silication
K-feldspar
Mica
Kaolinite
Gibbsite
at pH > 12.63 (metastable)
at pH > 10.43 (metastable)

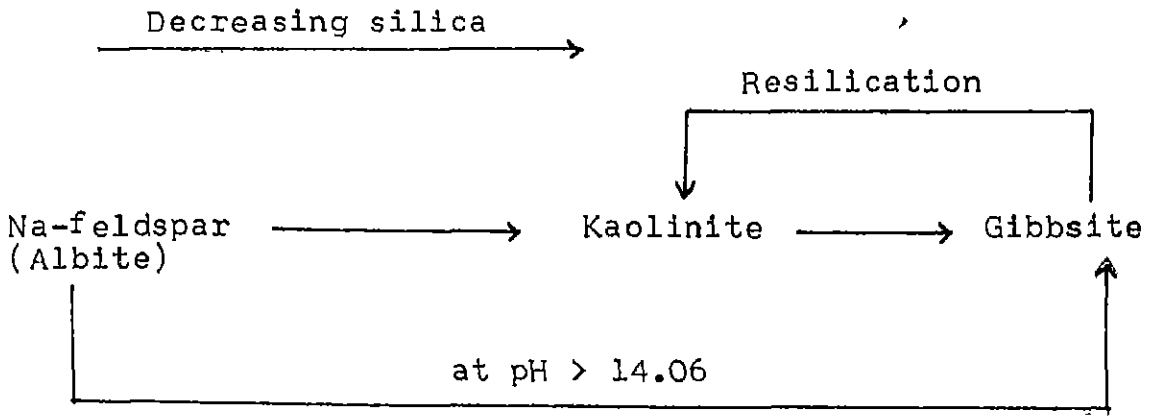
Decreasing silica
Resilication
Na-feldspar
(Albite)
Kaolinite
Gibbsite
at pH > 14.06

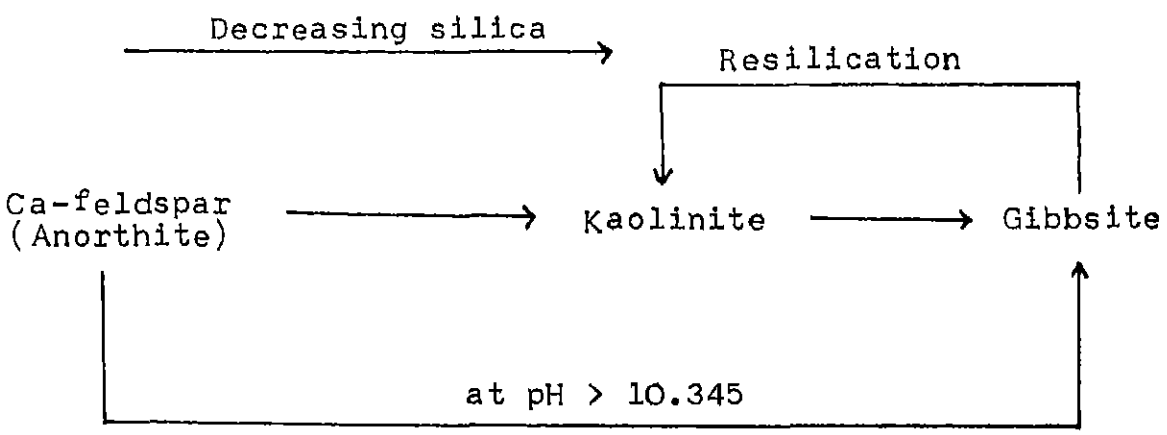
Decreasing silica
Resilication
Ca-feldspar
(Anorthite)
Kaolinite
Gibbsite
at pH > 10.345

CHAPTER 3

TIME OF WEATHERING

In the previous chapter, we have discussed the physico-chemical conditions for direct gibbsitization of feldspar. In the present chapter, we set out to investigate another quantitative aspect of feldspar weathering - that is - time. It is always interesting, both from an academic as well as from a practical point of view, to know the length of time involved to convert a given thickness of rock to its weathered product. Data from some known occurrences of bauxite/laterite are discussed below.

3.1. Paragominas Bauxite Deposit, Brazil

The feldspathic rocks have been weathered to bauxite in the Paragominas Bauxite Deposit, Brazil (Kronberg et al. 1979). The time of weathering can be estimated from a consideration of chemical mass balance of four highly soluble cations, viz. Na, K, Ca and Mg. The relevant data for these elements are presented in Table 3 1

Constraints : Average annual rainfall = 1000 m.m. = 1 m

Problem : To find the time required to leach Na, K, Ca and Mg from a 2.2 m column of average crustal rock and convert into a 2.2 m thick laterite/bauxite profile. Here, the

TABLE 3.1

Element	Average amount in Paragominas Bauxite Deposit ($\mu g.g^{-1}$)	Average amount in earth's crust $\mu g.g^{-1}$	Average amount in world river water $\mu g.g^{-1}$ (2)
Na	150 (1)	22700	6 3
K	800	18400	2.3
Ca	800	46600	15 0
Mg	2500	27640	4.1

Data from Kronberg et al (1979)

(1) value after intense leaching

(2) Data from Mason and Moore (1982)

thickness 2.2 m is the thickness of bauxite deposit in the Paragominas deposit.

Procedure

1) For Na ·

Area of the base of the rock column = 1 m^2 (say)

Height of the rock column = 2.2 m

Therefore, volume of the rock column = 1x2.2 m^3

= 2.2×10^6 cm^3

Density = 2.7 gm/cm^3

Therefore, weight of the rock column = $2.7 \times 2.2 \times 10^6$ gm

= 5.94×10^6 gm

Na content in parent rock = 22700 $\mu g.g^{-1}$

Na content in leached rock = 150 $\mu g.g^{-1}$

Therefore, amount of Na which contributes to water = (22700-150)

= 22550

= 22550×10^{-6} gm/gm of rock

Therefore, total Na contributed by a 2.2 m column of rock

= $5.94 \times 10^6 \times 22550 \times 10^{-6}$ gm

= 0.134×10^6 gm

In water, Na content = 6.3×10^{-6} gm/gm of water

So,

6.3×10^{-6} gm of Na is in 1 gm of water

Therefore, 0.134×10^6 gm of Na is in

0.021×10^{12} gm of water

= 0.021×10^{12} cm^3 of water

In 1 year, total volume of water through rainfall

$$= 1 \text{ m} \times 1 \text{ m}^2 = 1\text{m}^3 = 10^6 \text{ cm}^3$$

Therefore, time required for weathering

$$= 0.021 \times 10^{12} / 10^6 \text{ years}$$

$$= 0.021 \text{ m.y.}$$

ii) For k

By the approach as before, weight of a 2.2 m rock column = 5.94×10^6 gm

K content in the parent rock = 18400 $\mu g \cdot g^{-1}$

K content in the leached rock = 800 $\mu g \cdot g^{-1}$

Therefore, amount of K which is contributed to water

= (18400-800) μg/gm of rock

= 17600×10^{-6} gm/gm of rock

Total K contributed by a 2.2 m column of rock

= $5.94 \times 10^6 \times 17600 \times 10^{-6}$ gm

= 0.105×10^6 gm

In water, K content = 2.3×10^{-6} gm/gm of water

So, 2.3×10^{-6} gm of K is in 1 gm of water

Therefore, 0.105×10^6 gm of K is in

0.0456×10^{12} gm of water

= 0.0456×10^{12} cm^3 of water

In 1 year, total volume of water by rainfall

$= 1\ m \times 1\ m^2 = 1\ m^3 = 10^6\ cm^3$

Therefore, time required for weathering

$= 0.0456 \times 10^{12} / 10^6$ years

$= 0.0456$ m.y.

$= 0\ 046$ m y.

iii) For Ca

As before, weight of a 2.2 m column of parent rock

$= 5.94 \times 10^6$ gm

Ca content in parent rock = 46600 $\mu g . g^{-1}$

Ca content in leached rock = 800 $\mu g . g^{-1}$

Therefore, Ca contributed to water

= (46600-800) μg /gm of rock

$= 45800 \times 10^{-6}$ gm/gm of rock

Therefore, total Ca contributed by 2.2 m rock column

$= 5.94 \times 10^6 \times 45800 \times 10^{-6}$ gm

$= 0.272 \times 10^6$ gm

In water, Ca content = 15 μg /gm of water

So,

15×10^{-6} gm of Ca is in 1 gm of water

Therefore, 0.272×10^6 gm of Ca is in

0.018×10^{12} gm of water

$= 0.018 \times 10^{12}$ cm^3 of water

In 1 year, total volume of water by rainfall

$= 1\ m^3 = 10^6\ cm^3$

Therefore, time required for weathering

$= 0.018 \times 10^{12} / 10^6$ years

$= 0.018 \times 10^6$ years

$= 0.018$ m.y.

iv) For Mg ·

As before, weight of a 2.2 m column of parent rock

$= 5.94 \times 10^6$ gm

Mg content in parent rock = 27640 µg/gm of rock

Mg content in the leached crust = 2500 µg /gm of rock

Amount of Mg contributed to water

= (27640-2500) µg/gm rock

= 25140 µg/gm of rock

$= 25140 \times 10^{-6}$ gm/gm of rock

Therefore, total Mg contributed by a 2.2 m high column of parent rock

$= 5.94 \times 10^6 \times 25140 \times 10^{-6}$ gm

$= 0.15 \times 10^6$ gm

In water: Mg content = 4.1 µg /gm of water

$= 4.1 \times 10^{-6}$ gm/gm of water

So,

4.1×10^{-6} gm of Mg is in 1 gm of water

Therefore, 0.15×10^{6} gm of Mg is in

0.0366×10^{12} gm of water

$= 0.0366 \times 10^{12}$ cm^3 of water

In 1 year, total volume of water by rainfall

$= 1\ m^3 = 10^6\ cm^3$

Therefore, time required for weathering

$= 0.0366 \times 10^{12} / 10^6$ years

$= 0.0366 \times 10^6$ years

$= 0.0366$ m.y.

$= 0.037$ m.y.

The above calculations of time of weathering can be listed below . (Table 3.2)

From the above calculations, it can be seen that the time required for leaching of a 2.2 m high column of crustal rock to give rise to a deposit of laterite/bauxite has a narrow range. In this case, this range lies between 0.018 to 0.046 m.y. This, for all practical purposes, assigns the time required for weathering of a 2.2 m thick crustal rock at the Paragominas deposit, between 0.02 to 0.05 million years.

With the availability of accurate field data, this simple technique can be used in other cases also, to have an idea of the time involved in the process of weathering.

TABLE 3.2

For element	Calculated time of weathering (m.y.)
Na	0.021
K	0.046
Ca	0.018
Kg	0.037

3.2. East Coast Bauxite Deposit, India

In the present section, we undertake another case study, where the relevant data are more accurate because composition of weathered rock and ground water are also available. The deposit in the "East Coast Bauxite Deposit", of Orissa, India. The particular areas of interest are Pottangi and Panchpatmali villages of Koraput district. Sen and Guha (1987) conducted a detailed study of the mature weathering profile developed over a khondalitic parent rock From surface, upto a depth of about 21 m, they delineated a zone - the so called "laterite-bauxite" zone, where according to them, evidences in favour of direct in situ gibbsitization of Khoudalite are plenty. From a depth of 21 m upto a depth of about 70 m, the zone is called "saprolite" zone. This is also a zone of weathered/partially weathered material where evidence of directly altered gibbsite is less and amount of clay is predominant. Below this zone, lies the unaltered parent rock (Khondalite). In the subsequent calculations, we take the thickness of weathered zone as 70 m, upto the contact between the saprolite zone and unaltered parent rock.

Constraints :

Average annual rainfall = 1.6 m = 1600 mm

Depth of weathered zone below surface (i.e , depth taken

TABLE 3 3

Element	Average amount in parent rock (khondalite) ($\mu g.g^{-1}$)	Average amount in bauxite bearing weathered profile ($\mu g.g^{-1}$)	Average amount in local ground water from bauxite bearing horizons ($\mu g.g^{-1}$)
Na	15525 74	1990.75	0.537
K	47646.50	371.08	0.184
Ca	3466.00	tr	0.868
Mg	2133.81	tr	0.433

for calculations) = 70 m

The data for the four elements are presented in Table 3.3.

All the data are from Sen and Guha (1987). Except ground water analyses, all other values have been recalculated from percentage analyses.

Procedure for determination of time of weathering :

1) For Na

Area of the base of the rock column = 1 m^2 (say)

Height of the rock column = 70 m

Therefore, volume of the rock colum

$$= 70 \text{ m} \times 1 \text{ m}^2 = 70 \text{ m}^3$$

$$= 70 \times 10^6 \text{ cm}^3$$

Taking average density of the rock to be about 2.7 gm/cm^3,

weight of the rock column = $2.7 \times 70 \times 10^6$ gm

Now,

Na content of the parent rock = 15525.74 $\mu g \cdot g^{-1}$

Na content of the leached rock = 1990.75 $\mu g \cdot g^{-1}$

Therefore, amount of Na contributed to water

$$= (15525.74 - 1990.75)\ \mu g \cdot g^{-1} \text{ of rock}$$

$$= 13534.99 \mu g \text{ /gm of rock}$$

$$= 13534.99 \times 10^{-6} \text{ gm/gm of rock}$$

Therefore, Na contributed by a 70 m column of parent rock

$$= 2.7 \times 70 \times 10^6 \times 13534.99 \times 10^{-6} \text{ gm}$$

$$= 2.558 \times 10^6 \text{ gm}$$

In ground water, Na content = 0 537 $\mu g \cdot g^{-1}$

$$= 0.537 \times 10^{-6} \text{ gm/gm of water}$$

So,

0.537×10^{-6} gm of Na is in 1 gm of water

Therefore, 2.558×10^{6} gm of Na is in

4.763×10^{12} gm of water

$= 4.763 \times 10^{12}$ cm^3 of water

In 1 year, total volume of water through rain fall

$= 1.6 \times 1$ m^3 $= 1.6 \times 10^{6}$ cm^3

Therefore, time required

$= 4.763 \times 10^{12} / 1.6 \times 10^{6}$ years

$= 2.977 \times 10^{6}$ years

= 2.977 million years (m.y.)

3.0 m.y.

ii) For K

By the procedure shown as before, weight of a 70 m high column of khondalite = $2.7 \times 70 \times 10^{6}$ gm

Now,

K content of the parent rock (khondalite) = 47646.50 $\mu g.g^{-1}$

K content of the leached rock = 371.08 $\mu g.g^{-1}$

Therefore, amount of K contributed to water

= (47646.50-371.08) $\mu g.g^{-1}$

= 47275.42 μg/gm of rock

= 47275.42×10^{-6} /gm of rock

Therefore, total contributed by a 70 m column of parent rock = $2.7 \times 70 \times 10^{6} \times 47275.42 \times 10^{-6}$ gm

= 8.935×10^{6} gm

In ground water, K content = 0.184 $\mu g.g^{-1}$

= $0\ 184 \times 10^{-6}$ gm/gm of water

So,

$0\ 184 \times 10^{-6}$ gm of K is in 1 gm of water

Therefore, $8\ 955 \times 10^{6}$ gm of K

$48\ 56 \times 10^{12}$ gm of water

= 48.56×10^{12} cm^3 of water

In 1 year, total volume of water through rainfall

= 1.6x1 m^3 = 1.6×10^{6} cm^3

Therefore, time required = $48.56 \times 10^{12} / 1.6 \times 10^{6}$ years

= 30.35×10^{6} years

= 30.35 m.y.

iii) For Ca .

As before, weight of the 70 m column of khondalite

= $2.7 \times 70 \times 10^{6}$ gm

Now,

Ca content of the parent rock (khondalite) = 3466.00 $\mu g.g^{-1}$

Ca content of the leached portion i.e., bauxite material = 0 (actually it was reported to be "trace" in amount, which can be neglected for the present calculation)

Therefore, amount of Ca contributed to water = 3466 $\mu g.g^{-1}$

= 3466×10^{-6} gm/gm of rock

Therefore, total amount of Ca contributed by 70 m column of parent rock $= 2.7 \times 70 \times 10^{6} \times 3466.00 \times 10^{-6}$ gm

$= 0.655 \times 10^{6}$ gm

In water, Ca content $= 0.868\ \mu g \cdot g^{-1}$

$= 0.868 \times 10^{-6}$ gm/gm of water

So,

0.868×10^{-6} gm of Ca is in 1 gm of water

Therefore, 0.655×10^{6} gm of Ca is in

0.7546×10^{12} gm of water

$= 0.7546 \times 10^{12}$ cm^3 of water

In 1 yr., total volume of water by rainfall

$= 1.6 \times 1 \times 10^{6}$ cm^3

$= 1.6 \times 10^{6}$ cm^3

Therefore, time required $= 0.7546 \times 10^{12} / 1.6 \times 10^{6}$ years

$= 0.47 \times 10^{6}$ years

$= 0.47$ m.y.

iv) For Mg

As before, weight of a 70 m column of Khondalite

$= 2.7 \times 70 \times 10^{6}$ gm

Now,

Mg content in parent rock (khondalite) $= 2133.81\ \mu g \cdot g^{-1}$

Mg content in leached bauxite portion = 0 (reported to

be "trace" in amount)

Therefore, amount of Mg contributed to water

$= 2133\ 81\ \mu g.g^{-1}$

$= 2133\ 81 \times 10^{-6}$ gm/gm of rock

Therefore, total amount of Mg contributed by the 70 m column of parent rock $= 2.7 \times 70 \times 10^{6} \times 2133.81 \times 10^{-6}$ gm

$= 0\ 4033 \times 10^{6}$ gm

In water, Mg content $= 0.433\ \mu g.g^{-1}$

$= 0.433 \times 10^{-6}$ gm/gm of water

So, 0.433×10^{-6} gm of Mg is in 1 gm of water

Therefore, 0.4033×10^{6} gm of Mg is in

$0\ 9314 \times 10^{12}$ gm of water

$= 0.9314 \times 10^{12}$ cm^3 of water

Now, in 1 yr, total amount of water by rainfall

$= 1.6 \times 1 \times 10^{6}$ cm^3

Therefore, time required $= 0.9314 \times 10^{12} / 1.6 \times 10^{6}$ years

$= 0.5821 \times 10^{6}$ years

$= 0.5821$ m.y.

0.58 m.y.

So, on the basis of geochemical mass balance of four common soluble cations, the time required to weather a 70 m high column of khondalitic rock and to replace it by a column of

TABLE 3.4

For element	Calculated time (in million years)
Na	3.0
K	30.35
Ca	0.47
Mg	0.58

bauxite and clays of the same height can be listed below (Table 3.4)

However, in all these estimates, we have considered that all the water furnished by rain has infiltrated below. This is, however, not true as surface run off will constitute a large part of the total rain fall. Thus, effectively our age estimates are underestimates. The actual time of weathering will be more than what has been obtained These can be calculated if reliable data on percentage percolation are available

DISCUSSION

From Table 3.4, it can be seen that the age of weathering, for same thickness (70 m), calculated on the basis of four soluble cations vary among themselves. For Ca, it is least, being 0.47 m.y. while for K. it is largest, being equal to 30.35 m.y. so, the question that naturally arises, why is this discrepancy?

As the measurements of concentrations were carried out by Sen and Guha (1987) with utmost caution, inaccuracy of data cannot be a possible answer.

The explanation involves the aspect of relative mobility. Sen and Guha (1987) have measured the relative mobilities of all the cations by the ratio :

$$\text{Relative mobility} = \frac{\% \text{ cation in ground water}}{\% \text{ cation in average khondalite of the area}}$$

TABLE 3.5

Element	Relative mobility in ground water	Time of weathering (m.y.)
Na	3 495	3.0
K	0.445	30.35
Ca	20.00	0.47
Mg	19.295	0.58

The average relative mobilities for Na, K, Ca and Mg in ground water samples of Pottangi and Panchpatmali areas are presented below, along with the time of weathering furnished by each ion, in table 3.5

From the above table, it can be seen that the relative mobilities are inversely proportional to the "time" furnished by corresponding ions. This probably holds the key to the solution of the problem of time-discrepancy.

It is well known that mobility of cations depend on two factors

(a) the way a cation is bound up in a mineral mineral and the mineral stability, and

(b) rate of precipitation after a cation is released from the parent mineral due to weathering. With these, another factor can be coupled in order to get the true magnitude of relative mobility. This is the retention of ions in the system.

Three out of the above four ions, i.e., Ca, Mg and Na are released from their parent minerals more easily than K This is because, a ferro-magnesian mineral or calcic plagioclase has higher weatherability than that of potash feldspar. Moreover, the present case is an open system, where ground waters are collected from flowing springs. Hence, it is plausible to argue that at a certain point of time of weathering, there are much more quantity of Ca, Mg and Na in ground water, than K. Again among Ca, Mg and Na,

Ca and Mg exceed the quantity of Na. This is evidenced by the values of their relative mobilities in water. However, as the system is an open one, more and more Ca, Mg and Na are irretrievably lost compared to K Thus we get lower "time-values" by Ca, Mg and Na but significantly higher value by K This contention leads to the fact that the concept of geochemical mass balance seems more applicable in case of the balance of K than the other three ions, in this case Hence, the time required to weather a 70 m column of khondalite seems to be around 30 m.y.

With a different reasoning, Sen and Guha (1987) put the age of the laterite-bauxite duricrust as 50 $\pm$ 5 m.y. Their arguments are entirely qualitative and speculative. Hence, the age determined on the basis of K seems more acceptable as the real time of formation of a 70 m thick weathered profile.

3. 3. Evidence from Microscopic view, East Coast Bauxite

In this section, we will be applying the same principle as shown in Section 2 in order to calculate time of weathering in a much smaller scale. The principle of chemical mass balance is equally applicable in case of weathering of individual grains of feldspars. Figure 3.1 shows a single crystal of feldspar which has been altered to gibbsite directly, along its margins (figure from Sen and Guha, 1987). Now, from the principle of chemical mass

TABLE 3.6

For element	Calculated time (years)
Na	4.63
K	46 82
Ca	0.725
Mg	0.9

balance it follows that other factors remaining constant, the length of time furnished by each element is proportional to the thickness of weathered layer. We can directly apply this principle in the estimation of time of weathering of a single feldspar crystal. Fig 3.1 shows the altered layer in thin section. For accuracy, this layer of gibbsite is measured in four places and the average thickness is taken for calculation

Average thickness = 0 81 cm

Magnification = 75 times

Therefore, actual thickness= 0.81 cm/75 = 0.0108 cm

The procedure to obtain the time of weathering is illustrated below for K only. For other ions procedure is exactly similar.

In the previous section, we have obtained the time for weathering of a 70 m thick parent rock as 30.35 m.y., i.e., 30.35x10 years on the basis of K-leaching.

For weathering upto a thickness of 70 m, required time is

30.35×10^6 years

For weathering upto a thickness 0.0108 cm, required time

= 46.82 years.

Table 3.6 shows the time furnished by each ion, obtained by the procedure shown above.

Now, by the same arguments as have been outlined in Section

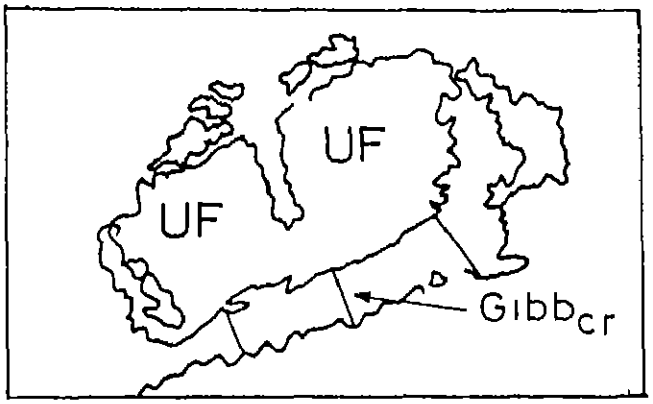

UF - Unaltered feldspar

Gibb$_{cr}$ - Cryptocrystalline gibbsite

Fig. 3.1 Feldspar crystal replaced by cryptocrystalline gibbsite along margins (X75) (After Sen and Guha, 1987)

2, we can accept the time furnished by K

So, the time required to create a 0 0108 cm thick band of gibbsite around the feldspar grain seems to be around 47 years, in the East Coast Bauxite Deposit, Orissa, India, (Pottangi and Ponchpatmali plateau areas) This fact can be schematically represented by the diagram shown in Fig 3.2.

3.4 KARNATAKA BAUXITE DEPOSIT, INDIA

Precambrian granitic gneisses (Tonalite gneisses) have extensively weathered to laterite-bauxite profiles, in the South Kanara district of Karnataka (Khanadali and Devaraju, 1987) There are evidences of development of gibbsite, both by the direct alteration of feldspar of the parent rock and by desilication of kaolinite

We have chosen the same four soluble cations, viz. Na, K, Ca and Mg for chemical mass balance. The quantities of these elements in parent rock and in weathered profile are recalculated from percentage analyses given by Khandali and Devaraju (1987). In the absence of ground water data, average world river water composition was used for the values of Na, K, Ca and Mg in water, from Mason and Moore (1982).

Constraints :

Average annual rainfall = 3500 mm (Ranganna et al., 1984; Krishna Rao, 1971)

= 3.5 m

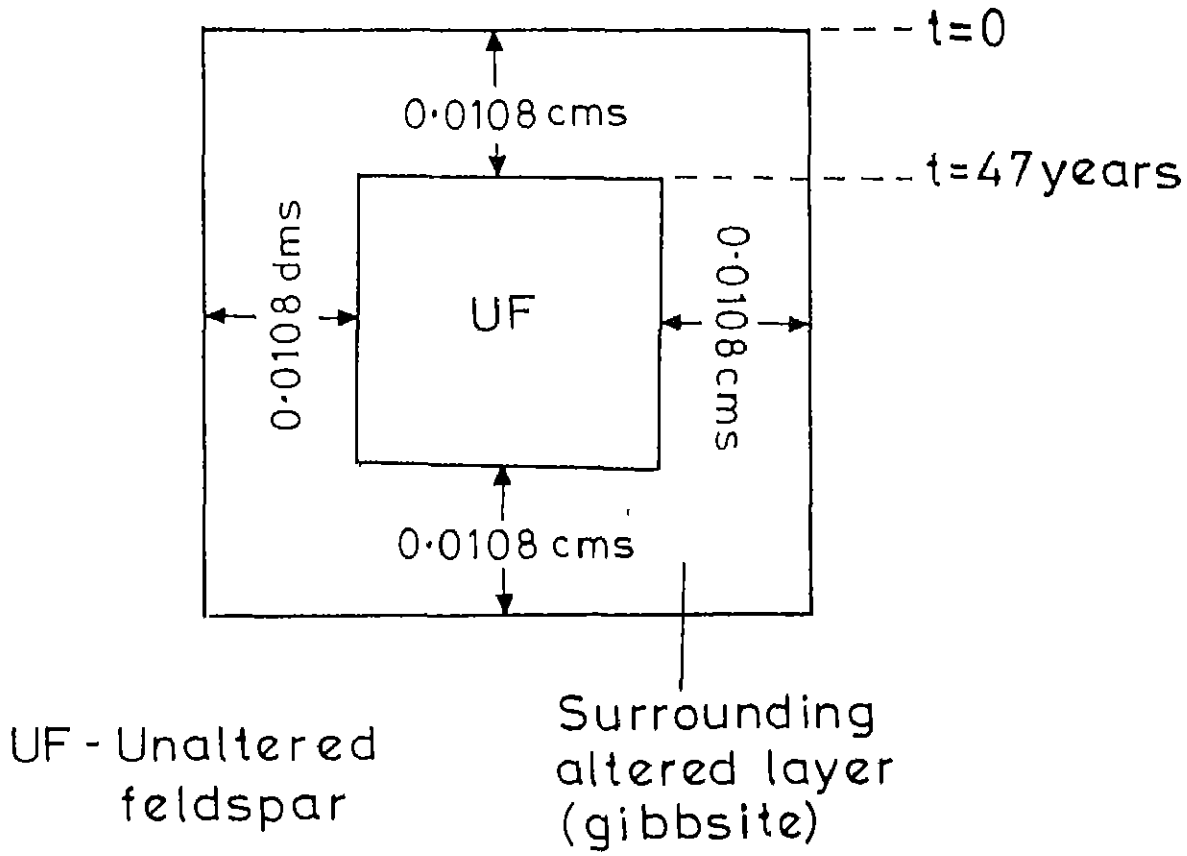

Fig. 3.2 Idealised diagram of weathering of a feldspar grain showing time of weathering

TABLE 3.7

Element	Average amount in parent rock (Tonalite gneiss) ($\mu g.g^{-1}$)	Average amount in gibbsite bearing weathered profile ($\mu g.g^{-1}$)	Average amount in world river water ($\mu g.g^{-1}$)
Na	32633.06	755.48	6.3
K	12193.56	1170.43	2.3
Ca	19339.00	205.13	15.0
Mg	9429.80	4890.95	4.1

Depth of the weathered zone below surface (i e., depth taken for calculations) = 26 m

The data for the four elements are presented below in tbaular form (Table 3.7).

Procedure for determination of time of weathering .

1) For Na

Area of the base of the rock column = 1 m^2 (say)

Height of the rock column = 26 m

Volume of the rock column = 26x1 m^3

= $26x10^6$ cm^3

Taking average density of the rock to be about 2.7 gm/cm^3

Weight of the rock column = $26x10^6$ x2.7 gm

Now,

Na content of the parent rock = 32633.06 $\mu g \cdot g^{-1}$

Na content of the weathered rock = 755.48 $\mu g.g^{-1}$

Therefore, amount of Na contributed to

water = (32633.06-755.48) $\mu g.g^{-1}$

= 31877 58 $\mu g \cdot g^{-1}$ of rock

= $31877.58x10^{-6}$ gm/gm of rock

Therefore, total Na contributed by a 26 m column of parent rock = $26x10^6$ x2.7x31877.58$x10^{-6}$ gm

= $2.238x10^6$ gm

In ave. world river water, Na content = 6.3 $\mu g \cdot g^{-1}$

= $6.3x10^{-6}$ gm/gm of water

So, $6.3x10^{-6}$ gm of Na is in 1 gm of water

Therefore, 2.238x10 gm of Na is in

0.355×10^{12} gm of water

$= 0.355 \times 10^{12}$ cm^3 of water

In 1 yr., total volume of water through rain fall

$= 3.5 \times 1 \times 10^{6}$ cm^3

Therefore, time required for weathering

$= 0.355 \times 10^{12} / 3.5 \times 10^{6}$ years

$= 0.1 \times 10^{6}$ years

$= 0.1$ *m.y.*

ii) For K .

By the procedure shown in case of Na, weight of a 26 m high column of granite gneiss (parent rock)

$= 26 \times 10^{6} \times 2.7$ gm

Now,

K content of the parent rock = 12193.56 $\mu g \cdot g^{-1}$

K content of the weathered rock = 1170.43 $\mu g \cdot g^{-1}$

Therefore, amount of K contributed to water

$= (12193.56 - 1170.43)\ \mu g \cdot g^{-1}$

$= 11023.13\ \mu g \cdot g^{-1}$

$= 11023.13 \times 10^{-6}$ gm/gm of water

Therefore, K contributed by a 26 m column of parent rock

$= 26 \times 10^{6} \times 2.7 \times 11023.13 \times 10^{-6}$ gm

$= 0.774 \times 10^{6}$ gm

In ave world given water, K content = 2 3 $\mu g.g^{-1}$

= $2.3x10^{-6}$ gm/gm of water

So,

$2.3x10^{-6}$ gm of K is in 1 gm of water

Therefore,

$0.774x10^{6}$ gm of K is in

$0.336x10^{12}$ gm of water

= $0.336x10^{12} cm^3$ of water

In 1 yr , total volume of water through rainfall

= $3.5x1x10^{6}$ cm^3

Therefore, time required = $0.336x10^{12}$ /$3.5x10^{6}$ years

= $0\ 096x10^{6}$ years

= 0.096 m.y.

iii) For Ca :

As before, weight of 26 m column of parent rock

= $26x10^{6}x2\ 7$ gm

Now,

Ca content of the parent rock = 19339.0 $\mu g.g^{-1}$

Ca content of the weathered rock = 205.13 $\mu g.g^{-1}$

Therefore amount of Ca contributed to water

= (19339.0-205.13) $\mu g.g^{-1}$

= 19133.87$\mu g.g^{-1}$

= $19133.87x10^{-6}$ gm/gm of rock

Therefore, total amount of Ca contributed by 26 m column of weathered gibbsitic product

$= 26\times10^{6}\times2.7\times19133.87\times10^{-6}$ gm

$= 1.343\times10^{6}$ gm

In ave: world river water, Ca content = 15 $\mu g.g^{-1}$

$= 15\times10^{-6}$ gm/gm water

So,

15×10^{-6} gm of Ca is in 1 gm of water

Therefore 1.343×10^{6} gm of Ca

0.0895×10^{12} gm of water

$= 0.0895\times10^{12}$ cm^3 of water

In 1 yr, total volume of water by rainfall = $3.5\times1\times10^{6}$ cm^3

Therefore, time required = $0.0895\times10^{12}/3.5\times10^{6}$ years

$= 0.0256\times10^{6}$ years

= 0.0256 m.y.

iv) For Mg

As before, weight of a 26 m column of parent rock

$= 26\times10^{6}\times2.7$ gm

Now,

Mg content in parent rock = 9525.8 $\mu g.g^{-1}$

Mg content in weathered rock = 4890.95 $\mu g.g^{-1}$

Therefore, amount of Mg contributed to water

$= (9529.8-4890.95)\ \mu g \cdot g^{-1}$

$= 4638.85\ \mu g \cdot g^{-1}$

$= 4638.85 \times 10^{-6}$ gm/gm of rock

Therefore, total amount of Mg contributed by the 26 m column of parent rock $= 26 \times 10^{6} \times 2.7 \times 4638.85 \times 10^{-6}$ gm

$= 0.326 \times 10^{6}$ gm

In water, Mg content $= 4.1\ \mu g \cdot g^{-1}$

$= 4\ 1 \times 10^{-6}$ gm/gm of water

So, 4.1×10^{-6} gm of Mg is in 1 gm of water

Therefore, 0.326×10^{6} gm of Mg is in $0\ 0795 \times 10^{12}$ cm^3 of water

In 1 yr., total amount of water by rain fall

$= 3.5 \times 1 \times 10^{6}$ cm^3

Therefore, time required $= 0.0795 \times 10^{12} / 3.5 \times 10^{6}$ years

$= 0.0227 \times 10^{6}$ years

$= 0.0227$ m y.

The time of weathering of a 26 m thick gneissic parent rock and its replacement by an equally thick layer of bauxite and/or latesite, calculated on the basis of chemical mass balance of four soluble cations (viz. Na, K, Ca and Mg) are presented in Table 3.8.

The above data indicate a rather narrow time range for weathering Thus, in the present case, an acceptable time for weathering of a 26 m thick parent rock can be around 0.1 m.y. However, in our calculations, we have considered

TABLE 3.8

For element	Calculated Time (million years)
Na	0 1
K	0 096
Ca	0 0256
Mg	0.0227

that all of the rain water have infiltrated in the rock. But, surface run off would constitute a considerable amount of rain water Hence, decrease in amount of water, which acted as leaching agent, would contribute in raising the time of weathering in all the above calculations. Thus, the times we have calculated are underestimates.

5 EVIDENCE FROM MICROSCOPIC VIEW, KARNATAKA BAUXITE DEPOSIT

In this section, we extend the calculations to microscopic scale. Fig. 3.3, reconstructed from the figure provided by Khanadali and Devaraju (1987) shows a central unaltered feldspar grain and the gibbsite band surrounding it along the periphery Here, we can assume direct gibbsitic alteration of plagioelase feldspar. We attempt to calculate the time required for the formation of this gibbsitic band around the feldspar grain, by means of chemical mass balance.

To ensure accuracy, we have measured the thickness of the altered rim in six places and the average was taken.

Average thickness of the gibbsite layer = 0.65 cm
(measured on Fig. 3.3)
Magnification = 70 times
Therefore, actual thickness = 0.65/70 = 0.00928 cm
When all other parameters remain constant, length of time of weathering becomes proportional to the thickness of

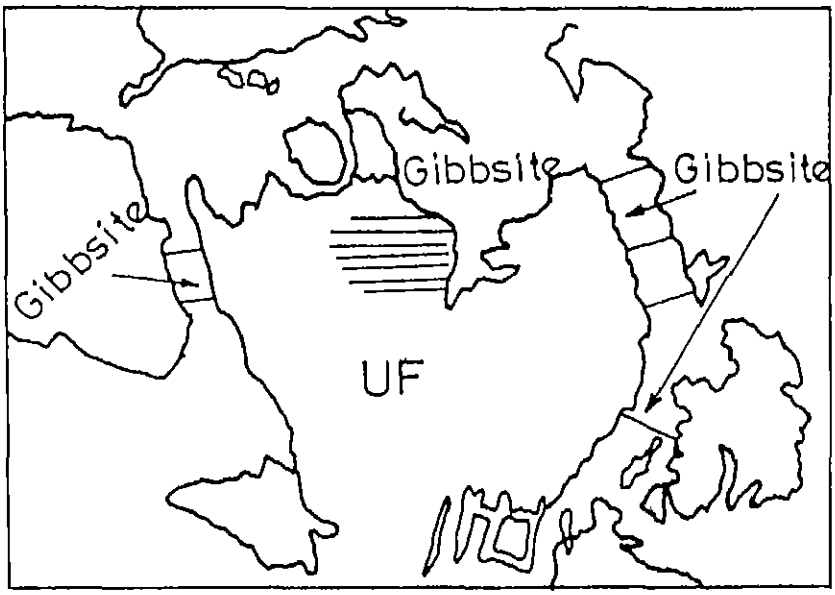

UF - Unaltered feldspar

Fig. 3.3 Schematic diagram drawn from photomicrograph showing transformation of plagioclase feldspar (centre) into gibbsite along grain boundaries, fractures and cleavage planes (X70) (After Khanadali and Devraju, 1988)

TABLE 3.9

For element	Time of weathering (months)
Na	4.34
K	4.17
Ca	1.11
Mg	1.00

weathered layer.

We can utilize the calculations of the previous section for release of various ions from a 26 m thick parent rock. Following this principle, the times of weathering of a feldspar grain, through a thickness of 0.00928 cms, for different ions are listed in Table 3.9. Geologically speaking, the above data indicate quite fast rate of weathering, inspite of the fact that these time values are underestimates The most plausible reason of this fast rate of weathering can be attributed to extremely high rainfall (3500 mm, annually) in the area from which the sample was taken (South Kanara district, Karnataka, India).

The following schematic diagram (Fig. 3.4) shows the idealised picture of weathering of the feldspar grain

The above discussions and calculations show the time required to weather a rock of given thickness to its weathered product of equal thickness under various natural physico-chemical conditions The variables include rock type, thickness of weathering, rainfall, prevailing P-T conditions, pH etc.

To sum up the above findings, all the relevant data and the derived time values are furnished in a tabular form below This serves the purpose of having a comparative view as well as rate of weathering in each case.

From Table 3.10, it can be seen that the rate of weathering varies drastically from region to region mainly

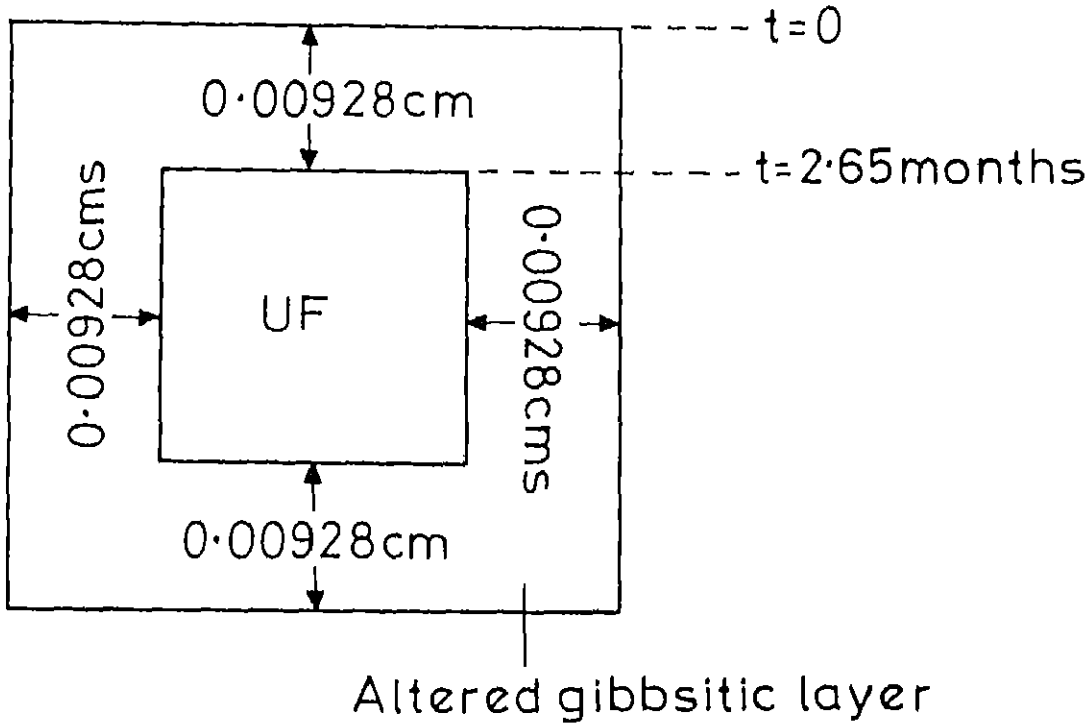

UF - Unaltered plagioclase feldspar

Fig. 3.4 Idealised diagram of weathering of a feldspar grain showing time of weathering

depending upon rainfall and rock types. A general survey reveals that the rate is more in areas of heavy rainfall than in areas of relatively less amount of rainfall.

Recently, Chen et al (1988) have calculated the rate of weathering of andesitic/andesitic tuffaceous rocks in Tatun valcanic area, N Taiwan According to them, the weathering rate, in the area, is indicated by the time required for accumulation of radioactive Be in the soil column They calculated the weathering rate to be around 12 cm Ka^{-1} or 120 $m/10^{6}$ years.

Comparison of this rate of weathering, measured by a completely different technique, with our calculations suggests similarity in the order of magnitude of the rates. This lends support in favour of the validity of the method of chemical mass balance as a simple but useful tool for quick estimate of time of weathering.

TABLE 3.10

Deposit	East Coast Bauxite Deposit, Orissa India			Bauxite Deposit of South Kanara district, Karnataka, India			Paragominas Bauxite Deposit Brazil	
Parent Rock Type	Khondalite Feldspar 56% by vol. Plag: K-fld = 65·35			Tonalite Gneiss Plag: >K-fld			Arenaceous sedimentary rock	
Average annual rain fall	1600 mm			3500 mm			1000 mm	
Thickness of the weathered layer	In field 70 m	For a single mineral grain in thin section ≃ 0.01 cm	Rate of weathering ($m/10^6$ yr)	In field 26 m	For a single mineral grain in thin section ≃ 0.009 cm	Rate of weathering ($m/10^6$ yr)	In field 2.2 m	Rate of weathering ($m/10^6$ yr)
For elements	Time of weathering (Million years)	(years)		Time of weathering (Million years)	(months)		Time of weathering (Million years)	
Na	3.0	4.63	23.33	0.1	4.34	260.0	0.021	104.76
K	30.35	46.82	2.3	0.1	4.17	260.0	0.046	47.83
Ca	0.47	0.725	149.0	0.02	1.11	1300.0	0.018	122.22
Mg	0.58	0.9	120.7	0.02	1.0	1300.0	0.037	59.46

CHAPTER 4

DEVELOPMENT OF A MATHEMATICAL MODEL OF WEATHERING

4.1 INTRODUCTION

In chapter 2, various physico-chemical factors governing the phenomenon of direct gibbsitization have been identified. Among them, one of the most important factors, viz., pH range has been derived with precision, by the help of equilibrium diagrams. Now, having proved the phenomenon of direct gibbsitization of feldspars to be operative in nature, we, here, attempt to investigate some aspects of the reaction mechanism. Before stating the problem, it is essential to mention the background of the investigation. Reaction mechanisms constitute one of the most significant but least studied aspects of weathering processes. We highlight the aspect of diffusion in the weathering of potash feldspar to gibbsite directly, in the following discussion.

4.2 STATEMENT OF THE PROBLEM

Two principal ideas have gained attention as probable

processes of mineral zonality evolution, i e., generation of layers of weathered products, in a weathering profile .

1. Weathering rate is controlled by diffusion of dissolved components through a layer of reaction products. In this process, the external reacting fluid has to traverse through an already formed product layer to come into contact with the fresh reacting solid. The reaction front thus proceeds inward, i.e., towards the direction of movement of the reacting fluid within the weathered rock. According to different authors, reactions of this type may be congruent or incongruent (Wollast, 1967, Dobrovolsky, 1987)

2. The other idea emphasizes that the limiting step in dissolution is not diffusion but chemical reaction, at the mineral-water interface, particularly at structurally controlled sites (Berner, 1978; Holdren and Berner, 1979; Colman and Dethier, 1986,).

3. A third mechanism is still on the anvil, which favours total dissolution of the ions from the parent mineral into the associated solution and thereafter insitu precipitation of the minerals after the ions have been recombined. This mechanism heavily depends on the relative mobility of various ionic species derived from the parent minerals

In the present thesis, we are concerned with the problem of direct gibbsitization of feldspars and its possible reaction mechanism. Here, we will confine ourselves to the investigation of the relative importance

of diffusion vis-a-vis chemical reaction in the process of direct gibbsitization of potash feldspar. In other words, we consider the alteration reaction to be diffusion controlled and with this assumption, try to find out the implications of the diffusion process.

4.3 FORMULATION OF THE PROBLEM

1) Background

According to Wollast (1967), direct gibbsitization can take place according to the following steps

Step 1 : Rapid exchange between H of the reacting solution (water) and K of the feldspar leading to breakage of feldspar structure and formation of a thin layer enriched in aluminium. According to Wollast (1967), this $Al(OH)_3$ (amorphous) layer forms all over the feldspar grain. However, according to others, like Berner and Holdren (1979), if it at all forms, it might be confined to the weak zones of the crystals, such as, along twin axes or cleavage planes of the crystal and presumably of sub-electron microscopic dimension, which is difficult to detect. No matter which mechanism is true, it does not rule out the importance of the presently adopted technique (i.e., diffusion controlled mechanism) to judge the relative significance of diffusion over chemical reaction.

This step is very fast and according to many workers

(e.g , Wollast 1967, Luce, 1972 and Lagace, 1965 in Dobrovolsky (1987)) goes into completion within few minutes in laboratory scale experiments.

Step 2 Once a thin layer (the so called "Protective layer" - of $Al(OH)_3$ amorphous) has been formed, now, silica starts coming out of the feldspar structure due to continuous reaction with the solution (water). Aluminium, because of its extremely low mobility is retained. In this stage, the rate of release of silica is controlled by two factors, viz., rate of diffusion of these species through the residual layer and the rate of the chemical reaction between feldspar and water, at the mineral-water interface.

Following Wollast (1967), a third mechanism can be included, which determines the kaolinization from the gibbsite, so formed.

Step 3 · Once the external silica concentration reaches a maximum value (dependent on pH), it starts reacting with the already formed $Al(OH)_3$ (amorphous) and gives rise to kaolinite ($Al_2Si_2O_5(OH)_4$) Here, silica reacts in the form of silicic acid (H_4SiO_4)

However, for the present, we shall confine ourselves only within the step 2.

ii) Qualitative formulation·

In the adjoining diagram (Fig. 4 1), ABCD is the cross-section of a potash feldspar block After certain time of weathering, A'B'C'D' becomes the cross-sectional area of the unweathered feldspar, while the annular region

of width x is the weathered product. Here, we assume that the water-rock interaction is isotropic and it always proceeds from the periphery to the centre of the mineral grain This allows us to visualize the weathering process as a one dimensional transient problem, where, a reaction front ABCD (Fig 4 1) existing at any time t takes the new position A'B'C'D' at some later time t' (t' > t). The weathered annular region, in this case, attains a composition of $Al(OH)_3$ (amorphous) (amorphous gibbsite).

In the present case, however, we extend the weathering reaction experienced by a single block of potash feldspar to a more general one, which involves a natural assemblage of several such feldspar grains

The problem can be formulated with reference to figure 4 2. PQRS represents the cross-section of a column of rock, initially rich in potash feldspar and having certain amount of porosity. Rain water flows continuously through this porous column with a certain range of velocity. Continuous weathering reaction is going on between the mildly acidic rainwater and potash feldspar. At any time t (t > 0), PQFE represents cross-section of the product layer adhering to the unreacted feldspar rich section EFRS. We assume that the reation is at equilibrium only along the line EF.

pH value at the boundary PQ is different from that at the reaction boundary EF. In the latter boundary, it is governed by the equilibrium reaction Hence, through this distance x_1 we monitor concentration of H^+ ions due to

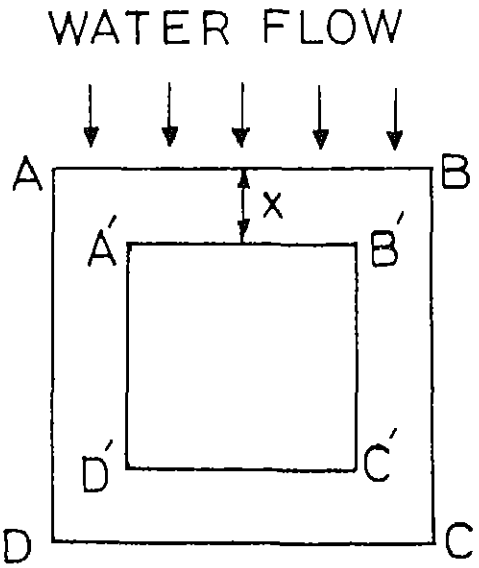

Fig. 4.1 Schematic diagram showing cross-section of a partially weathered feldspar grain

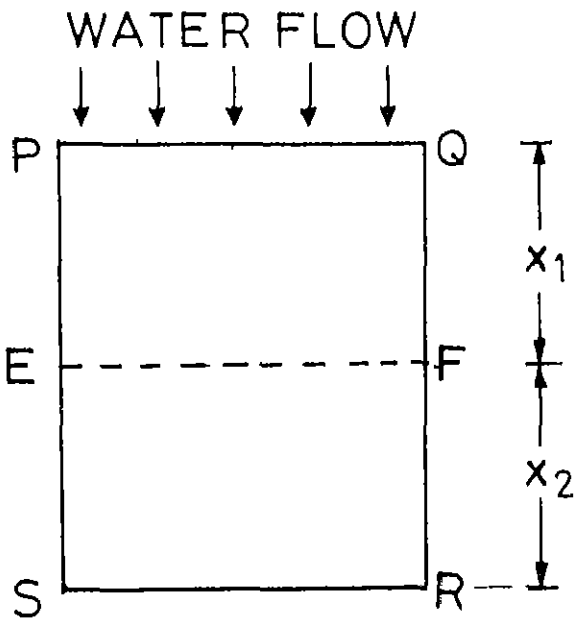

Fig 4.2 Schematic diagram showing vertical section of a partly weathered feldspathic rock body

connvective diffusion.

On the other hand, at the reaction boundary EF, silicic acid is produced as a result of the reaction

$$KAlSi_3O_8 + H^+ + 7H_2O = Al(OH)_3 + K^+ + 3H_4SiO_4$$

This silicic acid is carried out of the system by corrective diffusion. Hence, through the distance x_2 we will monitor concentration of H_4SiO_4 over known distances.

iii) Mathematical Formulation :

The equation of convective diffusion which arises from mass balance across a plane perpendicular to which diffusion takes place, is ·

$$\frac{\partial C_A}{\partial t} + V \cdot \frac{\partial C_A}{\partial x} = D_A \cdot \frac{\partial^2 C_A}{\partial x^2} \qquad (1)$$

where, C_A = concentration of the diffusing species A
(In the present problem, these are H^+ and H_4SiO_4)

x = distance

t = time

v = velocity of percolation of ground water

D_A = diffusion coefficient or diffusivity of the diffusing species A

4.4 SOLUTION PROCEDURE

One of the most suitable methods to solve the above partial differential equation is by "Finite Difference Method". In this case, an implicit finite difference scheme has been preferred over the explicit form of

solution in order to overcome the stability problem.

We define the following dimensionless variables x^*, t^* and C_A^* as follows

$$x^* = \frac{x}{x_{Ref}} \quad ; \quad t^* = \frac{t}{t_{Ref}} \quad ; \quad C_A^* = \frac{C_A}{C_{A_{Ref}}}$$

The abbreviation "Ref." stands for some reference value of the parameter

Now, $\frac{\partial}{\partial t}(C_A^* C_{A_{Ref}}) = C_{A_{Ref}} \frac{\partial C_A^*}{\partial t} = C_{A_{Ref}} \frac{\partial C_A^*}{\partial t^*} \cdot \frac{\partial t^*}{\partial t}$

$$= \frac{C_{A_{Ref}}}{t_{Ref}} \frac{\partial C_A}{\partial t^*}$$

$$\therefore \quad \frac{\partial C_A}{\partial t} = \frac{C_{A_{Ref}}}{t_{Ref}} \frac{\partial C_A^*}{\partial t^*} \tag{2}$$

Again,

$$\frac{\partial C_A}{\partial x} = \frac{\partial}{\partial x}(C_A^* \cdot C_{A_{Ref}}) = C_{A_{Ref}} \frac{\partial C_A^*}{\partial x}$$

or, $$\frac{\partial C_A}{\partial x} = C_{A_{Ref}} \frac{\partial C_A^*}{\partial x^*} \cdot \frac{\partial x^*}{\partial x} = \frac{C_{A_{Ref}}}{x_{Ref}} \cdot \frac{\partial C_A^*}{\partial x^*} \tag{3}$$

Again,

$$\frac{\partial^2 C_A}{\partial x^2} = \frac{\partial}{\partial x}\left(\frac{\partial C_A}{\partial x}\right) = \frac{\partial}{\partial x}\left(\frac{C_{A_{Ref}}}{x_{Ref}} \cdot \frac{\partial C_A^*}{\partial x^*}\right)$$

$$= \frac{C_{A_{Ref}}}{x_{Ref}} \cdot \frac{\partial}{\partial x^*}\left(\frac{\partial C_A^*}{\partial x^*}\right) \frac{\partial x^*}{\partial x}$$

or,

$$\frac{\partial^2 C_A}{\partial x^2} = \frac{C_{A_{Ref}}}{x_{Ref}^2} \cdot \frac{\partial^2 C_A}{\partial x^{*2}} \tag{4}$$

Substituting all these expressions in equation (1),

$$\frac{C_{A_{Ref}}}{t_{Ref}} \cdot \frac{\partial C_A^*}{\partial t^*} + V \cdot \frac{C_{A_{Ref}}}{x_{Ref}} \cdot \frac{\partial C_A^*}{\partial x^*} = D_A \frac{C_{A_{Ref}}}{x_{Ref}^2} \cdot \frac{\partial^2 C_A^*}{\partial x^{*2}}$$

or,

$$\frac{1}{t_{Ref}} \frac{\partial C_A^*}{\partial t^*} + \frac{V}{x_{Ref}} \cdot \frac{\partial C_A^*}{\partial x} = \frac{D_A}{x_{Ref}^2} \frac{\partial^2 C_A^*}{\partial x^{*2}} \qquad (5)$$

Multiplying both sides by x_{Ref}^2/D_A,

$$\frac{x_{Ref}^2}{t_{Ref} \cdot D_A} \cdot \frac{\partial C_A^*}{\partial t^*} + \frac{V\ x_{Ref}}{D_A} \cdot \frac{\partial C_A^*}{\partial x^*} = \frac{\partial^2 C_A^*}{\partial x^{*2}}$$

$$\text{or, } Pe1 \frac{\partial^2 C_A^*}{\partial t^{*}} + Pe2 \frac{\partial C_A^*}{\partial x^*} = \frac{\partial^2 C_A^*}{\partial x^{*2}}$$

where,

$$Pe1 = \frac{x_{Ref}^2}{t_{Ref} \cdot D_A} \quad \text{and} \quad Pe2 = \frac{V\, x_{Ref}}{D_A}$$

Pe1 and Pe2 are two dimensionless quantities known as Peclet numbers.

Now, while solving the above equation, we adjust the values of $t_{Ref} = \frac{x_{Ref}^2}{D_A}$, so that Pe1 becomes unity. As we are left with one Peclet number viz; Pe2, henceforth we denote Pe2 by Pe only.

So, the new dimensionless form of the equation becomes .

$$\frac{\partial C_A^*}{\partial t^*} + Pe \frac{\partial C_A^*}{\partial x^*} = \frac{\partial^2 C_A^*}{\partial x^{*2}} \qquad (6)$$

Now, in an implicit finite difference scheme (Carnahan, Luther and Wilkes, 1969), equation (6) can be written as :

$$\frac{C_{i,n+1} - C_{i,n}}{\Delta t} + Pe \frac{C_{i,n+1} - C_{i-1,n+1}}{\Delta x} = \frac{C_{i-1,n+1} - 2C_{i,n+1} + C_{i+1,n+1}}{(\Delta x)^2}$$

or,

$$(C_{i,n+1} - C_{i,n}) + Pe \frac{\Delta t}{\Delta x} (C_{i,n+1} - C_{i-n,n+1})$$

$$= \frac{\Delta t}{(\Delta x)^2} (C_{i-1,n+1} - 2C_{i,n+1} + C_{i+1,n+1})$$

multiplying both sides by $\frac{(\Delta x)^2}{\Delta t}$, we get,

$$(C_{i,n+1}-C_{i,n})\frac{(\Delta x)^2}{\Delta t} + Pe\ \Delta x(C_{i,n+1}-C_{i-1,n+1}) = C_{i-1,n+1}-2C_{i,n+1}+C_{i+1,n+1}$$

$$\text{or, } C_{i-1,n+1}(-Pe\ \Delta x-1)+C_{i,n+1}\left(\frac{(\Delta x)^2}{\Delta t}+Pe\ \Delta x+2\right)+C_{i+1,n+1}(-1) = \frac{(\Delta x)^2}{\Delta t}C_{i,n}$$

$$\text{or, } \alpha\, C_{i-1,n+1}+\beta\, C_{i,n+1}+\gamma\, C_{i+1,n+1} = \partial\, C_{i,n} \qquad (7)$$

where,

$$\alpha = -(Pe\ \Delta x + 1)$$

$$\beta = \frac{(\Delta x)^2}{\Delta t} + Pe\ \Delta x + 2$$

$$\gamma = -1$$

and $\partial = \frac{(\Delta x)^2}{\Delta t}$ are the coefficients of the generalized algebraic equation (7).

In the above formulation

i - variable representing distance nodes

n - variable representing time nodes

Δx - difference between two successive node points on the distance axis = distance interval

Δt - difference between two successive node points on the time axis = time-step interval

4.5 BOUNDARY CONDITIONS

The boundary conditions can be ascribed with reference

to the following diagram (Fig. 4.3). In case of investigation of hydrogen ion concentration, this grid represents the zone of product layer of composition $Al(OH)_3$ (amorphous), while, in case of investigation of silicic acid, this grid represents a zone inside the unweathered rock body, below equilibrium reaction zone of weathering This is further illustrated in the figure 4.4.

Boundary Conditions for Diffusion of Hydrogen ions .

At boundary AB (Fig. 4 3), $C(x=0, t=t) = 10^{-5.7}$ m/l (from average rainwater pH value)

At boundary CD (Fig 4.3), $c(x=1, t=t) = 10^{-10.43}$ m/l.

The second boundary condition arises from the equilibrium pH value derived from the point Q of the metastable boundary between K-feldspar and amorphous gibbsite (Chapter 2, Fig. 2.6)

Initial Condition for Diffusion of Hydrogen Ions :

A linear initial concentration profile between the two boundaries has been used throughout the investigation in a dimensionless form. As expected, this does not affect the final steady state solution as has been checked with various arbitrary concentration profiles as initial conditions.

Boundary Condition for Diffusion of Silicic Acid .

At the boundary AB, $C(x=0, t=t) = 10^{-5.5}$ m/l. This is the equilibrium concentration of silicic acid furnished by the point Q(Chapter 2, Fig. 2 6)

At the boundary CD, $C(x=1, t=t) = 2.K\ t^{1/2}$

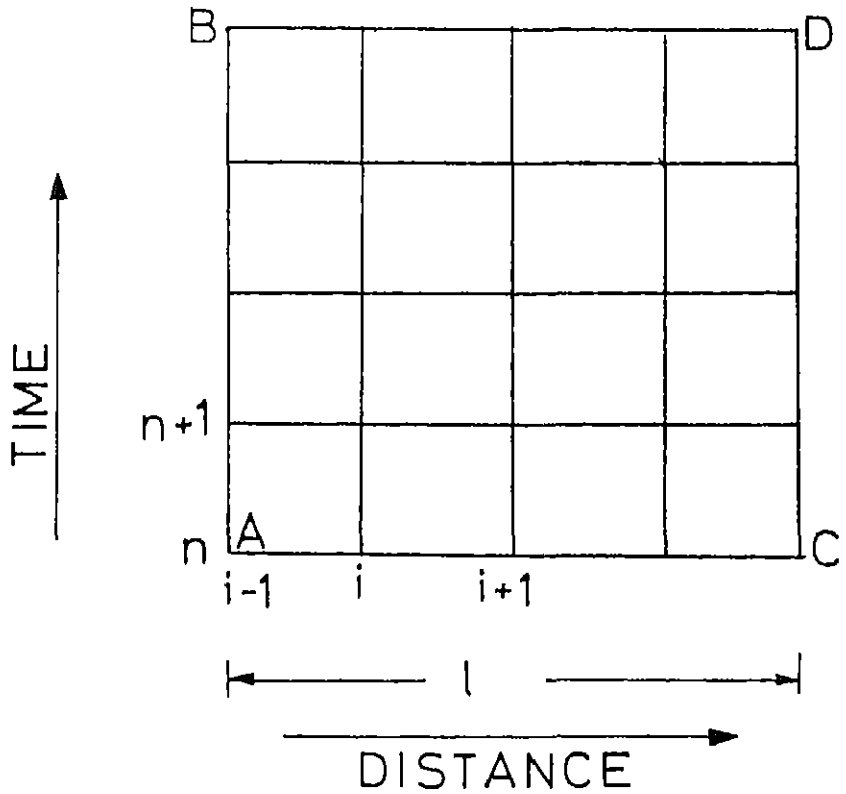

Fig. 4.3 Schematic representation of finite difference grid

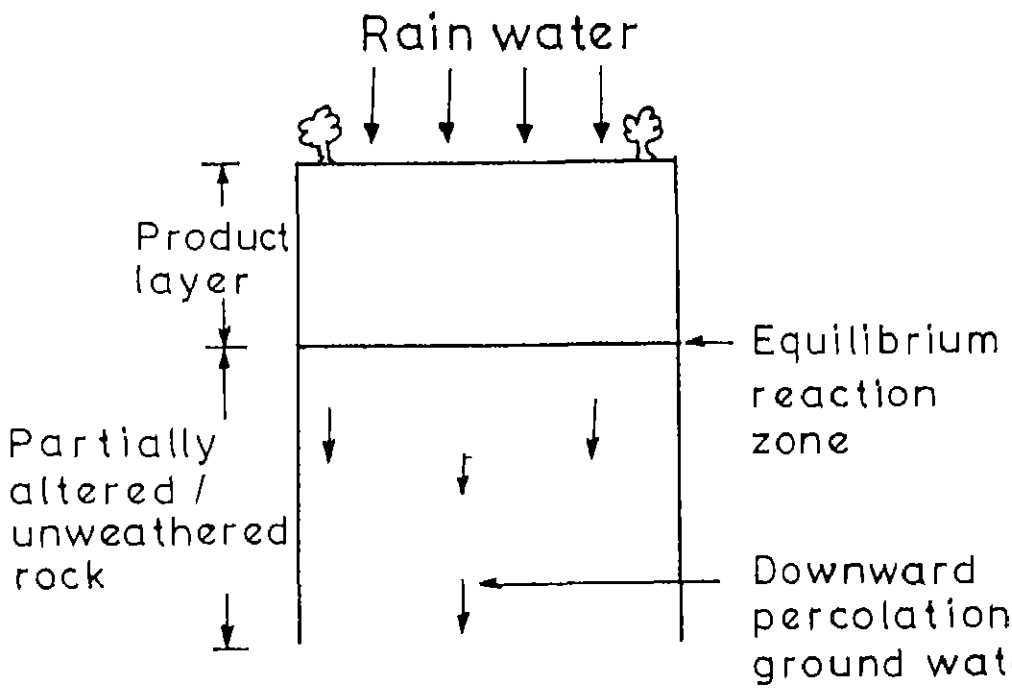

Fig. 4.4 Schematic diagram showing vertical section of a partly altered/unaltered rock capped by a product layer

(Assuming, parabolic rate law)

where, t = time

K = rate constant for release of silicic acid

At the boundary CD, we have applied the parabolic rate law of Wollast (1967)

Initial Condition for Diffusion of Silicic Acid

Same arguments are also applicable here, as in case of hydrogen ion diffusion.

In all the above cases, we have normalised all the variables to a range from 0 to 1 by dividing them with suitable reference values.

DATA SET :

A. For diffusion of hydrogen ions .

Percolation velocity of ground water (v) = 10^{-7} cm/sec.

Diffusion coefficient for H^+ in aqueous medium (D_H)

= 10^{-4} cm^2/sec (Garrels and Mackenzie, 1971)

Boundary conditions for concentration :

(Before normalisation)*

* : the term "Normalisation" here means division of the parameters by a reference value in order to make it dimensionless.

$C(x=0, t=t) = 10^{-5.7}$ m/l

$C(x=1, t=t) = 10^{-10.43}$ m/l

$C_{Ref} = 10^{-5.7}$ m/l

Boundary conditions for concentration (after normalisation)

C(x=0, t=t) = 1 0

$C(x=1, t=t) = 10^{-4.73}$ (Both dimensionless)

B. For diffusion of silicic acid

Percolation velocity of ground water(v) = 10^{-7} cm/sec

*Diffusion coefficient for silicic acid (H_4SiO_4) in aqueous solution (D_S) = 10^{-5} cm^2/sec (Applin, 1987).

*Different authors have reported different values for D_S, ranging from 10^{-5} to 10^{-6} cm^2/sec. However, as majority of the authors have chosen its value around 10^{-5} cm^2/sec at 25 °C, we have chosen so. (Applin, 1987).

Boundary conditions (before normalisation)

$C(x=0,\ t=t) = 10^{-5.5}$ m/l

$C(x=l,\ t=t) = 2\ K\ t^{1/2}$ m/l

where, K is the rate constant for silica release at the outer boundary CD (Fig. 4 3).

$$K = 10^{-4.5}\ \frac{mg}{l.(hour)^{1/2}} \quad \text{(Wollast, 1967)}$$

$$= 10^{-11.26}\ \frac{moles}{l.(sec)^{1/2}}$$

N.B. The value of K has been experimentally determined by Wollast (1967) for the pH values 4,6,8 and 10. In the present case,pH is 10 43,at equilibrium Thus, the K value corresponding to pH 10 has been chosen from Wollast's experiment, being the nearest).

Therefore, boundary conditions (after normalisation) :

$C(x=0,\ t=t) = 1.0$

$$C(x=1,\ t=t) = 2\ K\ t^{1/2}\ /10^{-5.5}$$

(Both dimensionless)

4.6 RESULTS AND DISCUSSION

The results were obtained by solving the appropriate finite difference equations in an interactive DEC-1090 computer housed at the computer centre of IIT Kanpur. All the relevant diagrams were also plotted in the same system, using a PLOT-10 package. Programmes have been written in FORTRAN language and have been incorporated in the appendix. 3.

(a) Diffusion of hydrogen ions through three separate distances, with percolation velocity remaining constant

Through three arbitrarily chosen distances (i.e., thicknesses of the product layer) viz· 200 cms, 400 cms and 600 cms, diffusion of H^+ was investigated under the given boundary conditions. In all the three cases, velocity of ground water was kept constant at 10^{-7} cm/sec. Table 4.1 displays the result of diffusion of H^+. Peclet numbers in the three cases and calculated time to attain steady state are also shown. Figure 4.5 diagrammatically shows the steady-state concentration profiles for the three cases.

It can be easily seen that as the value of Peclet

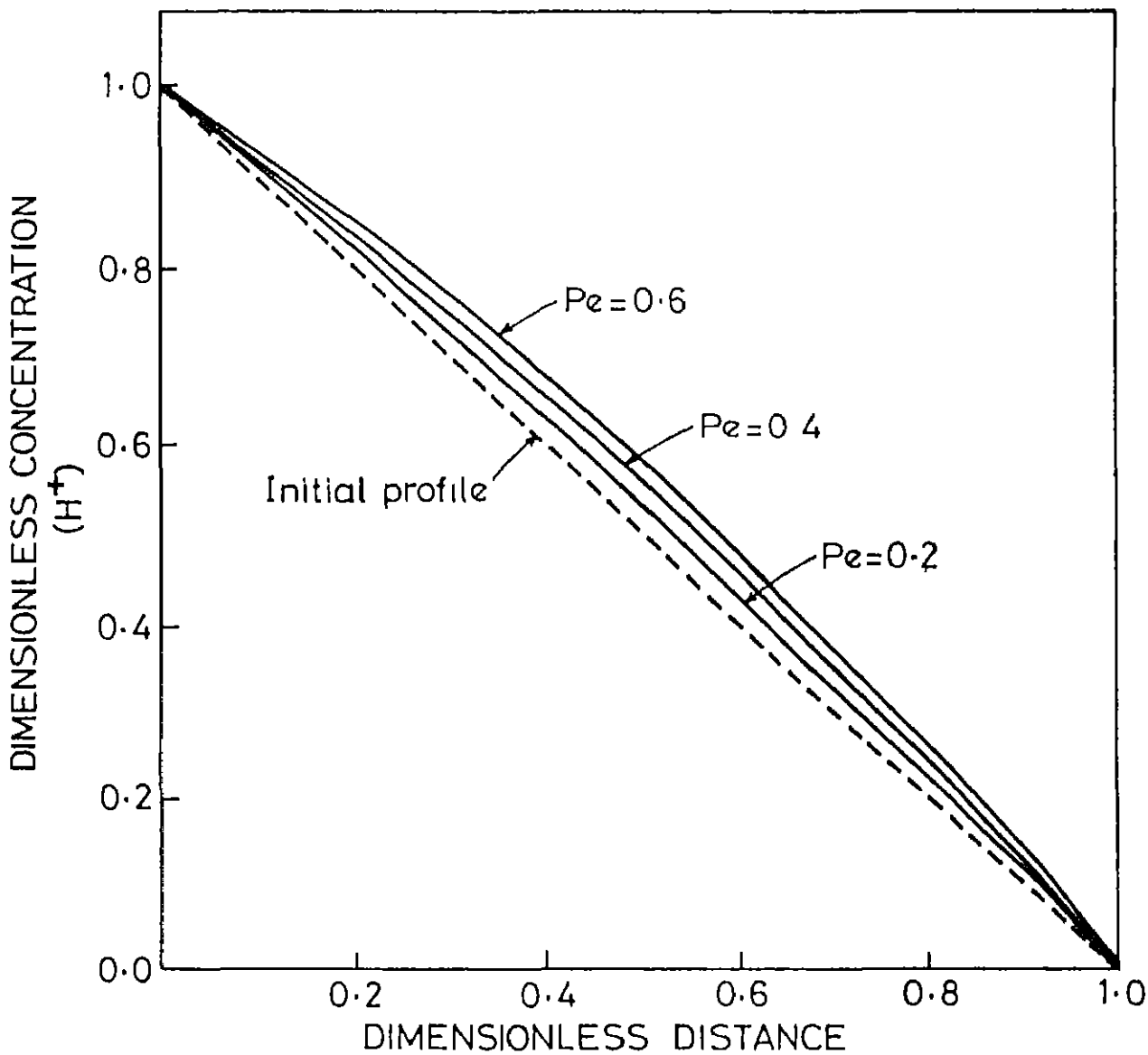

Fig. 4.5 Plot of steady state concentration profile of H^+ for three different Peclet numbers

TABLE 4.1

Case No	Distance (l) (cms)	Distance (Reference) (x_{Ref}) (cms)	Peclet Number ($Pe=V\ x_{Ref}/D_H$) (Dimensionless)	Calculated time to attain steady-state (years)
1.	200	200	0 2	3.8 ($=12\times10^7$ sec)
2	400	400	0.4	15.22 ($=48\times10^7$ sec)
3.	600	600	0.6	34.25 ($=108\times10^7$ sec)

numbers increases, the curvature of the steady-state profile also increases correspondingly

(b) Diffusion of silicic acid through three separate distances, with percolation velocity remaining constant

As in the case of hydrogen, in this case too, three separate distances (i.e., thickness of partially weathered/ unweathered rock) were chosen viz. 50 cms, 200 cms and 400 cms for diffusion of H_4SiO_4 under the relevant boundary conditions. Velocity of ground water was kept constant at 10^{-7} cm/sec.

Table 4.2 displays the result including Peclet number and time to attain steady state for the three cases. Fig. 4 6 diagrammatically shows the steady state concentration profiles over normalised distances for the three cases. As before, it is easily discernible that with increment in Peclet number the profiles progressively become more curved, i e., tend towards attaining the initial highest value (i.e., 1 0) of one end.

As expected from the theory, a high value of Peclet number would lead to the formation of a boundary layer. Although, the values of Peclet numbers used in these cases were not sufficient to show any concentration boundary layer in the real sense, the results, however, definitely show the real trend. In all the above cases, velocity of

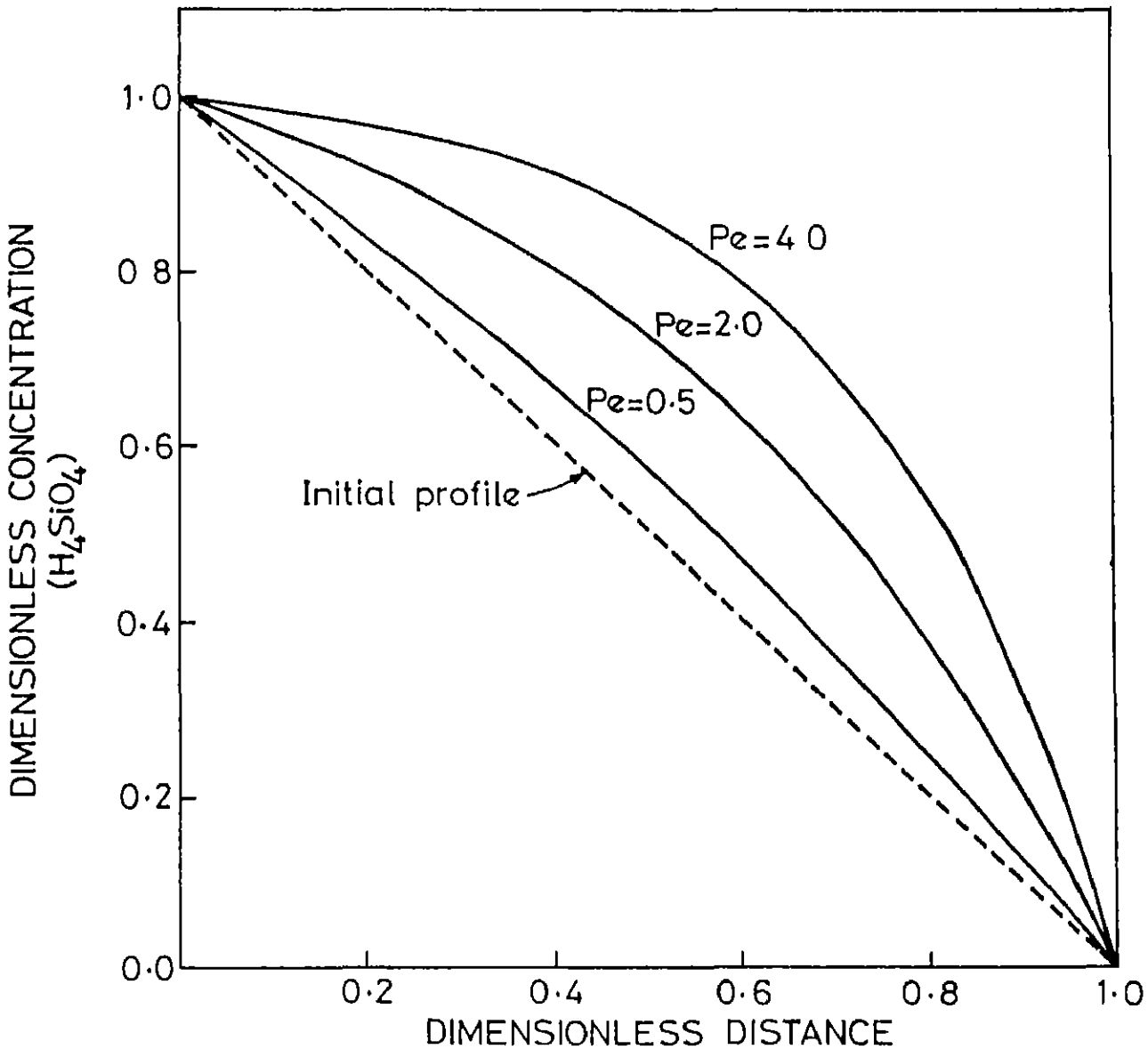

Fig. 4.6 Plot of steady state concentration profile of H_4SiO_4 for three different Peclet numbers

TABLE 4.2

Case No	Distance (l) (cms)	Distance (Reference) (x_{Ref}) (cms)	Peclet Number ($Pe=V.x_{Ref}/D_S$) (Dimensionless)	Calculated time to attain steady state (years)
1	50	50	0.5	3.17 ($=10^8$ sec)
2	200	200	2.0	38.05 ($=12\times10^8$ sec)
3	400	400	4.0	152.20 ($=48\times10^8$ sec)

water percolation (v) was kept constant at 10 cm/sec. So, the values of Peclet numbers become function of rock size only, for a constant value of diffusion coefficient.

In mass transport calculations, the final steady-state profile should be independent of initial concentration profile. To test the validity of this concept in the present cases, two other initial conditions (1 and 2) were used for the same set of boundary conditions It has been found that the steady state profiles do not change at all. These are shown in figures 4.7 and 4.8 for diffusion of H^+ and H_4SiO_4 respectively with one Peclet number for each case For other Peclet-Numbers, results are similar. However, in case of transient calculations, the number of time steps needed to achieve the final steady state depends on the initial condition. Correspondingly, the time calculated to achieve steady-state becomes dependent upon the initial condition. Thus, the times calculated for various Peclet numbers do not furnish the steady-state time unless the initial concentration profile is known. However, in the present cases, with the given boundary conditions, there is little scope for a very wide variation of initial conditions. Thus, the time calculated can be considered as real times.

The fact that with increasing Peclet numbers, i.e., with increase in rock sizes in these cases, the time required to attain steady state also increases correspondingly is shown in Figures 4.9 and 4 10. The

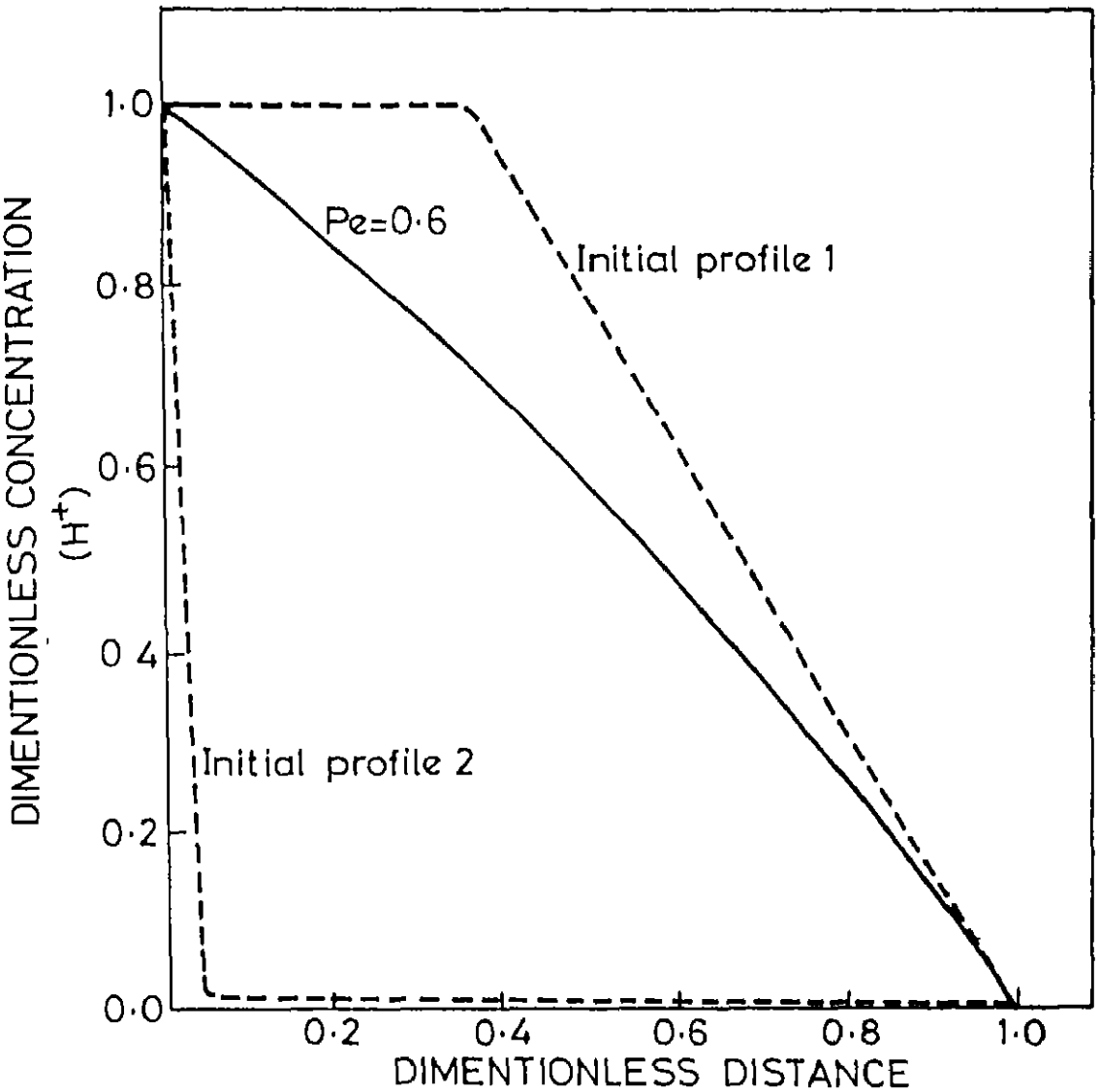

Fig. 4.7 Steady state concentration profile of H^+ (Peclet number = 0 6) for two different initial profiles

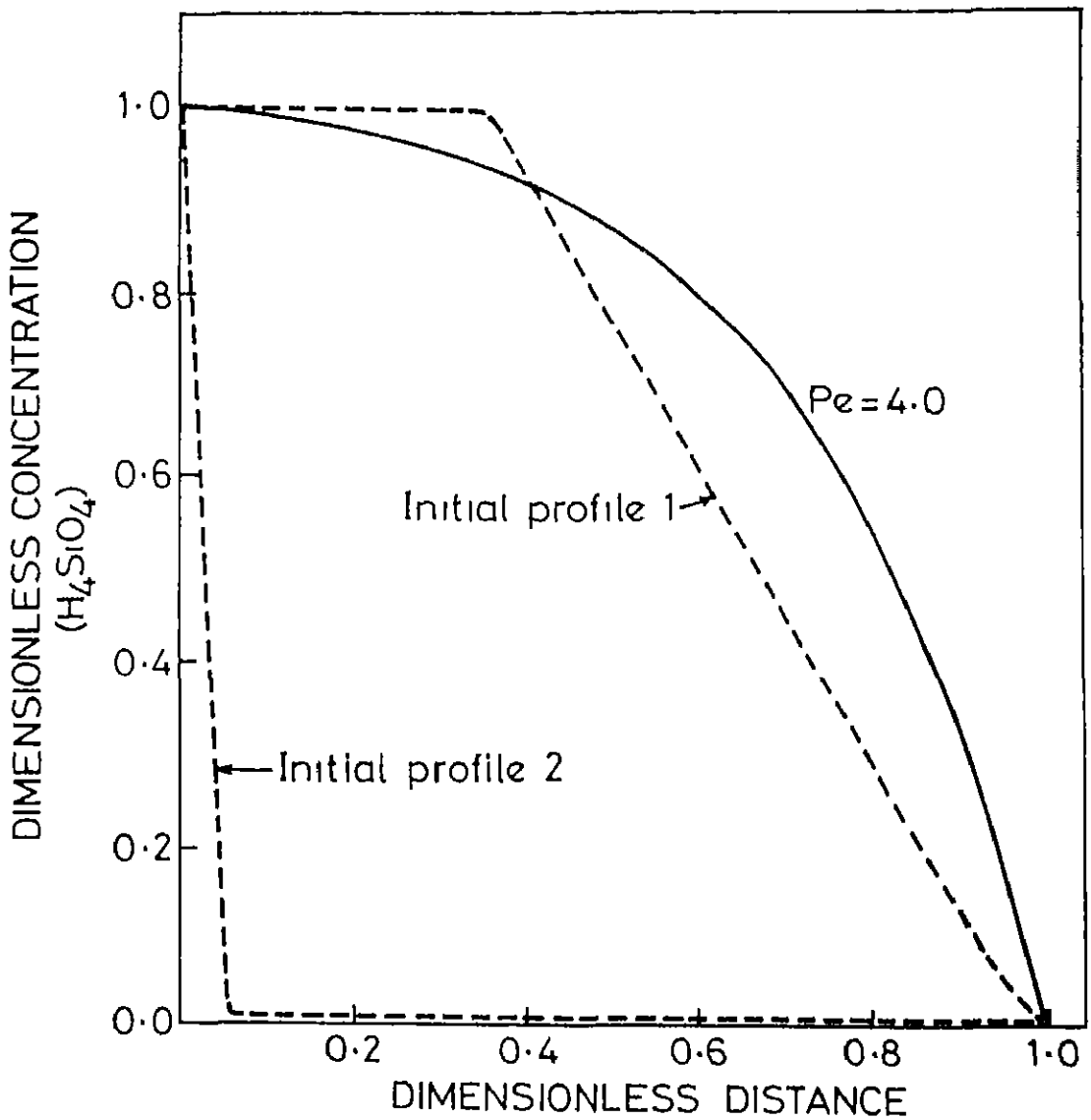

Fig 4.8 Steady state concentration profile of H_4SiO_4 (Peclet number = 4.0) for two different initial profiles

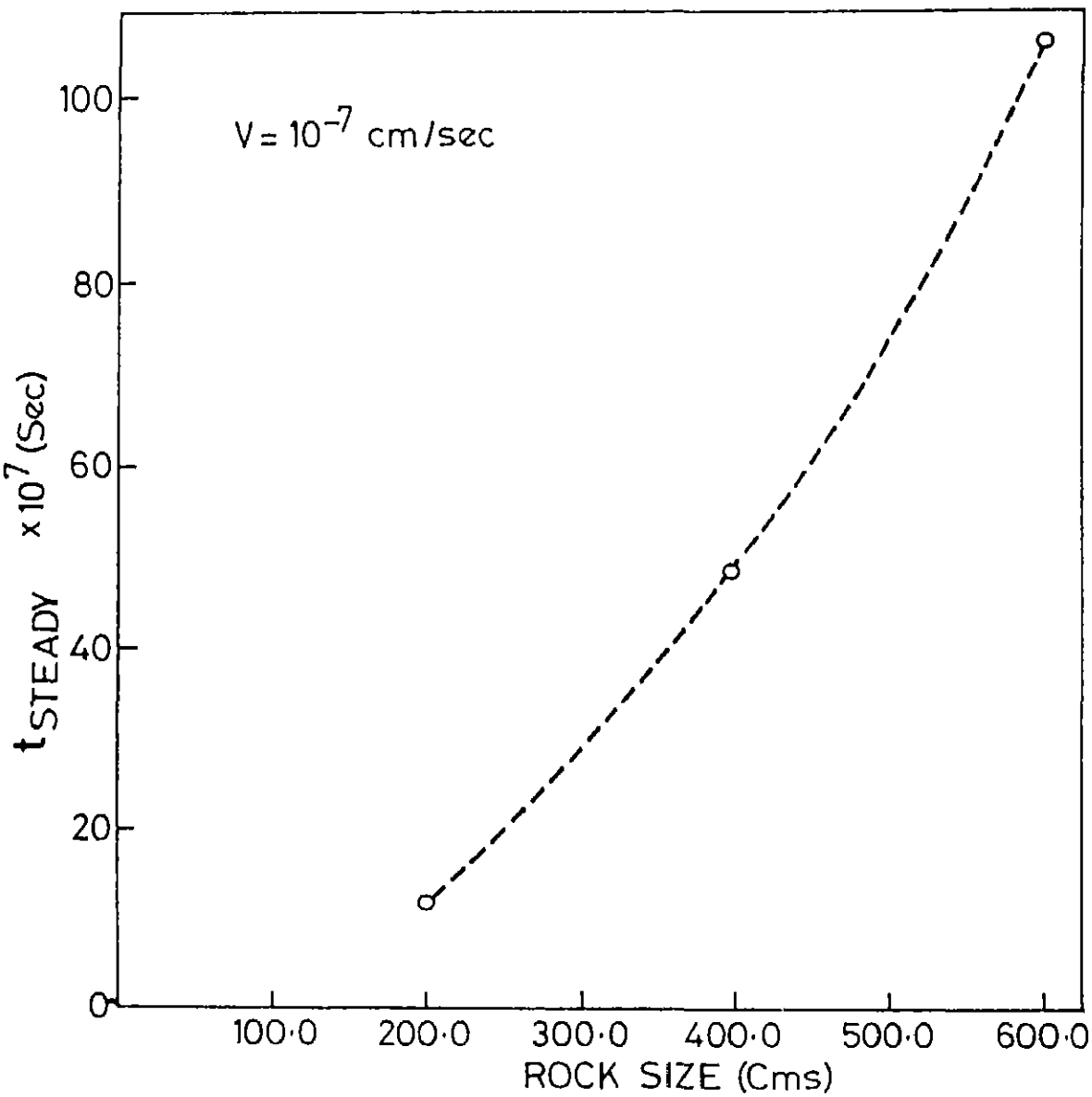

Fig. 4.9 Plots of time required to attain steady state against different rock sizes, for diffusion of H^+

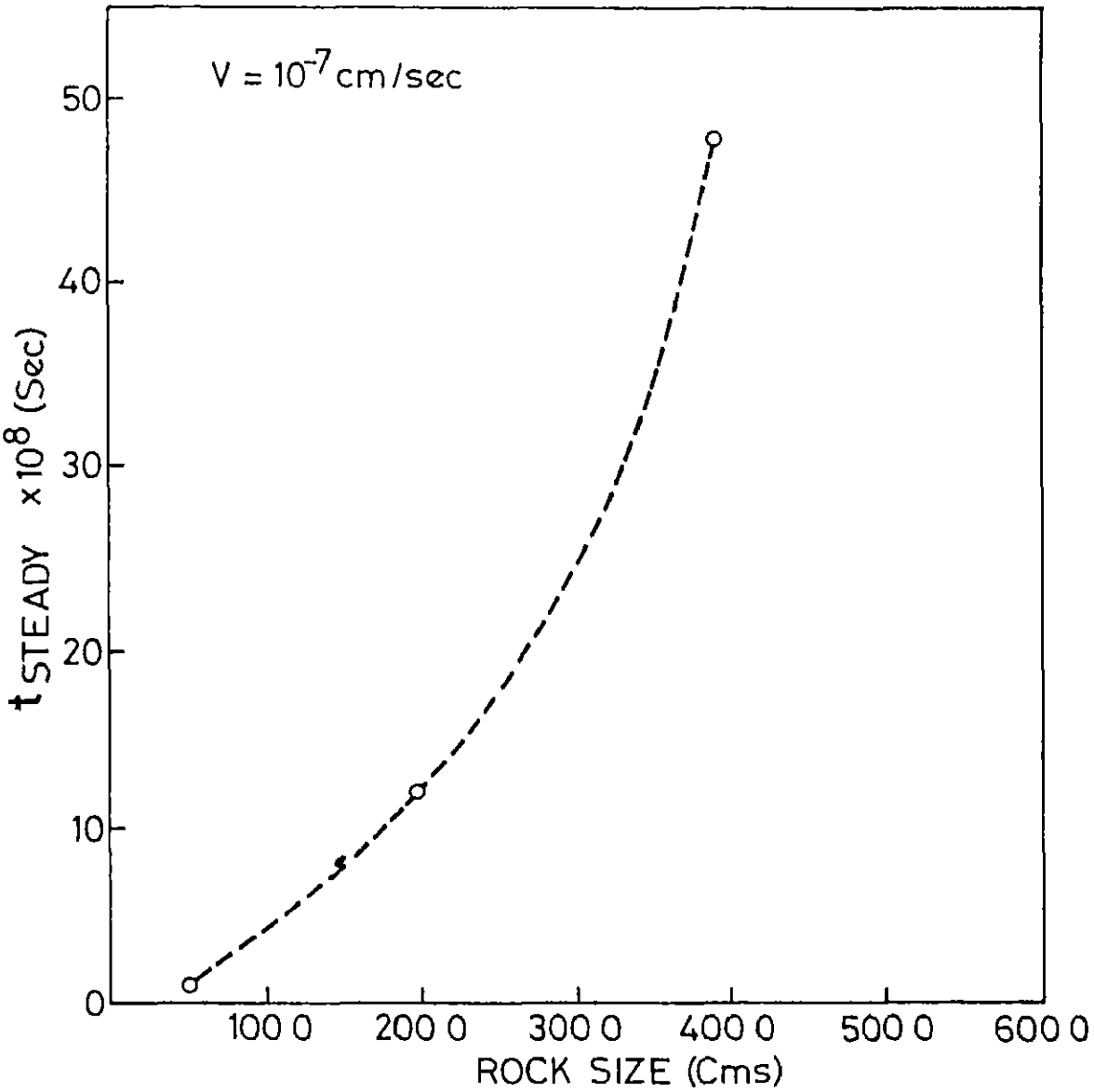

Fig. 4.10 Plots of time required to attain steady state against different rock sizes, for diffusion of H_4SiO_4

former shows the case of H diffusion and the latter shows the case of H_4SiO_4 diffusion. In both the cases, the increment is monotonic.

(c) Effect of Change in ground water percolation velocity on diffusion, with distance remaining constant.

Effects of change in ground water percolation velocity on the diffusion of H^+ and H_4SiO_4 have been studied by keeping distance constant for each case and changing the velocity of ground water in such a manner so as to keep the Peclet numbers unchanged This has has been done for comparison with the results given in Tables 4.3 and 4.4.

For diffusion of H^+, distance is kept constant at 20 cms and for diffusion of H_4SiO_4, it is kept constant at 50 cms. From Table 4.3 it can be seen that for the three different Peclet numbers, viz 0.2, 0.4 and 0.6, percolations velocities are 10^{-6} cm/sec, $2x10^{-6}$ cm/sec and $3x10^{-6}$ cm/sec respectively. However, this change fails to affect the calculated time to attain steady state, which in same (13.88 days) for all the three cases

For the diffusion of H_4SiO_4, table 4.4 furnishes similar result. In this case, for Peclet numbers 0.5, 2.0 and 4.0, velocities of percolations were 10^{-7} cm/sec, $4x10^{-7}$ cm/sec and $8x10^{-7}$ cm/sec. However, in all the cases, calculated time to attain steady state become same (7.93 years).

TABLE 4 3

Case No	Percolation Velocity of ground water (v) (cm/sec)	Peclet Number ($Pe=V.x_{Ref}/D_H$) (dimensionless)	Calculated time to attain steady-state (Days)
1.	10^{-6}	0.2	13.88
2	$2x10^{-6}$	0 4	13 88
3.	$3x10^{-6}$	0.6	13.88

TABLE 4 4

Case No.	Percolation velocity of ground water (v) (cm/sec)	Peclet Number ($Pe=V.x_{Ref}/D_S$) (Dimensionless)	Calculated time to attain steady-state (years)
1.	10^{-7}	0 5	7.93
2.	$4x10^{-7}$	2.0	7.93
3.	$8x10^{-7}$	4 0	7.93

These calculations show that as long as Peclet numbers remain the same, any change in percolation velocity of ground water or distance fails to affect the time required to attain steady state.

(d) Concentration profiles drawn over real distances ·

To see the dependence of steady state concentration profiles on rock sizes, for a given ground water velocity, concentrations (in dimensionless form) have been plotted against real (i.e., dimensionalised) distances (i e., rock thicknesses) in figures 4.11 and 4 12. The former shows the case of diffusion of H^+ while the latter that of H_4SiO_4. In both the cases, ground water velocity was kept constant at 10^{-7} cm/sec and the only variable was rock size. It can be seen that in both the diagrams, concentration profile is different for different rock sizes and no part is common among them. This proves that, at least for small thicknesses, rocks of different thickness weather in different ways.

(e) Study of diffusion when both distance (x) and ground water velocity (v) vary.

Figures 4.13 and 4.14 show the effects of small changes in the velocity of percolation from the value 10^{-7} cm/sec on the steady state profiles, over real rock thicknesses. Fig. 4.13 shows the case of diffusion of H^+.

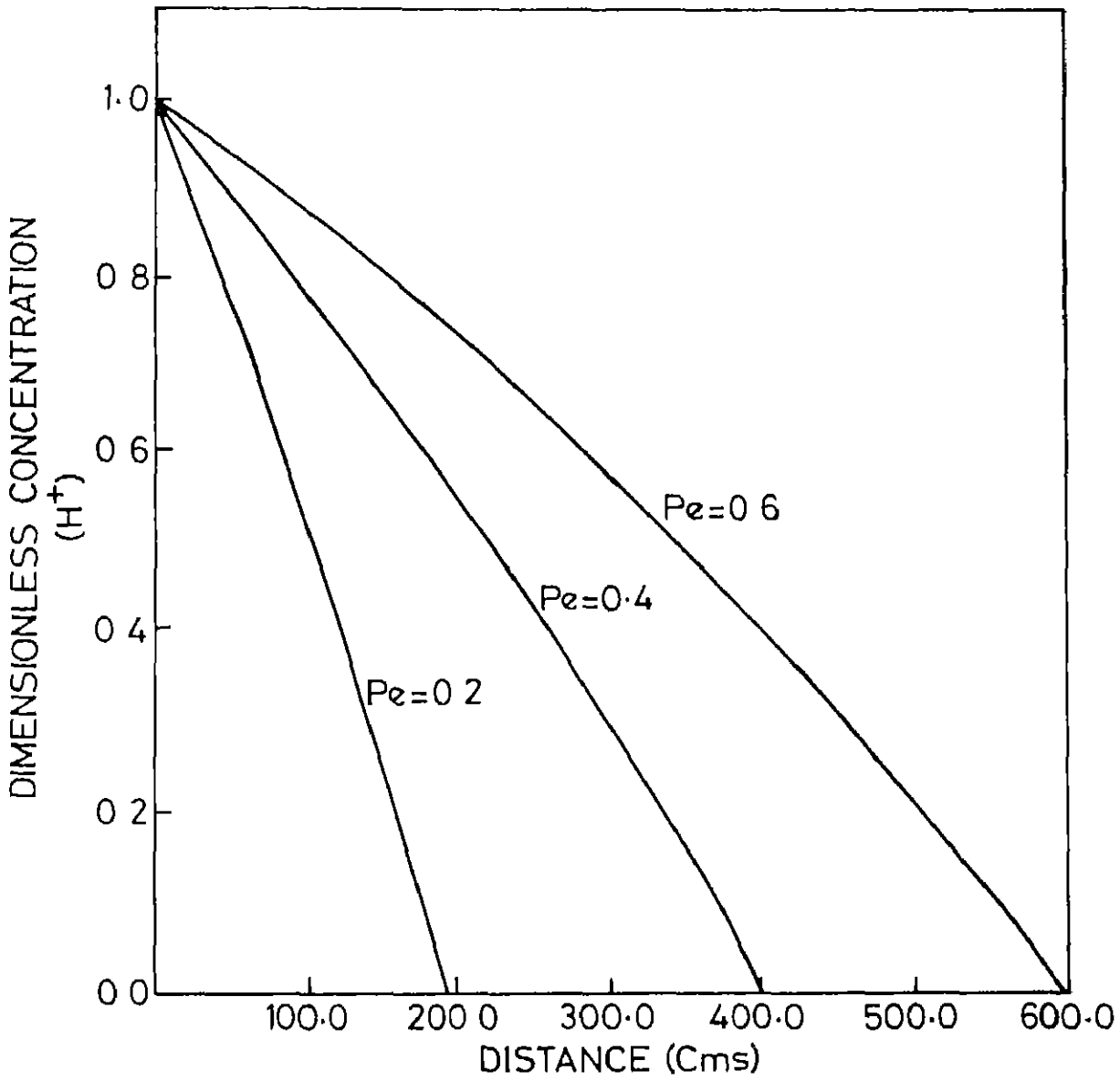

Fig. 4 11 Steady state concentration profiles of H^+ over different real distances, for three different Peclet numbers

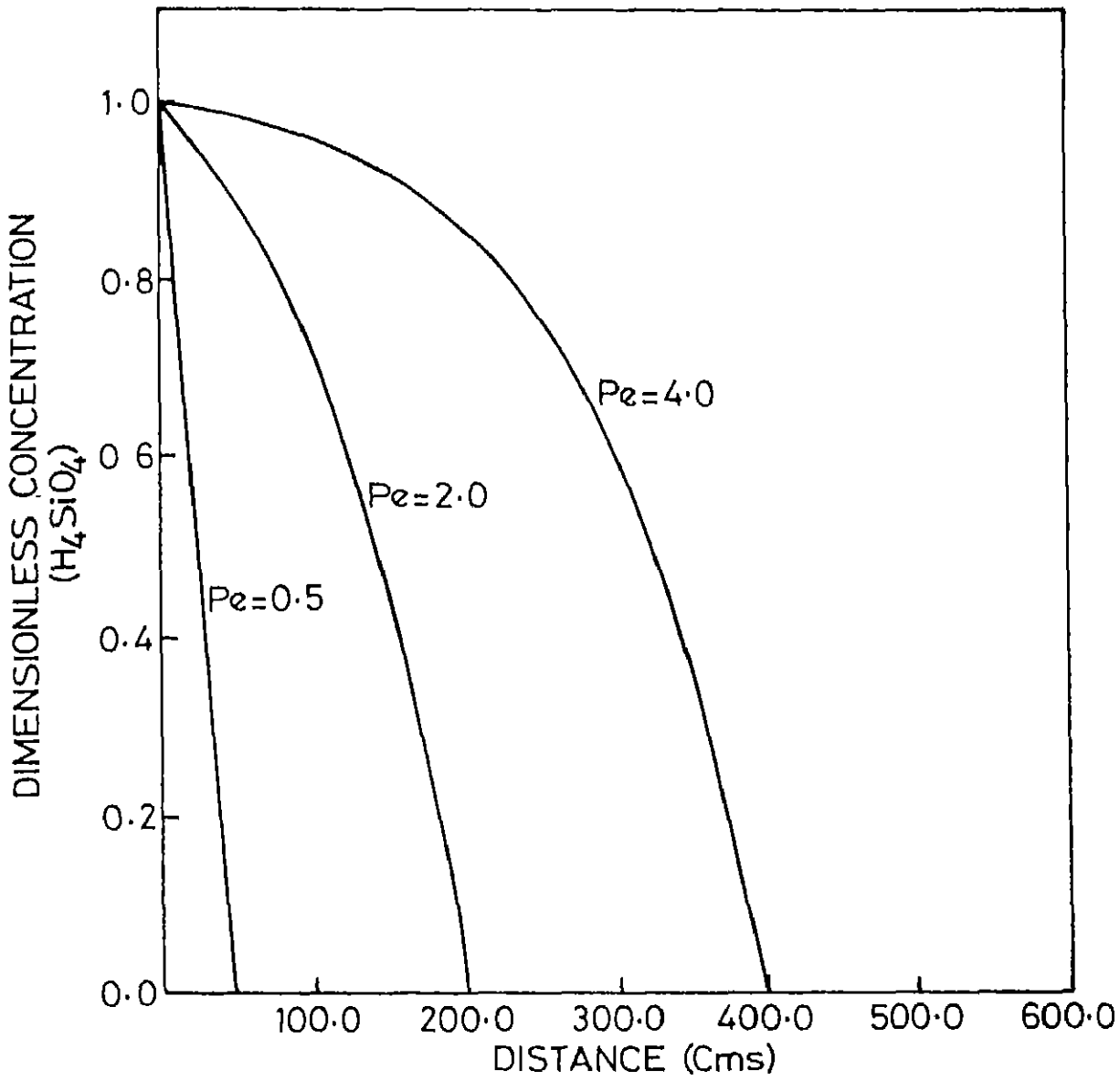

Fig. 4.12 Steady state concentration profiles of H_4SiO_4 over different real distances, for three differ, ent Peclet numbers

For the same rock thicknesses of 200 cms, 400 cms and 600 cms, the effect of two different velocities on steady states are shown It can be observed that for a small change in the magnitude of percolation velocity (v), the steady state profiles do not change appreciably for smaller Peclet numbers However, a large change in percolation velocity, with the thickness (i.e., distance) remaining same, will increase the value of Peclet number appreciably and as a consequence, steady state profile will also change markedly.

Fig 4.14 illustrates the same effect, as described above, in case of diffusion of H_4SiO_4 for three values of rock thicknesses, viz: 50 cms, 200 cms and 400 cms.

(f) Profiles over large-scale real distances ·

Till now, we have been dealing with diffusion of H^+ and H_4SiO_4 through arbitrarily chosen rock sizes (i.e.,distances). Now, we apply the same boundary conditions to a problem of diffusion of H^+ and H_4SiO_4 through a rock thickness of 70 m. This thickness has been chosen because in Chapter 3 of this thesis, we have calculated the time of weathering of a 70 m thick parent rock by chemical mass balance technique. So, it will help in comparing the results with the steady state time obtained by the method of diffusion. It may possibly suggest the relative role of diffusion in the total time required for the formation of a

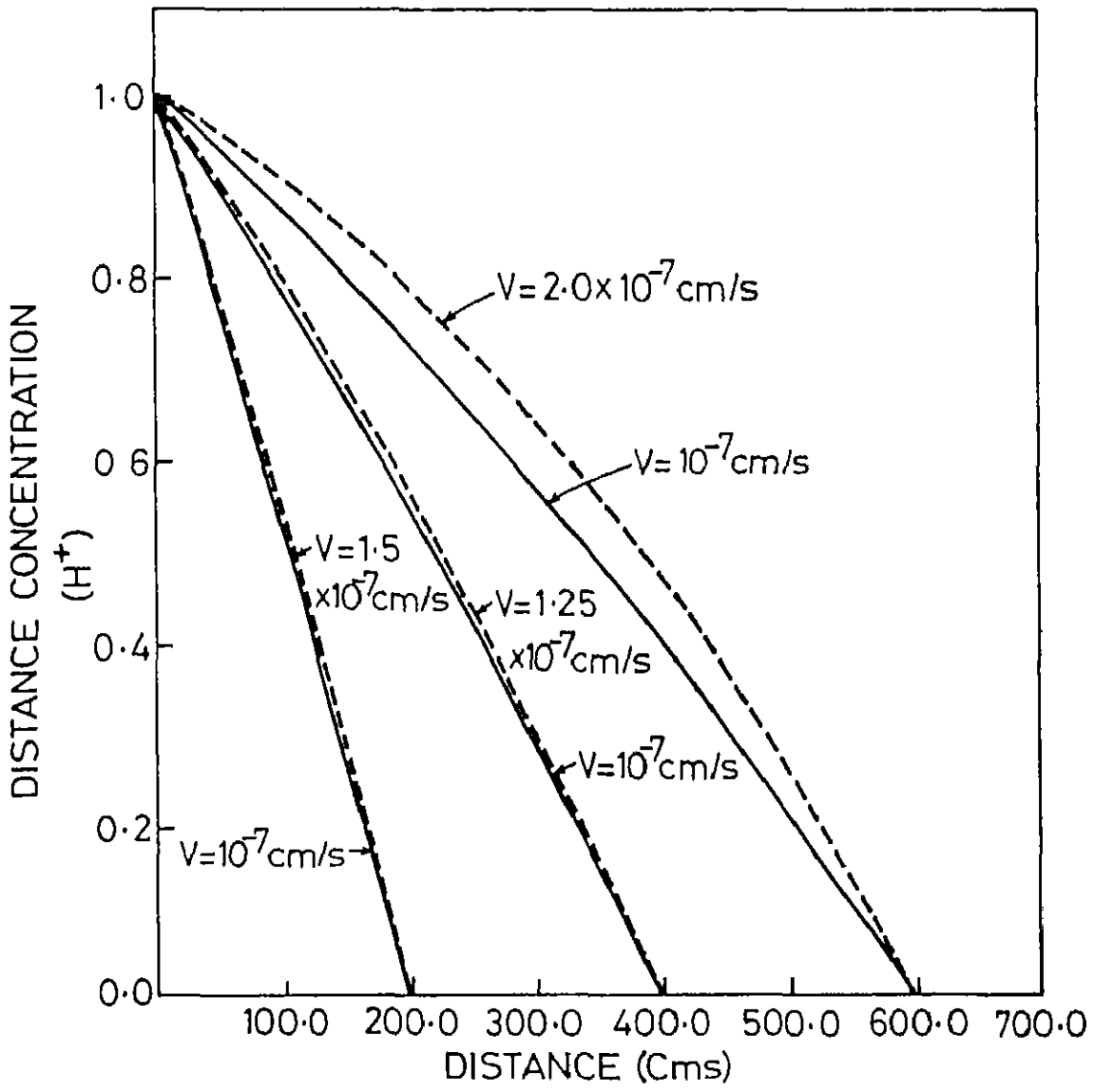

Fig. 4 13 Variation in steady state concentration profiles of H^+ for different values of ground water percolation velocity

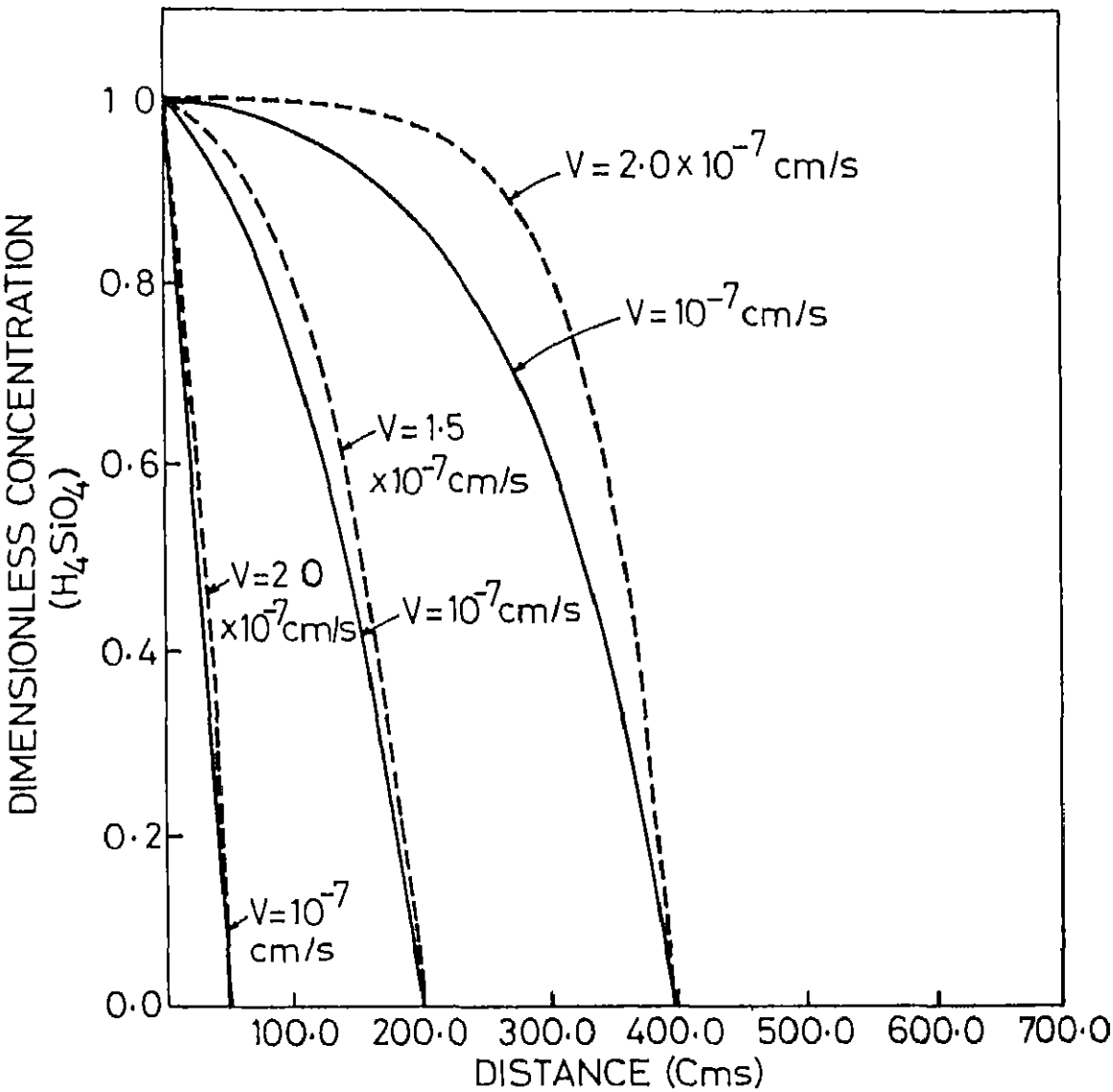

Fig. 4 14 Variation in steady state concentration profiles of H_4SiO_4 for different values of ground water percolation velocity

given thickness of weathered product.

Fig 4.15 shows the steady state profile of concentration of H^+ against distance, i.e., rock size (both in dimensionless form). Fig. 4 16 shows the same parameters for the diffusion of H_4SiO_4. Table 4.5 furnishes all the relevant data with the calculated time required for attaining steady-state.

From table 4.5, it can be seen that although the distance through which diffusion takes place, is same for both the cases, there is a marked difference in steady-state time. This is because of the difference in the value of diffusivity. Distance, i.e., rock thicknesses remaining same, the less the value of diffusivity, the more the time required to attain steady state.

A notable feature of these two diagrams is the existence of concentration boundary layer. For diffusion of H^+(Fig. 4.15), it can be seen that upto a distance of about (0.62x70) m, i.e., 43.4 m, concentration at every grid point is same as the upper boundary value (= 1.0, in dimensionless form) and while, for diffusion of H_4SiO_4 (Fig. 4.16), upto a distance (i.e., thickness) of about (0.88x70)m, i.e., 61.6 m, concentration is same as in the upper boundary (= 1.0, in dimensionless form). Beyond these thicknesses, boundary layers seem to exist where diffusion has a significant role in creating concentration gradient. In the former case, thickness of the boundary layer (δ) is 26.6 m while in the latter case, it is 8.4 m.

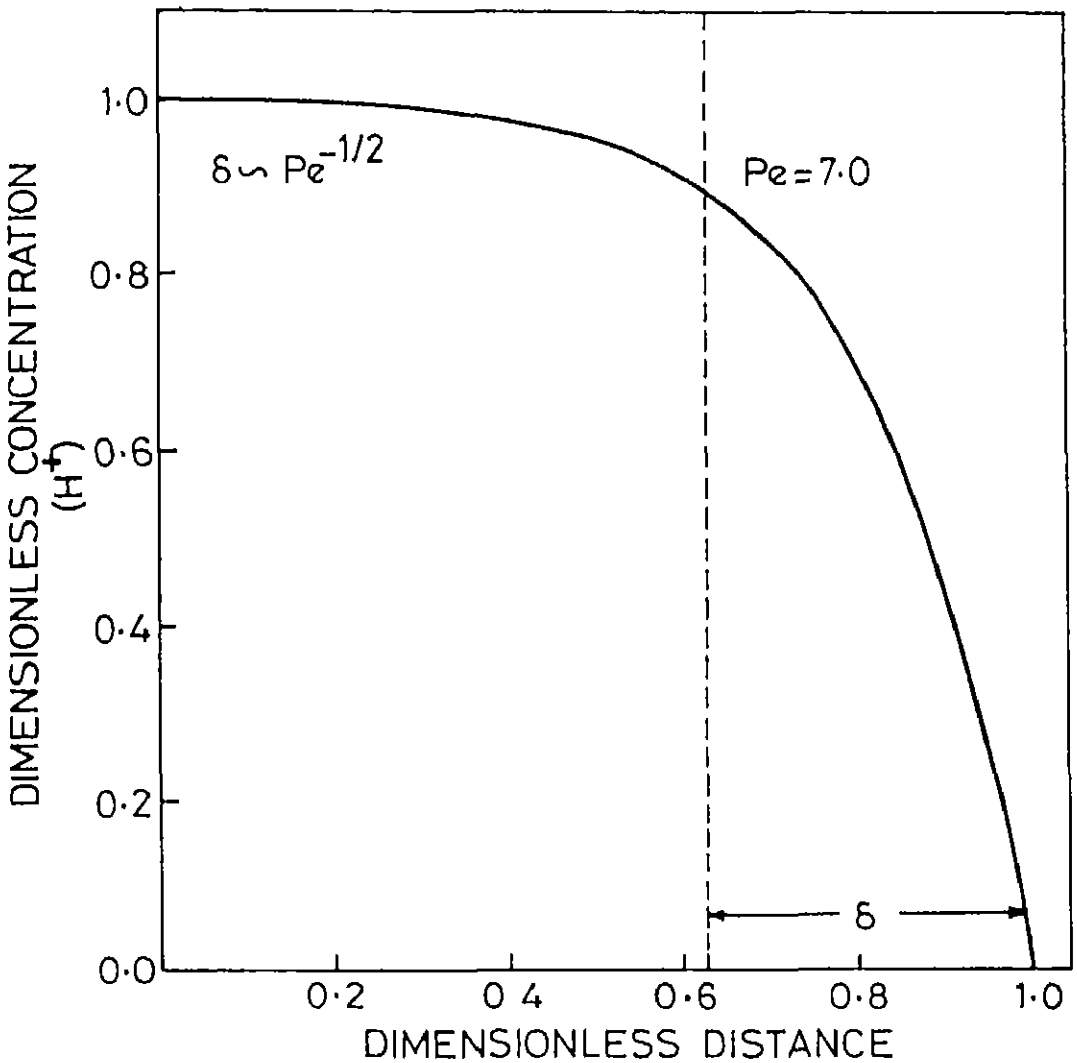

Fig 4.15 Diagram showing concentration boundary layer for diffusion of H^+ (Peclet number = 7 0)

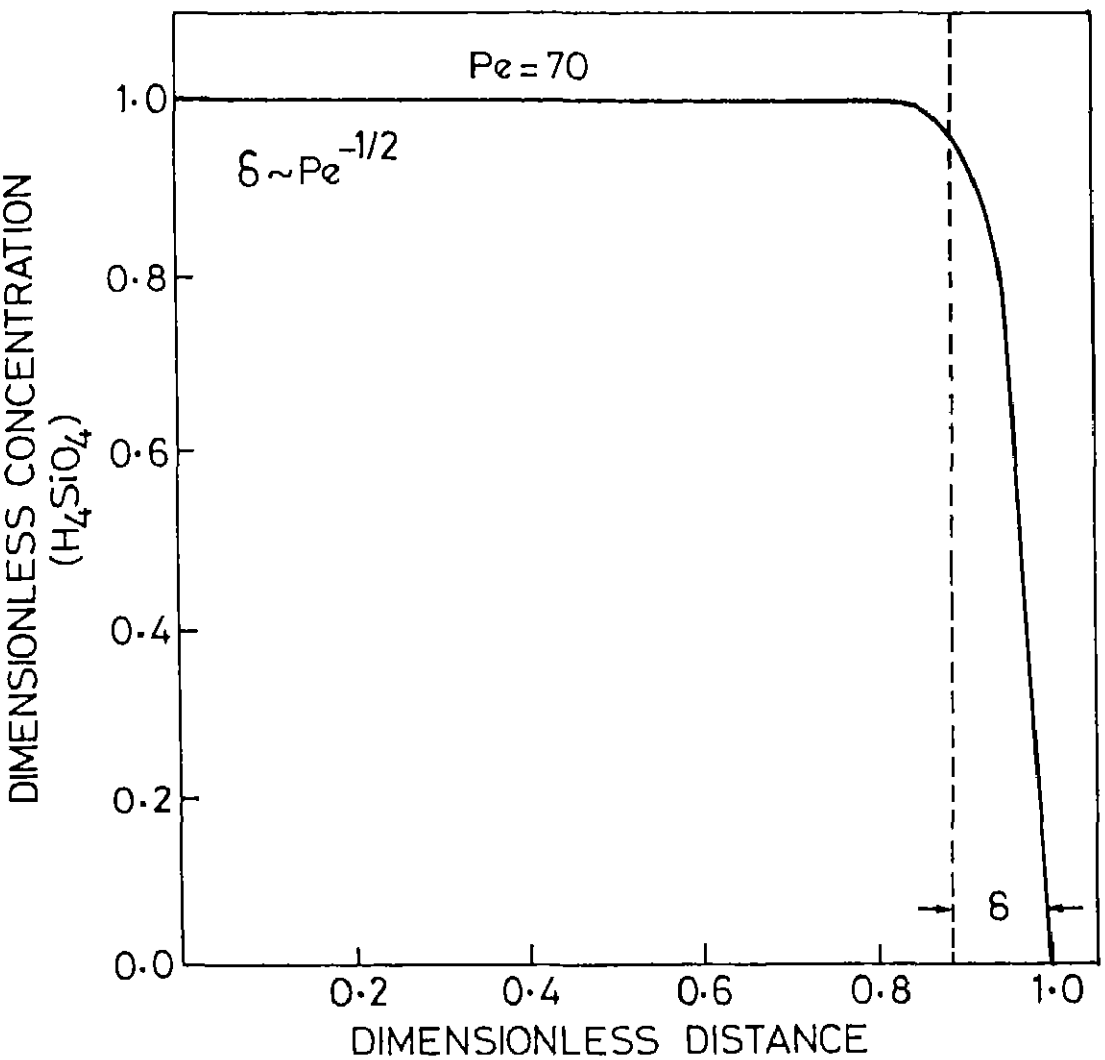

Fig. 4 16 Diagram showing concentration boundary layer for diffusion of H_4SiO_4 (Peclet number=70.0)

TABLE 4 5

,ase	Distance (ı.e., rock sıze)(l) (m)	Distance reference (X_{Ref}) (m)	Pecelet Number ($Pe=V.x_{Ref}/D$) (Dımensıonless)	Calculated tıme to attaın steady state (years)
Dıffusıon of H^+	70	70	7 0	7769.0
Dıffusıon of $H_4SıO_4$	70	70	70.0	77689.0

4 7 COMPARISON OF NUMERICAL SOLUTION WITH ANALYTICAL SOLUTION OF THE GOVERNING DIFFERENTIAL EQUATION

The differential equation for convective diffusion is:

$$\frac{\partial C}{\partial t} + V \cdot \frac{\partial C}{\partial x} = \eta \, D' \, \frac{\partial^2 C}{\partial x^2} \qquad (8)$$

where, c = concentration

t = time

x = distance

D' = diffusivity

η = tortuosity factor

v = percolation velocity of ground water

In our present study, we have not considered tortuosity as a separate parameter. On the contrary, we have used the value of an effective diffusivity (D) which takes into account the effects of tortuosity. So, this governing equation changes to

$$\frac{\partial C}{\partial t} + V \cdot \frac{\partial C}{\partial x} = D \cdot \frac{\partial^2 C}{\partial x^2} \qquad (9)$$

Golubev and Garibyants (1971) have discussed about the analytical solution of the above equation. The following account has been largely drawn upto from their treatment. They have treated the problem of convective diffusion through porous media with various boundary condition. The most appropriate of them, for the present study is the case

of - "Filtration from a steady source" This is because, in our cases, we have always maintained the concentration at one end fixed (i e., c(x=0, t=t) values are constants for the diffusion of H^+ and H_4SiO_4)

Thus, under the boundary and initial conditions of·

$x > 0,\ t = 0,\ c(x,t) = 0$

$x = 0,\ t > 0,\ c(x,t) = \text{constant}$

$= C_o$ (say)

The solution of the equation (9) has the form :

$$C(x,t) = \frac{C_o}{2}\left[\left(1-\text{erf}\left(\frac{x-Vt}{2\sqrt{Dt}}\right)\right) + e^{Vx/D}\left(1-\text{erf}\left(\frac{x+Vt}{2\sqrt{Dt}}\right)\right)\right] \qquad (10)$$

where, erfx is the error function of x defined as

$$\text{erfx} = \frac{2}{\sqrt{\pi}} \int_o^x \exp(-y^2)\, dy$$

In the subsequent analytical treatment, we take the initial concentration profile as given in the condition above, i.e., for $x > 0,\ t = 0,\ C(x,t) = 0$.

Comparison between analytical and numerical solutions - for diffusion of hydrogen ions (H^+) :

Out of the three distances (i.e., rock sizes) which we considered in numerical treatment, only two values, viz., 200 cms and 600 cms have been chosen for which diffusion of H^+ is compared.

For the present cases .

D = diffusivity of H^+ = 10^{-4} $cm^2/sec.$

t = time required to attain steady state for diffusion through rocks of 200 cms and 600 cms length

v = 10^{-7} cm/sec.

From the numerical result (obtained with the help of finite difference procedure), time required to attain steady state is first computed. This value of t along with the values of D and V are substituted in the equation (10). Defining dimensionless concentration variable C* as C* = $C(x,t)/C_o$, we arrive at a functional relationship between C* and the distance variable x. Figures 4 17 and 4.18 display the plots of C* against x (in cms), for two rock sizes viz· 200 cms and 600 cms respectively. In each plot, the dashed line shows concentration profile drawn from analytical result while the solid line shows concentration profile drawn from numerical results.

It can be noted that in both the cases, trends of concentration distribution are· similar and comparable. However, towards the boundary x = 1 (= 200 cms and 600 cms respectively), increasing disparity exists between the two profiles. This disparity is expected and can be explained in terms of dissimilar conditions at the boundary x = 1. In case of analytical treatment, solution was essentially obtained for a semi-infinite solid with no condition specified at x = 1, while, in case of numerical method, there is always a fixed concentration of H^+ specified by

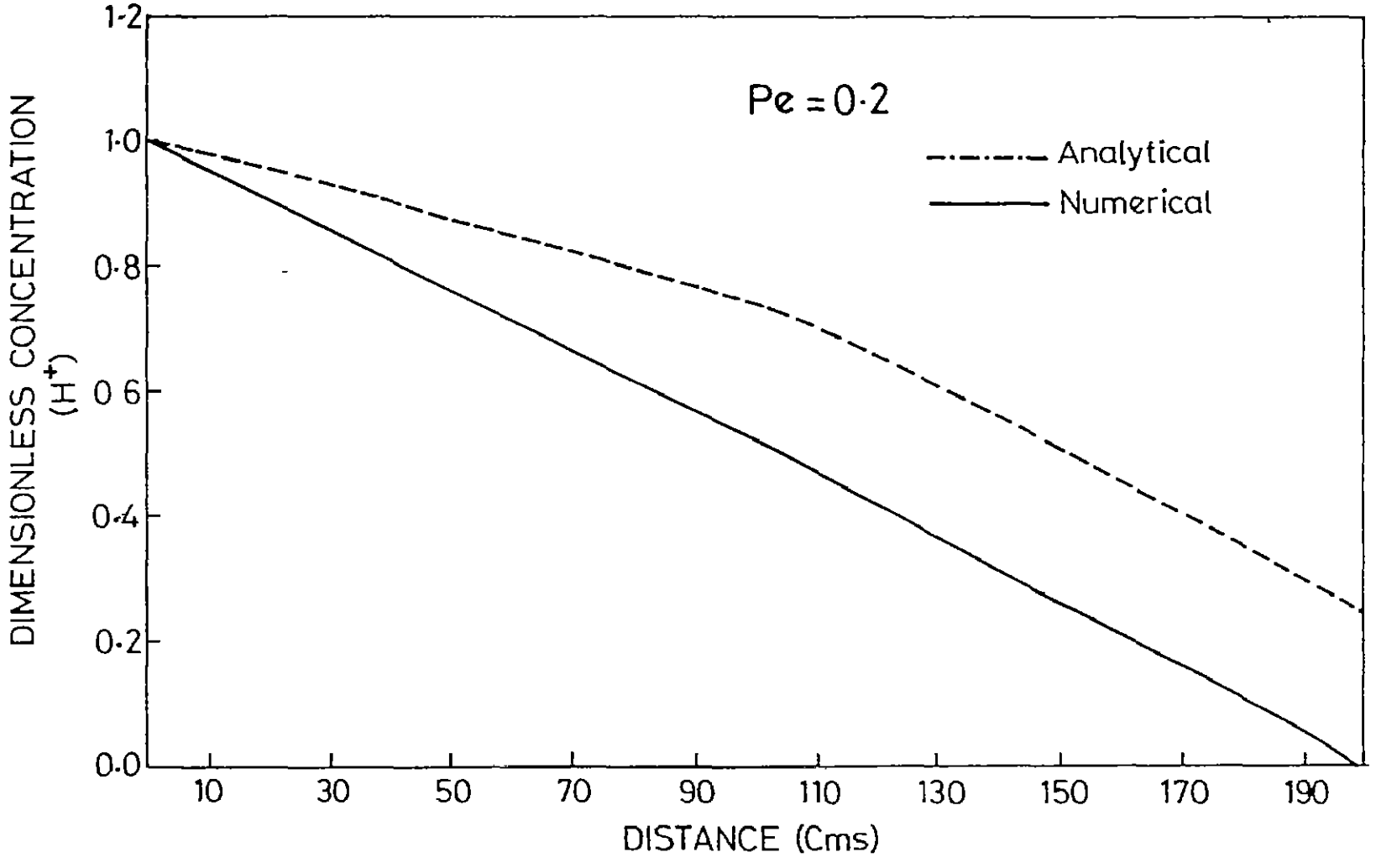

Fig. 4.17 Comparison of numerical and analytical results for diffusion of H^+ (Distance taken in numerical solution = 200 cm , Peclet number = 0.2)

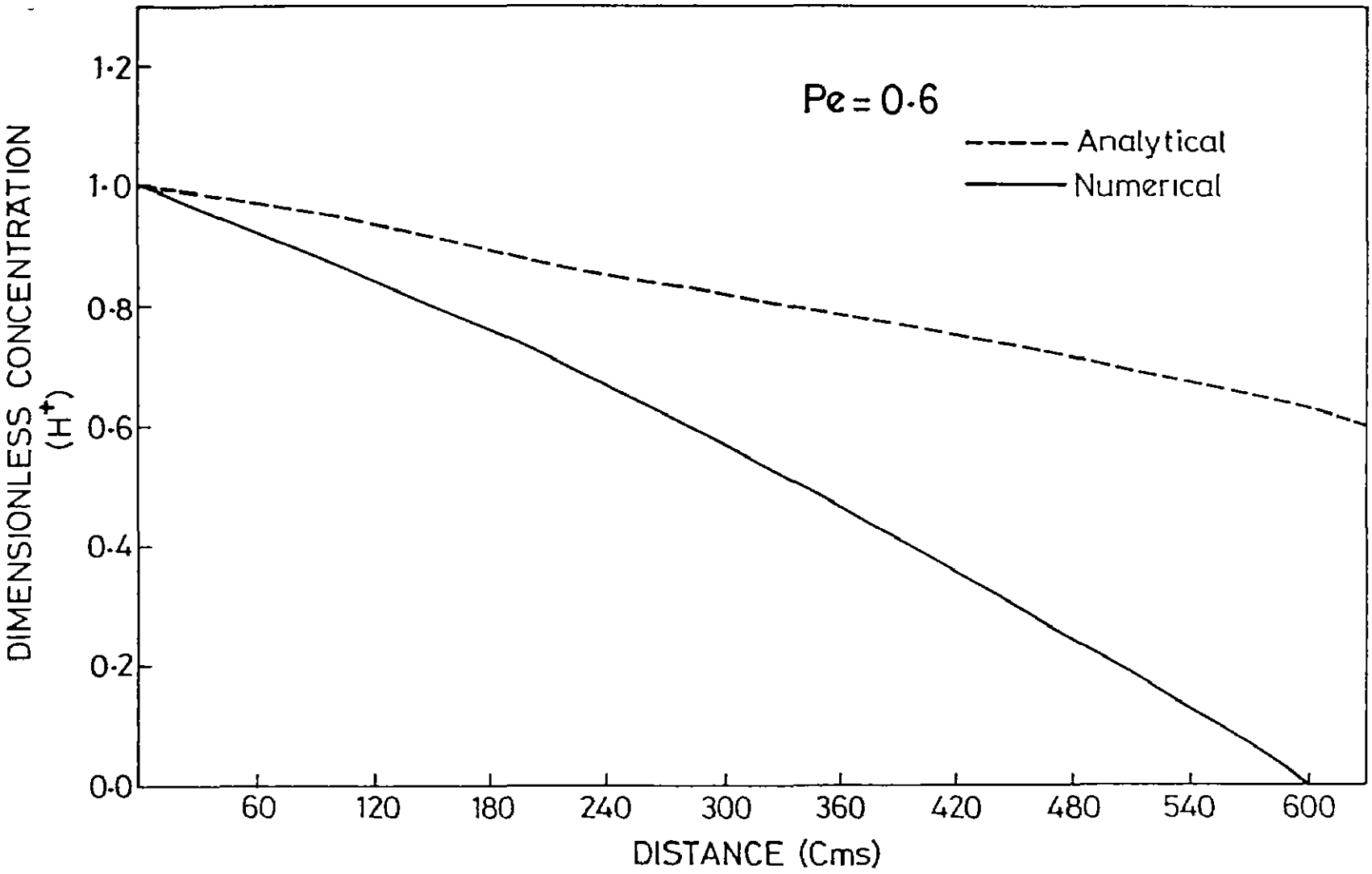

Fig. 4.18 Comparison of numerical and analytical results for diffusion of H^+
(Distance taken in numerical solution= 600 cms
Peclet number = 0.6)

the prevailing equilibrium reaction at x = 1.

Comparison between analytical and numerical solution - for diffusion of silicic acid

Out of the three rock-sizes which were taken into account for numerical investigation of diffusion of silicic acid, two cases, with rock sizes of 50 cms and 400 cms are now considered for comparison with analytical solution.

The same initial condition as taken before is applicable here too as well.

For these cases .

D = diffusivity of H_4SiO_4 = 10^{-5} $cm^2/sec.$

t = time required to attain steady-state

v = 10^{-7} cm/sec.

As done before, at first, time required to attain steady-state for diffusion of H_4SiO_4 is computed, numerically. With known values of t, V and D, we get a functional relationship between C* and x (in cms) in these cases also. Figures 4.19 and 4.20 show plots of C* against x for diffusion of H_4SiO_4 at steady-state time.

As in case of H^+, here also a progressive, disparity between the numerical and analytical profiles is observed as we approach towards the boundary x = 1 (= 50 cms and 400 cms respectively). In these cases, the reason of this disparity is the presence of a time dependent condition

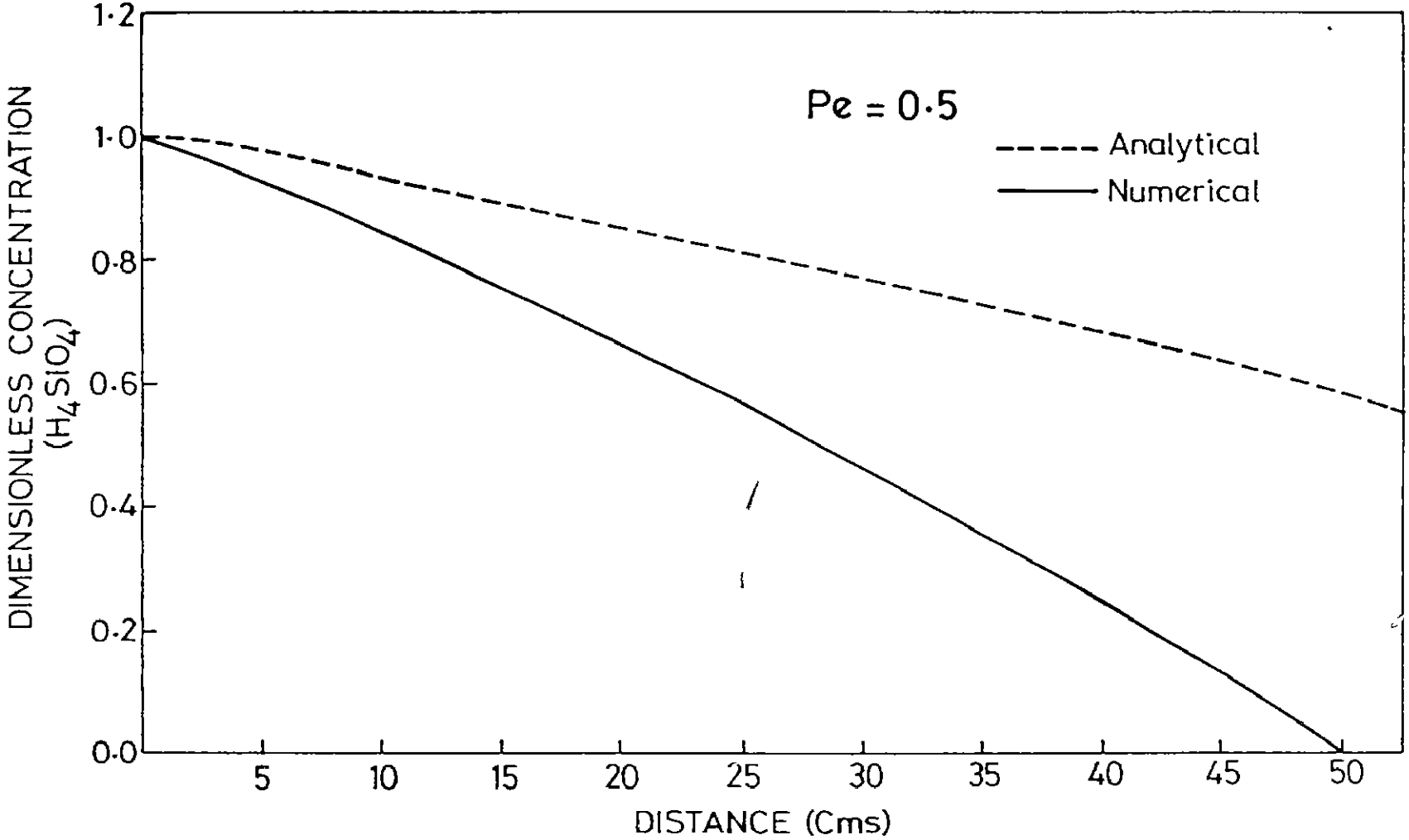

Fig. 4.19 Comparison of numerical and analytical results for diffusion of H_4SiO_4
(Distance taken in numerical solution = 50 cms
Peclet number = 0.5)

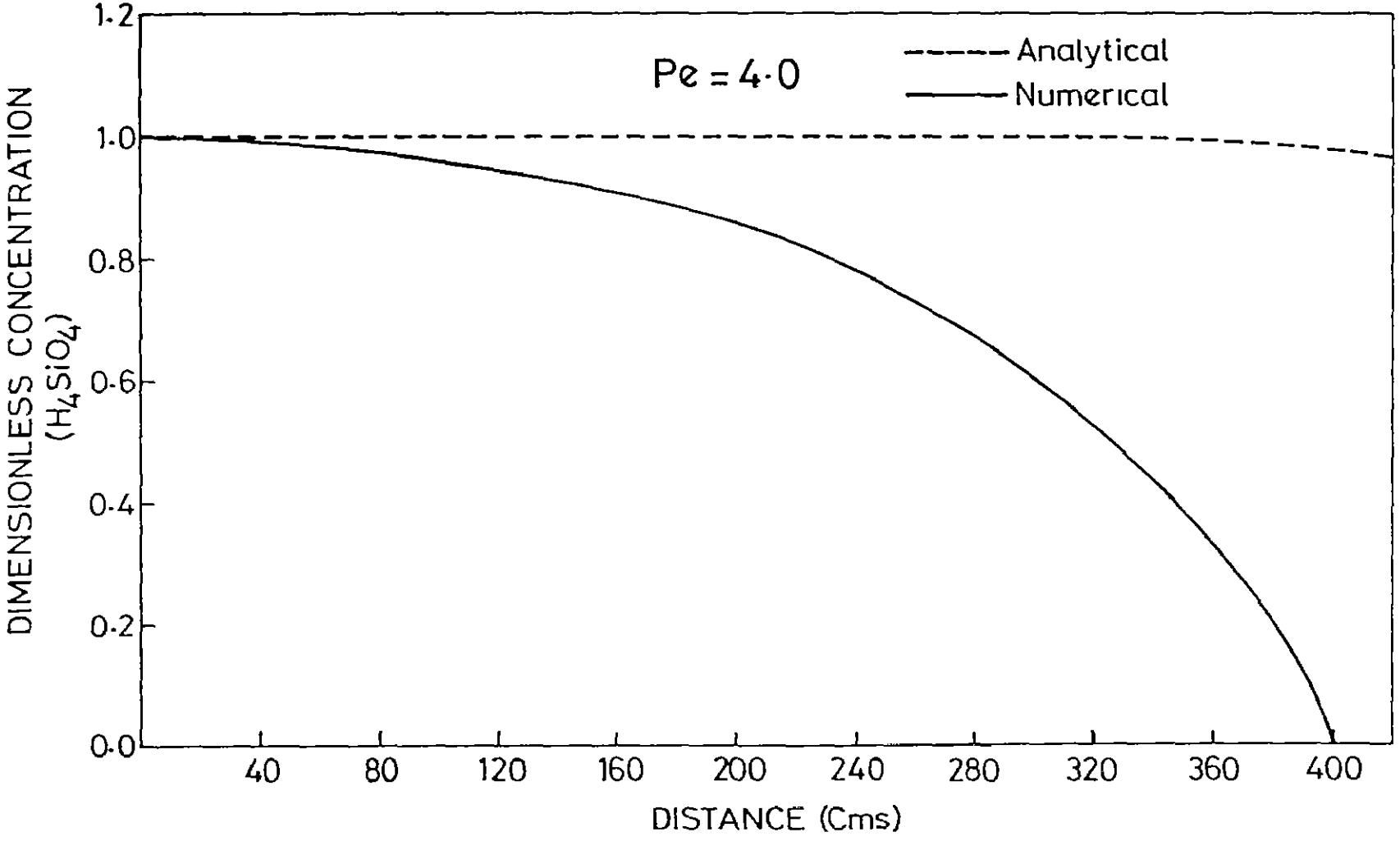

Fig. 4.20 Comparison of numerical and analytical results for diffusion of H_4SiO_4
(Distance taken in numerical solution=400 cms
Pecklet number = 4 0)

(Wollast-rate of release of silicic acid) at the boundary x = 1, which is ignored in case of analytical solution and once again semi-infinite formulation is used there with no specified condition at x = 1

Calculation of maximum distance traversed by the diffusing substances under semi-infinite mode of diffusion ·

With some reasonable assumptions, equation (10) can be expressed in such a way so that the maximum distance that a diffusing species will travel, can be computed The following treatment is adapted from Golubev and Garibyants (1971). If x and t are rather large, then expanding erf ($\frac{x + Vt}{2\sqrt{Dt}}$) into a series, it can be shown that the second term of the equation (10) is small as compared to the first term and may be neglected Therefore, the asymptotic solution of equation (9), for conditions as described before, has the following form

$$C(x,t) = \frac{C_o}{2} [1 - \text{erf} (\frac{x - Vt}{2\sqrt{Dt}})] \qquad (11)$$

Without any great error eqn (11) can be written as .

$$C(x,t) = \frac{C_o}{2} [1 - \frac{x - Vt}{\sqrt{\pi Dt}}] \qquad (12)$$

Now, for a minimal concentration which is still detectable in practice (i.e., chemically), we have,

$$C_{min} = \frac{C_o}{2} [1 - (\frac{x_{max} - Vt}{\sqrt{\pi Dt}})] \qquad (13)$$

where, x_{max} is the maximum distance of migration of the diffusing substance.

From eqn. (13),

$$x_{max} = Vt + (1 - 2.\frac{C_{min}}{C_o})\sqrt{\pi Dt} \qquad (14)$$

For $C_{min} << C_o$, we have,

$$X_{max} = Vt + \sqrt{\pi Dt} \qquad (15)$$

Among the two parts of the expression for X_{max}, Vt corresponds to the distance-component contributed by percolation velocity of the solution. The other part i.e., $\sqrt{\pi Dt}$ corresponds to the distance-component contributed by *diffusion only*

The parameter t in the expression of x_{max}, can be any time after the onset of diffusion. However, in present cases, we have used only the time required to attain steady state in each case. Using these time values along with appropriate values of V and D, theoretical values of x_{max} are calculated.

Tables 4.6 and 4.7 furnish the distance of diffusion (i.e., rock sizes) as taken in numerical analyses along with the calculated values of x_{max}.

Figures 4.21 to 4.24 show the concentration distribution upto theoretical x_{max} along with the concentration distribution furnished by numerical solution upto the pre-defined distances. The first two plots show the case of diffusion of H^+ while the last two show that

TABLE 4.6

Diffusing substance Hydrogen ions (H^+)

Case No	Peclet Number (Dimensionless)	Distance (l) (cm)	Calculated X_{max} using eqn (15) (cms)
1.	0.2	200	372
2.	0.6	600	1422

TABLE 4.7

Diffusing substance : Silicic acid (H_4SiO_4)

Case No.	Peclet Number (Dimensionless)	Distance (l) (cm)	Calculated X_{max} using eqn.(15) (cms)
1.	0.5	50	113.5
2.	4.0	400	2308.0

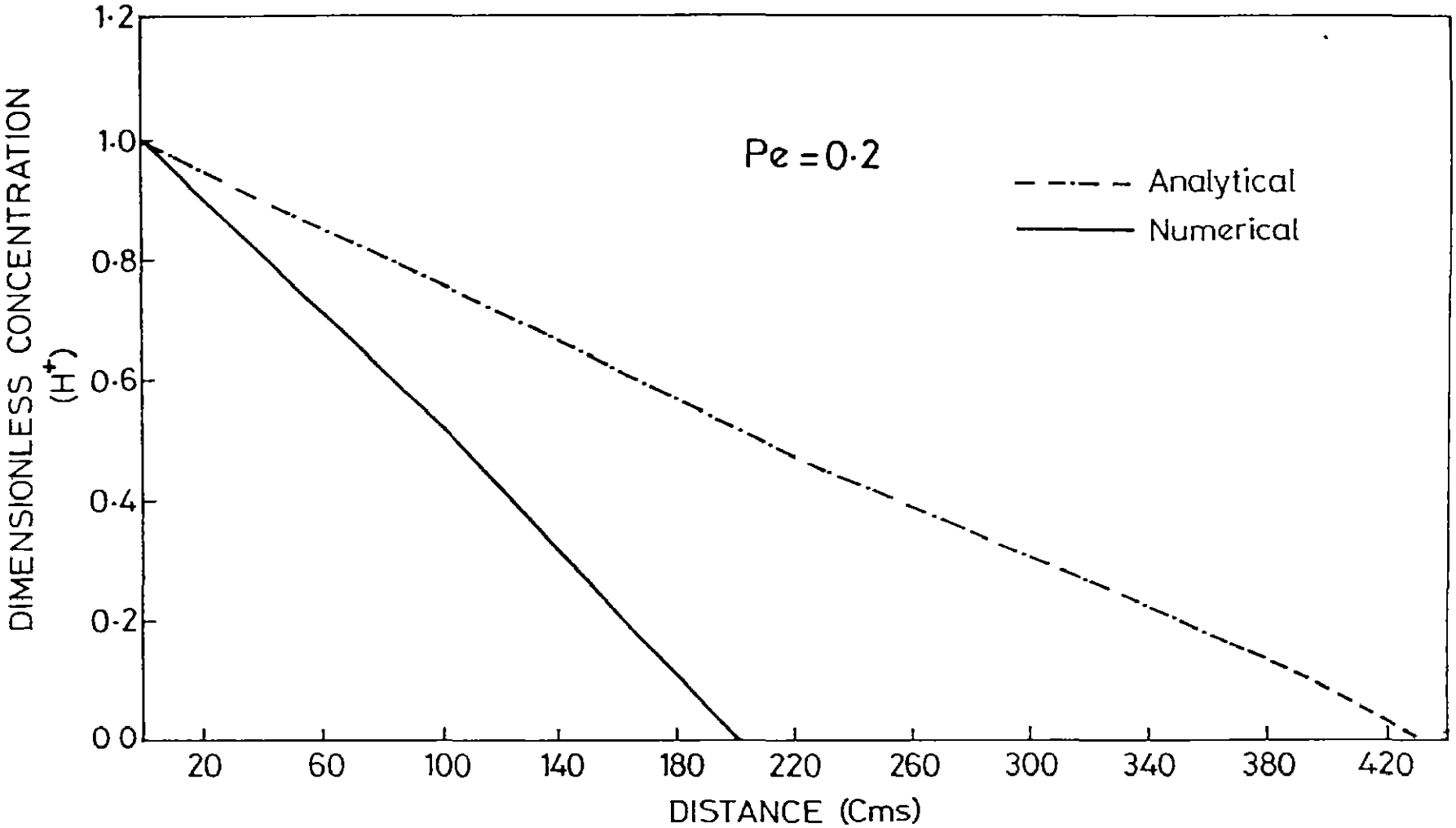

Fig 4.21 Plot of steady state concentration profile of H^+ obtained numerically along with analytical result plotted upto X_{max}. (Distance taken in numerical solution=200 cms)

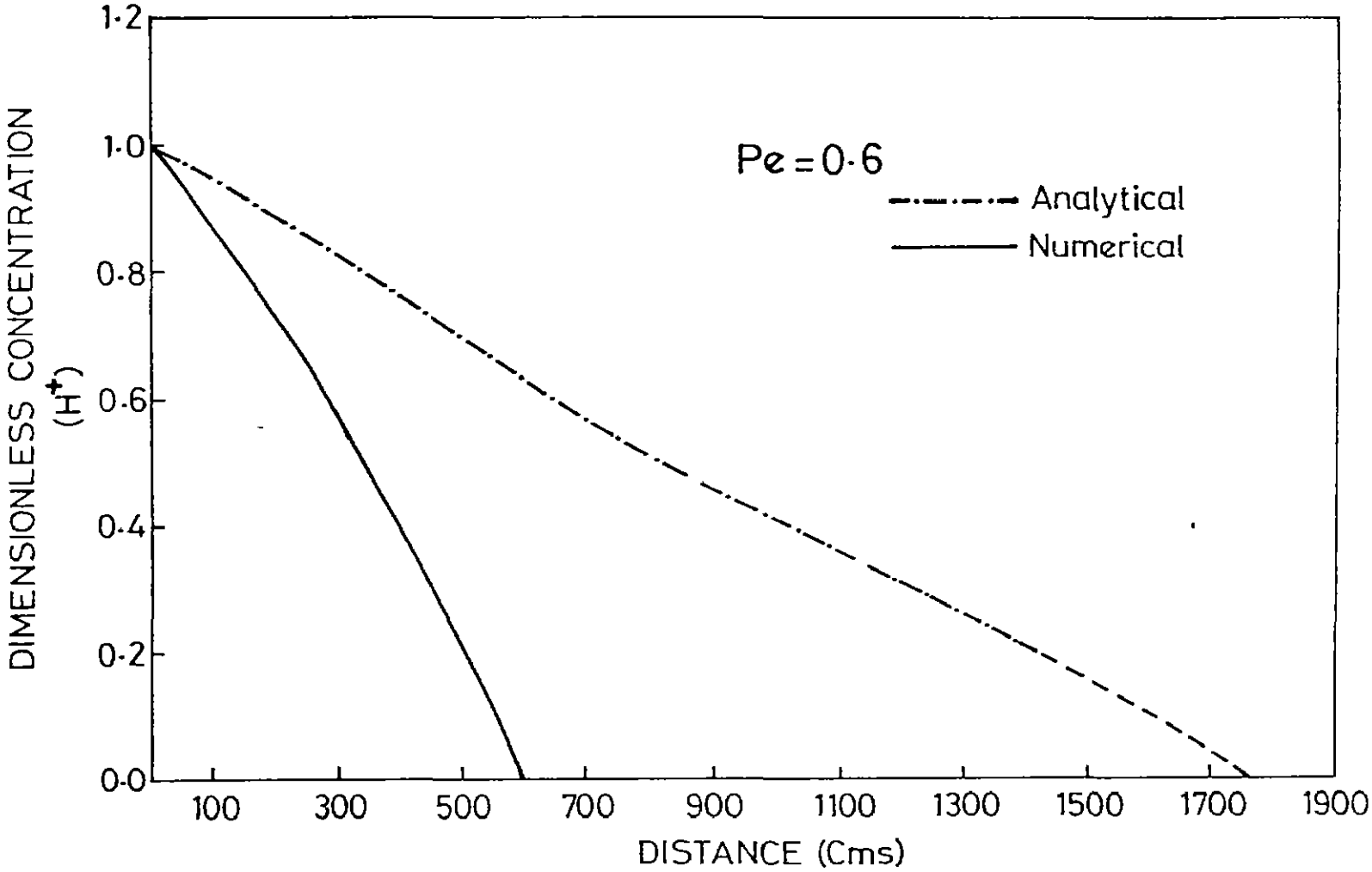

Fig. 4.22 Plot of steady state concentration profile of H^+ obtained numerically along with analytical result plotted upto X_{max} (Distance taken in numerical solution = 600 cms)

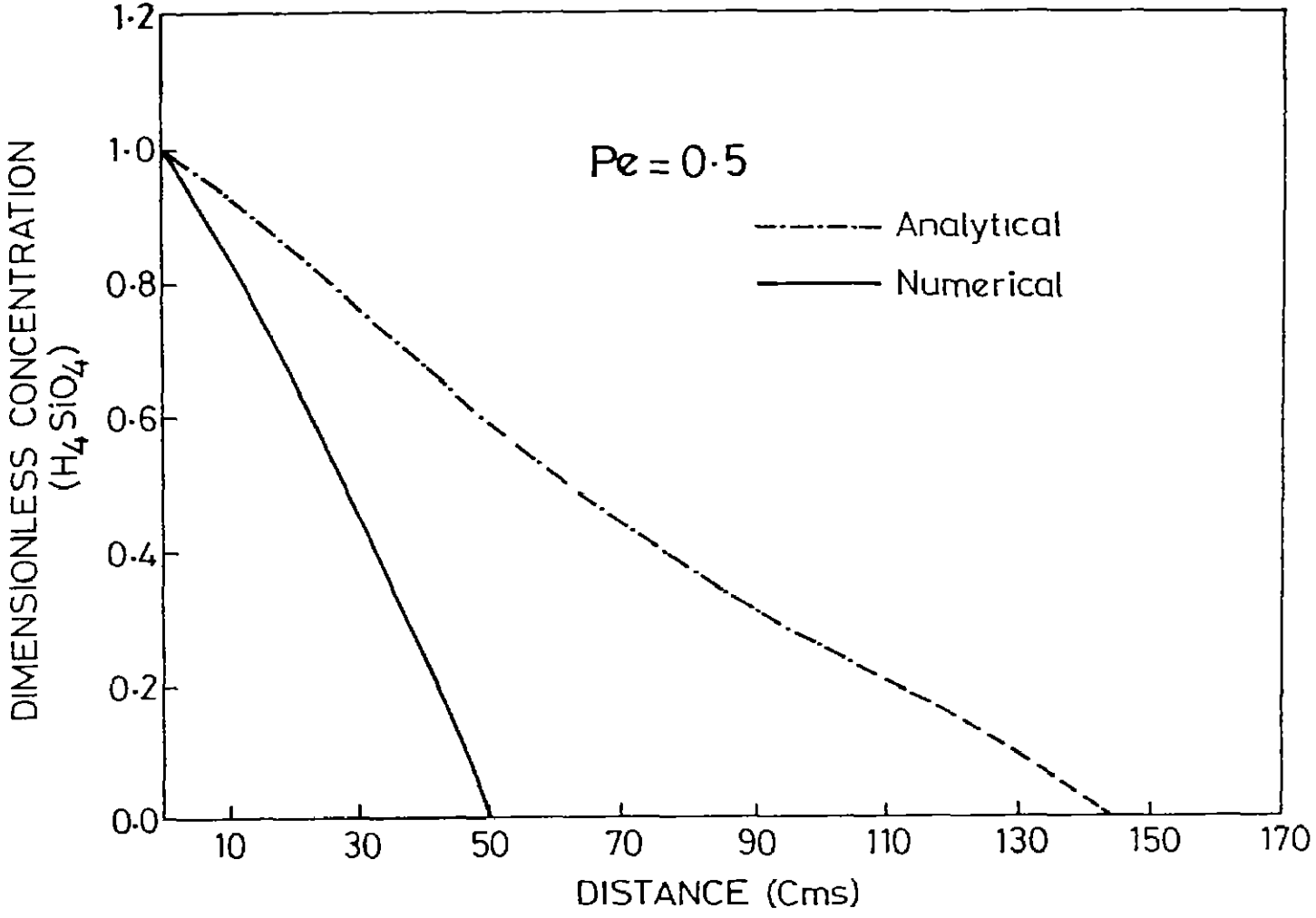

Fig 4.23 Plot of steady state concentration profile of H_4SiO_4 obtained numerically along with analytical result plotted upto X_{max}
(Distance taken in numerical solution=50 cms)

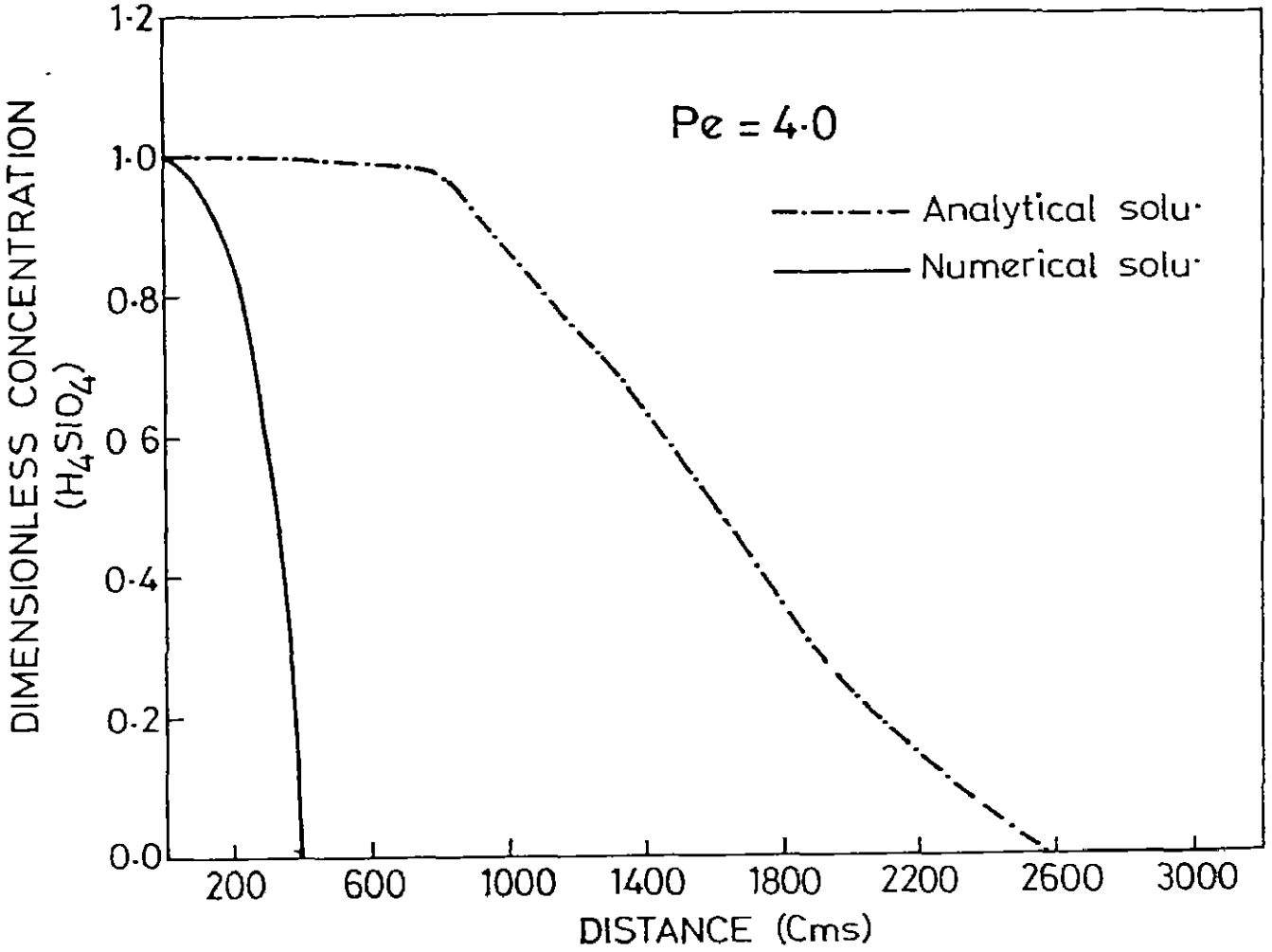

Fig. 4.24 Plot of steady state concentration profile of H_4SiO_4 obtained numerically along with analytical result plotted upto X_{max}
(Distance taken in numerical solution=400 cms)

of H_4SiO_4.

From these diagrams as well as from earlier plots, the following observations can be made :

(a) We have always investigated the aspect of diffusion through finite rock-size. The pre-assigned boundary conditions confine our steady state concentration profiles within the given distance (length of rock body). However, in case of analytical treatment, no condition is imposed at the other boundary towards the direction of flow. This essentially makes the problem semi-infinite type.

(b) It is noticeable that near the boundary having maximum concentration (= 1.0 in dimensionless forms), the concentration profiles displayed by both the methods are close to each other. This is because, at this boundary, conditions are same for both the methods. However, in the other boundary disparity increases rapidly This is because of dissimilar boundary conditions.

(c) It is noteworthy that in all the cases, for the same time (time required to attain steady state in case of numerical solution) x_{max} is always larger than the rock-size through which numerical solution was obtained. This is expected. Because, instead of imposing a boundary condition at other end ($x = 1$), if we would have allowed the substances to diffuse freely through the rock, then this x_{max} would have been such a distance where concentration is smallest as compared to the source strength, but still measurable.

(d) The analytical solution, however, furnishes the actual distance through a rockbody upto which diffusion is significant in case of convective diffusion from a steady source along with a free boundary. In numerical solutions between fixed rock-sizes, diffusion has significance throughout that rock body before the formation of a concentration boundary layer Once a boundary layer is formed, after that diffusion is only significant within that layer in generating a perceptible concentration profile.

(e) In reality, the analytical solution with semi-infinite mode of conditions corresponds to an open system, where reaction products (e.g., silicic acid in the present case) are continually lost in the surrounding medium. On the other hand, numerical solution with fixed boundaries is more appropriate in case of a closed system (e.g., laboratory simulation of weathering of a mineral grain) where rate of release of products can be measured at a fixed a boundary. In natural system, such as ours, as the ground water percolation velocity is very slow, for all practical purposes, within short period of time (geologically) numerical technique with fixed boundaries are applicable. This is because within short period of time not much of material will be out of the system. This is further favoured by the very slow movement of the reaction front.

4.8 GEOLOGICAL IMPLICATION OF THE RESULTS

We started our investigation in order to find out the role played by convective diffusion in the process of weathering. On the way, we have picked up a specific example, viz: direct gibbsitic alteration of feldspars. All the boundary conditions considered are consistent within the thermodynamic framework of direct gibbsitization of potash feldspar. Thus, the results obtained highlight the diffusive aspect of the transformation. Here, we have not considered the aspect of chemical reaction rate Conclusion regarding this will however appear logically.

From the analyses that have been carried out so far, the following conclusions emerge out ·

1. Assuming equilibrium reaction between rock and water, precise measurements of parameters like concentration, pH etc can be made of the diffusing species.
2. For a given thickness, when steady-state will be attained, it appears, that the reaction will come to a standstill and no further weathering will take place. This

contention, however, is not true In our treatment, we have not coupled the problem of boundary movement. But, in reality, the reaction boundary will be moving at a definite rate (however small the rate may be). For this reason of continuous change in distance of effective diffusion, reaction will never cease, until whole of the rock is weathered or the weathering agent ceases to operate. Another reason for cessation of the weathering reaction may be the formation of an optimum thickness of the product layer which, due to its increasing resistance, hinders further diffusion significantly

3. As we have outlined, at the very beginning, two aspects play significant role in the generation of weathered profiles. These are - (a) reaction rate and (b) diffusion of reacting species as well as of reaction products, through the rock mass. In the present case, for distances around few hundreds of centimetres, the steady-state time values are of the order of few years to hundreds of years. On the otherhand, in natural weathering of feldspars, the time required to weather through few hundreds of centimetres is much more. This leads us to conclude that in a natural weathering process, reaction rate is slower than the rate of convective diffusion. It thus acts as rate limiting step and actually determines the time required for weathering of a given thickness of rock and its replacement by the weathered product of equal thickness.

CHAPTER 5

CONCLUDING REMARKS

The present work has dealt with the process of weathering of feldspars with particular reference to its direct conversion to gibbsite. Three aspects of feldspar weathering have been investigated. These are :

(a) Crystallo-chemical changes and thermodynamic viability of weathering of feldspars to gibbsite, both directly and indirectly.

(b) Calculation of time of weathering by chemical mass balance of four soluble elements (Na, K, Ca and Mg) from their fractionation in the parent rock, weathered product and ground water.

and, (c) Role of convective diffusion and chemical reaction in direct gibbsitization of feldspars.

Following are the conclusions drawn from the investigation.

1. Weathering of feldspars, when viewed as a successive structural simplification should follow the normal course of, feldspar mica kaolinite gibbsite. Direct gibbsitization bypasses the intermediate stages.

2. The thermodynamic stability of K-feldspar shows that direct conversion of K-feldspar to gibbsite is not possible. However, a metastable boundary has been shown to exist between K-feldspar and gibbsite. This implies that if gibbsite forms directly from K-feldspar, it will be in metastable form.

From stability diagrams involving Na- and Ca-feldspars, direct conversion of these feldspars to gibbsite appears to be thermodynamically viable.

3. In all the above mentioned cases, direct gibbsitization should take place at high pH conditions (pH > 10).

4 The rates of weathering leading to formation of bauxite vary widely. Mass balance calculations have shown that among different rocks for the same element and for different elements in the same rock, weathering rates are different.

5. On an average, in tropical regions, rate of weathering seems to be a few metres to a few hundred metres per million years.

6. When the velocity of the percolating ground water remains constant, the time taken to reach steady state for any diffusing species (H^+ or H_4SiO_4) increases with increas-

ing rock-size.

7. If the rock-length, through which diffusion occurs is kept constant but percolation velocity of ground water is varied within realistic range, it does not affect the time required to attain steady state.

This is true for the diffusion of both H^+ and H_4SiO_4. For example, for diffusion of H through a distance of 20 cms, under three different percolation velocities of ground water (10^{-6} cm/sec, $2x10^{-6}$ cm/sec and $3x10^{-6}$ cm/sec), the time required to attain steady state has been found to be 13.88 days irrespective of ground water percolation velocity.

8. Plots of steady state concentration profiles over rock-lengths (through which diffusion occurred) show that the steady state profiles are different for different rock-lengths and no part of the profiles is common between them. This shows that rocks of different size weather in a different way.

9. For very large rock-size, which contributes in increasing the value of Peclet-number significantly, a prominent concentration boundary layer is formed. Thus, the zone of effective diffusion is reduced and is henceforth confined only within that boundary layer. In other portion, diffusion does not produce any additional

change in concentration profile as there is no appreciable concentration gradient.

10. It seems that diffusion process attains steady state well before the time required to weather a rock of given thickness This indicates that diffusion plays an important role only during the initial stages of the weathering process.

11. After the attainment of the steady state concentration profile through diffusion, the process is likely to be controlled by chemical reaction.

Two chemical reactions are dominant in the weathering of K-feldspar to gibbsite. These are :

(i) $K^+ \rightleftharpoons H^+$ (Surficial ionic exchange between H^+ of water and K^+ of K-feldspar)

(ii) $KAlSi_3O_8 + H^+ + 7H_2O = Al(OH)_3 + K^+ + 3H_4SiO_4$
amorphous

As experimental evidences suggest that the first reaction is very fast, therefore the second reaction which produces H_4SiO_4 is most likely to be rate controlling.

SCOPE OF FURTHER WORK

The theoretical approach outlined in this thesis can

be further extended and supplemented in several ways :

1. In this work, we have assigned the initial concentration profile arbitrarily. However, from a partially weathered rock-profile (or in small scale from a partially weathered piece of mineral) the exact concentration of different species, at various points can be measured by using electron microprobe analyser.

The calculated concentration profiles for a given size of rock can also be measured and verified by this instrument. All these refinement will enhance the accuracy of the model.

2. In the present treatment, we have assumed regular geometry for the shape of the cross-section of the weathered zone. In reality, this may not be true. Thus, for irregular shapes, advanced method like FEM (Finite Element Method) can be used for better results.

3. Differential equation containing both diffusive and chemical reaction rate terms should be developed and solved. This will help in establishing mathematical relationships between diffusion parameters and chemical reaction rate terms in case of weathering.

4. Experimental work should be carried out to calculate rate constants for important weathering reactions.

REFERENCES

APPLIN , KENNETH. R , (1987) The diffusion of dissolved silica in dilute aqueous solution, Geochimica et cosmochimica acta, vol 51, pp 2147-2151

BERNER, R.A (1978) Rate control of mineral dissolution under earth surface conditions, Am.J.Sci. vol. 278, pp 1235-1252.

BHAVANA, P.R. (1983) Mineralogy and water chemistry in laterite profiles near Calicut, Kerala, unpub: M.Tech. Thesis, I.I T. Kanpur, pp. 68.

CARNAHAN, B, LUTHER, H A. and WILKES, J.O. (1969): Applied Numerical Methods, John Wiley and Sons Inc., pp· 604.

CHEN, C-H, LIU, K.K., SHIEH, Y-N. (1988): Geochemical and Isotopic studies of bauxitisation in the Tatun Volcanic area, Northern Taiwan, Chemical Geology, vol: 68, pp· 41-56.

COLMAN, S.M. and DETHIER, D.P. (1986) An overview of rates of chemical weathering, Chapter 1, in Rates of chemical weathering of rocks and minerals (Colman and Dethier, Eds.), Academic Press, N.Y., pp. 1-18.

DEER, W.A., HOWIE, R.A. and ZUSSMAN (1979): Introduction to the Rock-Forming Minerals, ELBS and Longman, London, pp: 528.

DOBROVOLSKY, E.V (1987). Physico-chemical mechanisms of weathering processes and corresponding models of dynamics of mineral zonality evolution, Chemical Geology, vol: 60, pp: 89-94

GARRELS, R.M and CHRIST, C.L (1965): Solutions, Minerals and Equilibria, Harper and Row, New York, pp: 450.

GARRELS, R M. and MACKENZIE, (1971) Evolution of Sedimentary Rocks, W.W. Norton and Co. Inc., New York, pp. 397.

GOLUBEV, V.S. and GARIBYANTS, A.A. (1971): Heterogeneous Processes of Geochemical Migration, Consultants Bureau, N.Y., pp: 150.

GRUBB, P.L.C. (1970): Mineralogy, Geochemistry and Genesis of the bauxite deposits on the Gove and Mitchell plateaux, Northern Australia, Mineralium Deposita, vol: 5, pp: 248-272.

GRUBB, P.L.C. (1979): Genesis of bauxite deposits in the tower Amazon basin and Guianas Coastal plain - Economic Geology, vol. 74, pp: 735-750.

HOLDREN, Jr. G R. and BERNER, R.A. (1979a) Mechanism of feldspar weathering-I- Experimental Studies· Geochimica et. Cosmochimica acta, vol. 43, pp 1161-1171.

---- AND ---- (1979b). Mechanism of feldspar weathering-II - Observations of feldspars from soils: Geochimica ... acta, vol 43, pp: 1173-1186.

ILER, R.K. (1955). The Colloid Chemistry of Silica and Silicates, Cornell Univ. Press

KELLER, W.D. (1979) Bauxitization of Syenite and Diabase illustrated in scanning electron microscope, Economic Geology, vol 74, pp· 116-124.

KHANADALI, S.D. and DEVARAJU, T.C. (1987) Laterite-Bauxite of Padurai Plateau, South Kanara, Karnataka States, Jour. Geol. Soc. India, Bangalore, vol· 30, October, pp. 255-266.

KITTRICK, J. (1966): Free Energy of formation of kaolinite from solubility measurements, Am. Mineralogist, vol· 51, pp: 1457-1466.

KRAUSKOPF, K.B. (1979): Introduction to Geochemistry, 2nd Edn, McGraw-Hill Kogakusha, Tokyo, pp: 617.

KRISHNA RAO, P.R. (1971): Hydrometeorological aspects of estimating ground water potential. Proc Seminar ground water potential in hard rock areas of India, Geol Soc India, Bangalore, pp 1-11.

KRONBERG, B.I., COUSTON, J.F., STILTANIDI FILHO, B., FYFE, W.S., NASH, R.A. and SUGDEN, D. (1979). Minor element geochemistry of the Paragominas bauxite, Brazil. Economic Geology, vol· 74, pp: 1869-1875.

LOUGHNAN, F.C. (1969). Chemical weathering of the silicate minerals, American Elsevier, New York, pp: 154.

LUCE, R.W., BARTLETT, R.W. and PARKS, G.A. (1972): Dissolution Kinetics of Magnesian silicates Geochimica et Cosmochimica acta, Vol· 36, pp 35-50.

MASON, B. and MOORE, C.B. (1982). Principles of Geochemistry, 4th ed:, Wiley Eastern Ltd., pp: 350.

PETERSEN, U. (1971). Laterite and Bauxite Formation, Economic Geology, vol: 66, pp: 1070-1071.

RANGANNA, G., GAJENDRAGAD, M.R., GURAPPA, K.M., NAYAK, I.V. and SEETHARAM, A.N. (1984): Groundwater development and its impact on agriculture along coastal Karnataka - A case study. Proc. of Central Board of Irrigation and Power; 51st

Annual research and development session, vol II, pp 91-102.

RAYMAHASHAY, B C. (1984). "Thermodynamics of Weathering Reactions". In Product and Processes of Rock Weathering, Recent Research in Geology, vol 11, pp 188-193. Hindustan Pub Corp. New Delhi, India.

ROBIE, R.A., HEMINGWAY, B.S., and FISHER, J.R., (1978). Thermodynamic properties of minerals and related substances at 198.15 K and 1 bar pressure and at higher temperatures, U.S. Geol. Surv. Bull No. 1452, pp 456.

SEN, A.K. and GUHA, S. (1987) The geochemistry of the weathering sequences - Present and past - in and around the Pottangi and Panchpatmali bauxite - bearing plateaus, Orissa, India Chemical Geology, vol. 63, pp 233-274

VALETON, I. (1972). Bauxites, Development in Soil Science 1, Elsevier Publishing Co., Amsterdam, pp 226.

WOLLAST, R. (1967). Kinetics of the alteration of K-feldspar in buffered solutions at low temperature. Geochimica et Cosmochimica acta, vol. 31, pp 635-648.

APPENDIX 1

List of minerals, their composition and ΔG_f^o values :

Mineral	Composition	ΔG_f^o in k.cal/mole (1978)*
1. Quartz	SiO_2	-204.853
2. Gibbsite (crystalline)	$Al(OH)_3$	-276.289
3. Gibbsite(Amorphous)	$Al(OH)_3$	-271.9[1]
4. Kaolinite(crystalline)	$Al_2Si_2O_5(OH)_4$	-908.939
5. Kaolinite (Poorly crystalline)	$Al_2Si_2O_5(OH)_4$	-901.0[2]
6. K-mica(muscovite)	$KAl_3Si_3O_{10}(OH)_2$	-1339.873
7. K-feldspar (microclinne)	$KAlSi_3O_8$	-895.294
8. Albite	$NaAlSi_3O_8$	-887.972
9. Anorthite	$CaAl_2Si_2O_8$	-961.068
10. H_4SiO_4		-312.918
11. H_2O		- 56.732
12. K^+		- 67.581
13. Na^+		- 62.656
14. Ca^{++}		-132.426
15. H^+		0
16. $Al(OH)_4^-$		-310.2
17. Al^{3+}		-116.0

* - Data from Robie et al.(1978), recalculated from J/mole into k.cal/mole by P.R. Bhavana (1983).

1 - From Krauskopf (1979) and the references therein.

2 - From Kittrick (1966).

Abbreviation : X/n = Crystalline ; Amorp:= Amorphous

1. Kaolinite (X/n) - Gibbsite (X/n) equilibrium

$$Al_2Si_2O_5(OH)_4 + 5H_2O = 2Al(OH)_3 + 2H_4SiO_4$$

$$\log K_1 = -10.4$$

2. K-mica - Kaolinite (X/n) equilibrium

$$2\ KAl_3Si_3O_{10}(OH)_2 + 2H^+ + 3H_2O = 3Al_2Si_2O_5(OH)_4 + 2K^+$$

$$\log K_2 = 8.82$$

3. K-mica - Poorly crystalline Kaolinite equilibrium

$$2KAl_3Si_3O_{10}(OH)_2 + 2H^+ + 3H_2O = 3Al_2Si_2O_5(OH)_4 + 2K^+$$

$$\log K_3 = -8.636$$

4. K-mica - Gibbsite (X/n) Equilibrium

$$KAl_3Si_3O_{10}(OH)_2 + H^+ + 9H_2O = 3Al(OH)_3 + 3H_4SiO_4 + K^+$$

$$\log K_4 = -11.187$$

5. K-feldspar-K-mica Equilibrium

$$3KAlSi_3O_8 + 2H^+ + 12H_2O = KAl_3Si_3O_{10}(OH)_2 + 6H_4SiO_4 + 2K^+$$

$$\log K_5 = -10.354$$

6. K-feldspar - Kaolinite (X/n) : Equilibrium)

$$2KAlSi_3O_8 + 2H^+ + 9H_2O = Al_2Si_2O_5(OH)_4 + 2K^+ + 4H_4SiO_4$$

$$\log K_6 = -3.961$$

7. K-feldspar-Poorly Crystalline Kaolinite Equilibrium

$$2KAlSi_3O_8 + 2H^+ + 9H_2O = Al_2Si_2O_5(OH)_4 + 2K^+ + 4H_4SiO_4$$

8. K-feldspar - Gibbsite (Amorph.) Equilibrium

$$KAlSi_3O_8 + H^+ + 7H_2O = Al(OH)_3 + K^+ + 3H_4SiO_4$$

$$\log K_8 = -10.398$$

9. K-feldspar - Gibbsite (X/n) Equilibrium

$$KAlSi_3O_8 + H^+ + 7H_2O = Al(OH)_3 + K^+ + 3H_4SiO_4$$

$$\log K_9 = 7.18$$

10. Poorly Crystalline Kaolinite - Gibbsite (Amorph.) Equilibrium

$$Al_2Si_2O_5(OH)_4 + 5H_2O = 2Al(OH)_3 + 2H_4SiO_4$$

$$\log K_{10} = -11.014$$

11. Albite-Kaolinite (X/n) Equilibrium

$$2NaAlSi_3O_8 + 2H^+ + 9H_2O = Al_2Si_2O_5(OH)_4 + 2Na^+ + 4H_4SiO_4$$

$$\log K_{11} = -0.44$$

12. Albite-Gibbsite (X/n) Equilibrium

$$NaAlSi_3O_8 + H^+ + 7H_2O = Al(OH)_3 + Na^+ + 3H_4SiO_4$$

$$\log K_{12} = -5.423$$

13. Anorthite-Kaolinite (X/n) Equilibrium

$$CaAl_2Si_2O_8 + 2H^+ + H_2O = Al_2Si_2O_5(OH)_4 + Ca^{++}$$

$$\log K_{13} = 17.27$$

14. Anorthite-Gibbsite (X/n) Equilibrium

$$CaAl_2Si_2O_8 + 2H^+ + 6H_2O = 2Al(OH)_3 + Ca^{++} + 2H_4SiO_4$$

$$\log K_{14} = 6.87$$

N.B: K-feldspar and K-mica (muscovite) are always considered to be in crystalline state and so also albite and anorthite.

APPENDIX 2

Dissolution of various ionic species of aluminium

Reaction in acid range -

1. $Al(OH)_3 + 3H^+ = Al^{3+} + 3H_2O$
   (crystalline gibbsite) $\log K_1 = 7.263$

Reaction in alkaline range -

2. $Al(OH)_3 + H_2O = Al(OH)_4^- + H^+$
   (crystalline gibbsite) $\log K_2 = -16.731$

* Data taken from Appendix 1

```
C      ********************************************************************
       DIFFUSIONAL CONCENTRATION DISTRIBUTION OF HYDROGEN ION/SILICIC
       ACID WITHIN WEATHERED LAYER OF K-FELDSPAR
       ********************************************************************
       PROGRAMMER: PARTHA PRATIM DE
       M.TECH THESIS WORK(I.I.T KANPUR/1987-88
       ********************************************************************
       DX=DISTANCE INTERVAL,DTIME=TIME INTERVAL,PE=PECLET NUMBER
       CK=RATE CONSTANT FOR SILICA RELEASE,N=DISTANCE NODES
       A=SUB-DIAGONAL COEFF.,B=DIAG.COEFF.,CC=SUPER-DIAG COEFF.
       ISTEP=PRINTING INTERVAL, C=CONCENTRATION
       CST=CONCENTRATION
       ********************************************************************
       DIMENSION A(20),B(20),CCK(20),D(20),C(20)
C      INPUT DATA
       DX=0.05,N=21;DTIME=0.1;PE=300.0
       CK3=0.55E-11;CST=0.316E-6
       ISTEP=10
       ALPHA=-(PE*DX+1)
       BETA=(DX*DX)/DTIME+(PE*DX)+2
       GAMMA=-1
       DELTA=(DX*DX)/DTIME
       P=1.0
C      C(2)=0.95
       C(2)=0.0
       DO 20 IP=2,N-2
20     C(IP+1)=CK(IP)-2.0
C20    C(IP+1)=C(IP)-1.05
       Q=0.186E-4
C      Q=0.0
       WRITE(22,200) P, (C(IP+1),IP=1,N-2),Q
C      R=0.0
       TIME=0.0
       ILIM=0
       WRITE(24,193)
       WRITE(24,200) TIME,P,(C(IP),IP=2,N-1),R
40     TIME=TIME+DTIME
       ILIM=ILIM+1
       DO 30 I =3,N-2
       A(I)=ALPHA/DELTA
       B(I)=BETA/DELTA
30     CC(I)=GAMMA/DELTA
       A(2)=0.0
       B(2)=BETA/DELTA
       CC(2)=GAMMA/DELTA
       A(N-1)=ALPHA/DELTA
       B(N-1)=BETA/DELTA
       CC(N-1)=0.0
C      CK(N)=2.0*CK*SQRT(TIME)/CST
       C(1)=1.0
C      C(N)=0.0
       C(N)=0.186E-4
       DO 50 I =3,N-2
50     D(I)=CK(I)
       D(2)=C(2)-(ALPHA/DELTA)*C(1)
       D(N-1)=CK(N-1)-(GAMMA/DELTA)*C(N)
C
       CALL TRIDAG(2,N-1,A,B,CC,D,C)
       IF((ILIM/ISTEP)*ISTEP.NE.ILIM) GO TO 40
       WRITE(22,200) (CK(I),I=1,N)
       IF (TIME.GE.4.5) GO TO 10
       WRITE(24,205)
       WRITE(24,210) ALPHA,BETA,GAMMA,A(3),B(3),CC(3)
199    FORMAT(8H0  TIME,18X,43HVALUES OF CONCENTRATION AT ALL GRID-POIN
       1TS)
200    FORMAT(1H ,3H0.6//(1H ,7X,21E17.6))
202    FORMAT(2X,21H2.4)
205    FORMAT(13X,'ALPHA',13X,'BETA',12X,'GAMMA',13X,'A(I)',13X,'B(I)',
       113X,'CC(I)')
210    FORMAT(5X,6(5X,E13.6))
       STOP
       END
C      ********************************************************************
       SUBROUTINE TRIDAG(IF,L,A,B,CC,D,V)
       DIMENSION A(20),B(20),CC(20),D(20),V(20),BET(101),GAM(101)
       BET(IF)=B(IF)
       GAM(IF)=D(IF)/BET(IF)
       IFP1=IF+1
       DO 1 I =IFP1,L
       BET(I)=B(I)-A(I)*CC(I-1)/BET(I-1)
1      GAM(I)=(D(I)-A(I)*GAM(I-1))/BET(I)
       V(L)=GAM(L)
       LAS1=L-IF
       DO 2 K =1,LAST
       I=L-K
2      V(I)=GAM(I)-CC(I)*V(I+1)/BET(I)
       RETURN
       END
```

```
C     ********************************************************
C     THIS PROGRAM PLOTS DIMENSIONLESS CONCENTRATION AGAINST
C     DIMENSIONLESS DISTANCE
C     PROGRAMMER:SARITA PRATIM DE
C     M.TECH THESIS WORK/I.I.T KANPUR/1987-88
C     ********************************************************
      DIMENSION X(25),Y(25,25)
      READ(21,*) ((I,M),M=1,21)
C     READ(24,*) ((X(J,M),M=1,21),J=1,14)
      N=21;XSTEP=0.05;YSTEP=0.05
      X(1)=0.0
      DO 20 IP = 1,20
20    X(IP+1)=X(IP)+0.05
      XWIN=X(N)+0.1
C     YWIN=Y(K,N)+0.1
      YWIN=X(N)+0.1
      CALL GRSTRT(1010,1)
      TYPE 1212
1212  FORMAT(4X,'MANUAL CHECK #') ; ACCEPT *,I
      CALL WINDOW(-XWIN/5.0,XWIN,-YWIN/5.0,YWIN)
      CALL VWPORT(-XWIN/5.0,XWIN,-YWIN/5.0,YWIN)
      CALL MOVE(0.0,0.0)
      CALL DRAW(XWIN,0.0)
      CALL DRAW(XWIN,YWIN)
      CALL DRAW(0.0,YWIN)
      CALL DRAW(0.0,0.0)
      CALL SMOOTH
C     DO 9 J = 1,K
C     CALL SKIP
      DO 8 M = 1,N
      CALL DRAW(X(M),Y(I,M))
8     CONTINUE
C9    CONTINUE
      CALL MOVE(0.0,0.0)
      CALL VECROT
      Y1=YWIN/100.0
      DO 25 I = 1,5
      CALL MOVE(4.0*XSTEP,0.0)
      CALL DRAW(0.0,-Y1)
      CALL MOVE(0.0,-4*Y1)
      CALL TXTCUR(3);CALL TXPCUR(3)
      A=XSTEP*FLOAT(I*4)
      CALL RNUMBR(A,1,4)
      CALL MOVE(0.0,5.0*Y1)
25    CONTINUE
      CALL MOVE(-1.0,0.0)
      X1=XWIN/100.0
      DO 30 J = 1,5
      CALL MOVE(0.0,4.0*YSTEP)
      CALL DRAW(-X1,0.0)
      CALL MOVE(-8.0*X1,0.0)
      CALL TXTCUR(3);CALL TXPCUR(3)
      B=YSTEP*FLOAT(J*4)
      CALL RNUMBR(B,1,4)
      CALL MOVE(9.0*X1,0.0)
30    CONTINUE
      CALL VECABS
      CALL MOVE(XWIN/2.0,-YWIN/5.0)
      CALL TXTCUR(8)
      CALL TEXT(22,'DIMENSIONLESS DISTANCE')
C     CALL TEXT(18,'DIMENSIONLESS TIME')
      CALL MOVE(-XWIN/5.0,YWIN/2.0)
      CALL TXANGL(90.0)
      CALL TEXT(27,'DIMENSIONLESS CONCENTRATION')
      CALL GRSTOP(' ACCEPT *, J
      STOP
      END
```

```
C     ***************************************************
C     THIS PROGRAM PLOTS DIMENSIONLESS CONCENTRATION
C     AGAINST DIMENSIONALISED DISTANCE
C     PROGRAMMER:PARTHA PRATIM DE
C     M.TECH THESIS WORK/I.I.T KANPUR/1987-88
C     ***************************************************
      DIMENSION X(25),X1(25),Y(25,25)
      READ(22,*) ((Y(J,M),M=1,21),J=1,3)
C     READ(21,*) (Y(3,M),M=1,21)
      N=8;XSTEP=100.0;YSTEP=0.05;K=3,NN=21
      X(1)=0.0
      DO 100 I = 1,7
100   X(I+1)=X(I)+XSTEP
      XWIN=X(N)+1.0
      YWIN=Y(1,1)+0.1
      X1(1)=0.0
      DO 110 IP =1,23
110   X1(IP+1)=X1(IP)+0.05
      CALL GPSIRT(1010,1)
      TYPE 121
121   FORMAT(1X,'READY');ACCEPT *,I
      CALL WINDOW(-XWIN/5.0,XWIN,-YWIN/5.0,YWIN)
      CALL VWPORT(-XWIN/5.0,XWIN,-YWIN/5.0,YWIN)
      CALL MOVE(0.0,0.0)
      CALL DRAW(XWIN,0.0)
      CALL DRAW(XWIN,YWIN)
      CALL DRAW(0.0,YWIN)
      CALL DRAW(0.0,0.0)
C     CALL VECABS
      CALL SMOOTH
      DO 200 JJ = 1,NN
      XT1=X1(JJ)*200.0
      CALL DRAW(XT1,Y(1,JJ))
200   CONTINUE
C     CALL SKIP
      CALL MOVE(0.0,0.0)
      CALL SMOOTH
      DO 300 KK = 1,NN
      XT2=X1(KK)*100.0
      CALL DRAW(XT2,Y(2,KK))
300   CONTINUE
C     CALL SKIP
      CALL MOVE(0.0,0.0)
      CALL SMOOTH
      DO 400 LL = 1,NN
      XT3=X1(LL)*500.0
      CALL DRAW(XT3,Y(3,LL))
400   CONTINUE
      CALL MOVE(0.0,0.0)
      CALL VECREL
      XX=XWIN/100.0
      DO 500 I = 1,5
      CALL MOVE(0.0,4.0*YSTEP)
      CALL DRAW(-XX,0.0)
      CALL MOVE(-3.0*XX,0.0)
      CALL TXTCUR(3) ; CALL TXFCUR(3)
      B=YSTEP**FLOAT(I*4)
      CALL RNUMBR(3,I,4)
      CALL MOVE(9.0*XX,0.0)
500   CONTINUE
      CALL MOVE(0.0,-11.0)
      YY=XWIN/3333.0
      DO 600 J = 1,6
      CALL MOVE(XSTEP,0.0)
      CALL DRAW(0.0,-YY)
      CALL MOVE(0.0,-4*YY)
      CALL TXTCUR(3) ; CALL TXFCUR(3)
      A=XSTEP**FLOAT(J)
      CALL RNUMBR(A,1,5)
      CALL MOVE(0.0,5.0*YY)
600   CONTINUE
      CALL VECABS
      CALL MOVE(XWIN/2.0,-YWIN/6.0)
      CALL TXTCUR(3)
      CALL TEXT(1,'DISTANCE (IN CMS)')
      CALL MOVE(-XWIN/6.0,YWIN/2.0)
      CALL TXANGL(90.0)
      CALL TEXT(2,'DIMENSIONLESS CONCENTRATION')
      CALL GRSTOP;ACCEPT *,J
      STOP
      END
```